THERMAL HAZARD ANALYSIS OF NITROAROMATIC COMPOUNDS

A Thesis

by

WEN ZHU

Submitted to the Office of Graduate and Professional Studies of
Texas A&M University
in partial fulfillment of the requirements for the degree of

DOCTOR OF PHILOSOPHY

Chair of Committee,	Chad Mashuga
Committee Members,	James Holste
	Benjamin Wilhite
	Debjyoti Banerjee
Head of Department,	M. Nazmul Karim

August 2019

Major Subject: Chemical Engineering

ABSTRACT

Nitroaromatic compounds are among the largest group of industry chemicals. Due to the high bond-association energy (BDE) of the C-NO_2 in nitroaromatic compounds (297 $\pm$ 17 kJ/mole), once the runaway reaction is triggered, the compounds will release massive heat and gases that accelerate the system temperature and pressure increase that lead to an explosion instantly.

Mononitrotoluenes (MNT) is among most important nitroaromatic compounds used as intermediates for the synthetic pharmaceuticals, agrochemicals and precursors for TNT. However, in the past 30 years, serious incidents, owing to its thermal decomposition, have killed 88 people and injured more than 900.

To help prevent future thermal runaway behavior of the nitroaromatic compounds, this work presents using both the experimental and simulation methodologies to figure out the thermochemistry and thermodynamics starting from MNT. The understanding of the thermal behaviors and mechanisms can yield safer handling and storage of the reactive chemicals. To investigate the mechanisms that cause the *ortho*-nitrotoluene (2-NT, isomer of MNT) decomposition reactions, the effects of different incompatible substances and surrounding conditions, such as confinement, heating rate, induction effect and sample sizes, were studied using three types of calorimetry – DSC, ARSST and APTAC.

Experimental results suggest that:

2-NT is the most hazardous reactive chemical among the three isomers of MNT with the much higher pressure rise rate than the others. It is an autocatalytic reaction follows

three stages: induction phase, acceleration phase and decay phase. The induction phase follows the zero order reaction with activation energy (170-174 kJ mol^{-1}) and pre-exponential factor ($10^{11.6}$-$10^{11.7}$ s^{-1}). The main decomposition pathway during reduction phase is the generation of anthranil and water.

The six common contaminants (NaOH, Na_2SO_4, $CaCl_2$, NaCl, Na_2CO_3 and Fe_2O_3) that exist in the manufacturing process of MNT lower the thermal stability of 2-NT with the three proposed mechanisms (generation of OH^-, impact of chloride ions and Iron (III) oxide catalyzed nitroarenes reduction).

This work demonstrates the complexity and the multiple studies required for making MNT safer, providing suggestions to the nitroaromatics industry. It can also serve as an example for comprehensive studies on various reactive chemicals.

DEDICATION

To

My mother Xiuyu Li, my father Jiancheng Zhu and

My husband Dai Li

ACKNOWLEDGEMENTS

Many people have been part of my journey through Texas A&M University. They helped me overcome challenges, achieve my goals, supported me in hard time, or simply made graduate life happier and enjoyable, and I want to express my gratitude to each of them.

I want to give my special appreciation to my deceased advisor, Dr. M. Sam Mannan. Dr. Mannan was someone you would never forget once you meet him. He was professional, thoughtful and kind. He was a good leader, good researcher as well as a good person. His dedication to chemical process safety impacted me a lot and I believe his legacy in process safety will continue to impact the world. I want to thank him for his encouragement, help and support since my first day joined the Texas A&M University. He gave me various opportunities to practice my skills in solving the real-world problems, contribute to the solutions and gain valuable experience.

I also want to give my special thanks to my advisor, Dr. Chad Mashuga for mentoring me during these past five years. Dr. Mashuga is the funniest advisor and one of the smartest people I know. He is gentle and warmhearted. He has been supportive and provided insightful discussions about my research. I want to thank both of my advisor Dr. Mashuga and Dr. Mannan for supporting me not only in academic level, and also cheering me up during the hard times of my life.

I also very appreciate the time and advice from Dr. James Holste, Dr. Debjyoti Banerjee and Dr. Benjamin Wilhite. I want to thank them for serving as my committee members and their assistant during the doctoral program.

I want to express my deep gratitude toward Dr. Maria Papadaki from the University of Patras, Greece for her contributions. Dr. Papadaki's scientific advice and expertise allowed me to pursue the research work more confidently and fearlessly. She also always there to encouragement for making me realized my potential and working hard to be a stronger person.

I would also like to extend my thanks to the members of the Mary Kay O'Connor Process Safety Center. I want to thank Dr. Simon Waldram and Dr. Zhe Han who taught me the basic principles of reactive chemicals and the usage of calorimeter. Thanks also go to my colleagues and the department faculty and staff for making my time at Texas A&M University a great experience.

I want to thank my parents and my grandma in China. They taught me importance of study hard, work hard and to be a warm and kind person. Their contributions shaping the person I am today. Without their support and love, I would not be able to keep ambitious and trying hard for my goals. I also want to thank my husband, Dai Li for his love, accompany and support. I also want to thank his family for their care and encouragement. I want to thank my best friends, Lu Chen, Xingyue An, Yanpu Zhang, Xiaolei Wang, Yifei Yang, Lubna Ahmed for the love and support they have showered on me always.

Finally, I want to thank all the people I have met during my PhD and thank them for their advices, accompany and support.

NOMENCLATURE

A: Pre-exponential factor [s^{-1}]

a: Thermal expansion coefficient [K^{-1}]

b: Isothermal compressibility [pa^{-1}]

C: Concentration of the reactant at time t [mol m^{-3}]

C_0: The reactant initial concentration [mol m^{-3}]

C_p: Heat capacity at constant pressure [J g^{-1} K^{-1}]

C_v: Heat capacity at constant volume [J g^{-1} K^{-1}]

$C_{p,c}$: Heat capacity of the glass cell [J g^{-1} K^{-1}]

$C_{p,s}$: Heat capacity of sample [J g^{-1} K^{-1}]

dP/dt: Pressure increase rate [psi min^{-1}]

$(dP/dt)_{max}$: Maximum pressure increase rate [psi min^{-1}]

dT/dt: Self-heat rate [°C min^{-1}]

$(dT/dt)_{max}$: Maximum self-heat rate [°C min^{-1}]

$\left(\frac{dT}{dt}\right)_{\varphi>1}$: Experimental self-heat rate [°C min^{-1}]

$\left(\frac{dT}{dt}\right)_{\varphi=1}$: Adiabatic self-heat rate (corrected by the phi factor) [°C min^{-1}]

Ea: Activation energy [kJ mol^{-1}]

ΔHrxn: Heat of the reaction [kJ mol^{-1}]

k: Kinetic constant [dependent of reaction order]

k^*: Pseudo zero order rate constant at temperature T

m: Mass [g]

m_c: Mass of cell [g]

n: Order of the reaction

NCG: non-condensable gas generated by the reaction [mole]

n_{final}: The total moles of non-condensable gases [mole]

$n_{initial}$: The moles of non-condensable gases at the beginning of the test [mole]

$n_{r \times n}$: Moles of chemical reacted [mole]

P: Pressure [Pa]

$P_{initial}$: Initial pressure before starting the experiment [Pa]

P_{final}: Pressure inside the test cell after cooling down [Pa]

P_{max}: Maximum Pressure [Pa]

P_{onset}: Onset Pressure [Pa]

q_L: Heat release rate to the environment [J s^{-1}]

$\dot{q}$: Heat release rate [W kg^{-1}]

r: Reaction rate [mol m^{-3} s^{-1}]

R: Universal gas constant [J mol^{-1} K^{-1}]

R^2: Coefficient of determination

S: Wetted surface area [m^2]

t: Time [min]

T: Temperature [K]

t_{mr}: Time to maximum rate [min]

T_a: The self-accelerating decomposition temperature (SADT) [K]

T_e: The ambient temperature [°C]

T_f: Temperature when the reaction completed, when dT/dt equals to zero [°C]

T_{max}: Temperature at the maximum self-heat rate (ºC), the temperature at which $(dT/dt)_{max}$ occurs [°C]

T_{NR}: Temperature of no return [K]

T_o: Onset temperature [°C]

$(T_0)_{\varphi=1}$: Adiabatic onset temperature after phi factor correction [K]

T_p: The peak temperature of a DSC scan at that rate [K]

T_{SADT}: The self-accelerating decomposition temperature [K]

$(T)_{\varphi=1}$: Adiabatic temperature after phi factor correction [K]

ΔT_{ad}: Adiabatic temperature rise [°C]

$\Delta T_{external}$: External heating source caused temperature rise [K]

U: The heat transfer coefficient [J s^{-1} m^{-2} K^{-1}]

$\hat{V}$: Volume [m^3]

α: Extent of conversion/fractional conversion

β: Heating rate [K min^{-1}]

φ: PHI factor or thermal inertia factor

ρ: Density [g ml^{-1}]

TABLE OF CONTENTS

Page

LIST OF FIGURES

Page

LIST OF TABLES

Page

1. INTRODUCTION

Chemical reactivity is the tendency of the substances to react with other media [1]. People use chemicals' reactivity to produce goods and provide services to assist society. However, insufficient understanding and improper usage of the reactive chemicals can cause the uncontrolled runaway reactions to happen. When the uncontrolled runaway reactions happen, they will lead to

- Uncontrolled energy releases
- Uncontrolled generation of gaseous/hazardous products

These two results have been the most significant in leading to major chemical incidents, which present severe threat to the chemical process industry and local community.

Nitroaromatic compounds are one of the most important groups of industrial chemicals in use today with high chemical reactivity. Nitroaromatic is an organic chemicals and has at least one nitro group ($-NO_2$) attached to an aromatic ring (Figure 1). Due to the high bond-association energy (BDE) of the $C-NO_2$ in nitroaromatic compounds (297 ± 17 kJ/mole)[2][3], once the runaway reaction is triggered, the compounds will release massive heat and gases that accelerate the system temperature and pressure increase that lead to an explosion instantly.

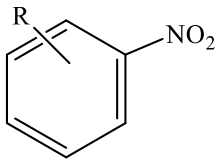

Figure 1. Formula structure of nitroaromatics. R can be –NO2, –CH3, –OH, –NH2 etc.

The simplest formula nitroaromatic compound is nitrobenzene (Figure 2) that has only one nitro group on the benzene ring. Dinitrobenzenes have two nitro groups with three isomers and 1,3,5-Trinitrobenzene (TNB) is a common explosive which has three nitro groups.

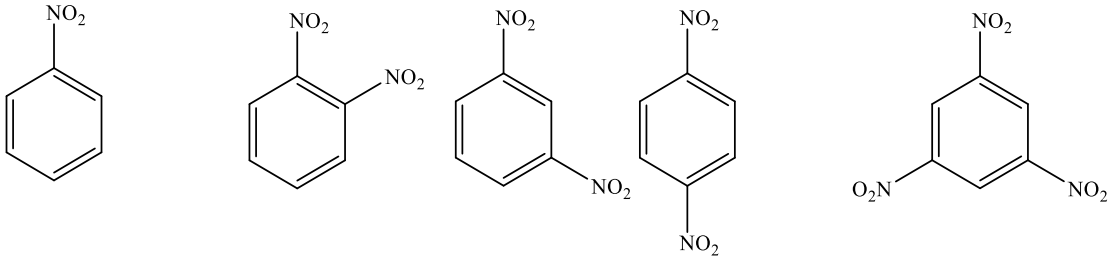

Nitrobenzene Dinitrobenzenes 1,3,5-Trinitrobenzene

Figure 2. Formula structure of Nitrobenzene, Dinitrobenzenes and 1,3,5-Trinitrobenzene

Another important family of the simple aromatics is nitrotoluenes. Nitrotoluenes are widely used as intermediates for the normal chemical production. MNT has one nitro group attached on the methylbenzene and it has three different isomers (*ortho*-, *meta*- and *para*- nitrotoluene). DNT has two nitro groups attached on the methylbenzene and it has

six different isomers. Toluene nitrated with three NO_2^- is the famous explosive TNT. TNT has low sensitivity to impact and friction which is safe for transportation and higher stability but generate large amount of power once decompose.

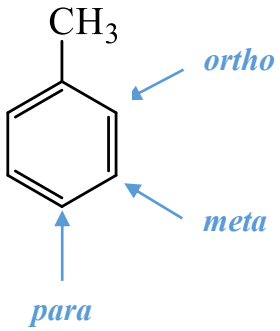

Figure 3. Structural formulas of three isomers of MNT

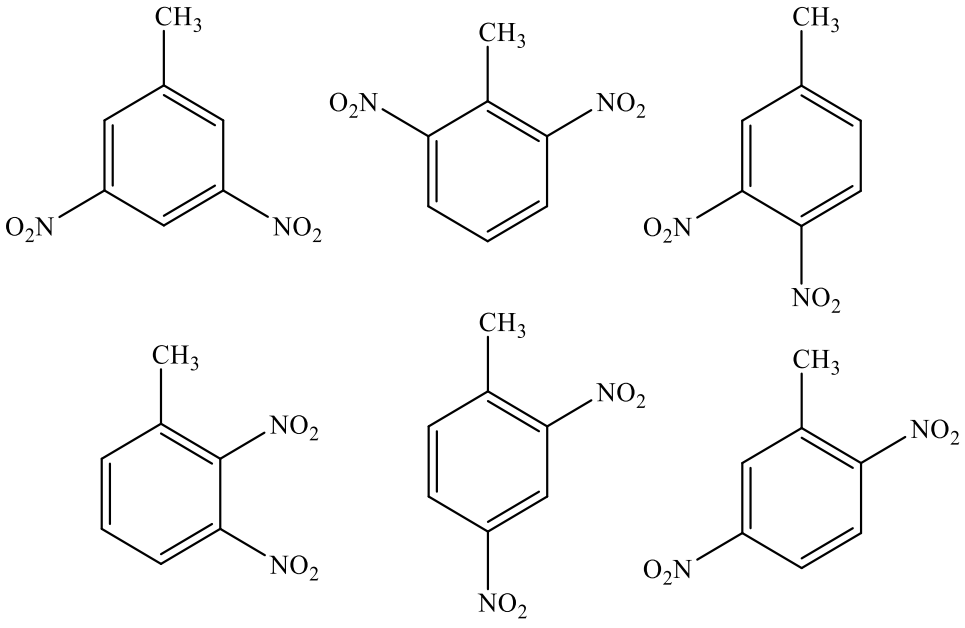

Figure 4. Structural formulas of six isomers of DNT.

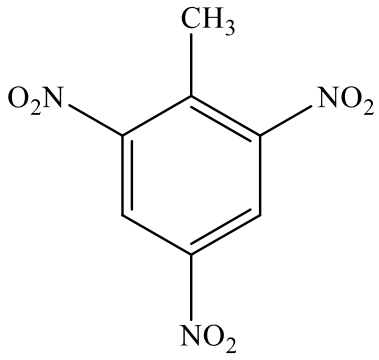

Figure 5. Structural formulas of TNT.

MNT and DNT are reactive chemicals due to the easy to break and energetic nitro groups on the methylbenzene. A number of incidents have occurred due to the thermal decomposition reactions of MNT and DNT, which caused fatalities and great loss of property. Incident history demonstrates inadequate recognition and evaluation of reactive hazards of nitro aromatic compounds.

The work mainly focusses on investigation possible mechanisms of the MNT & DNT decompositions, and the MNT & DNT's chemical reactivity under different conditions. Additionally, the predictive models will help to have safer storage, handling and transportation of these chemicals. Due to the measurement limitation of the calorimetry, the experimental part mainly focuses on the study of mononitrotoluenes (MNT).

1.1 Manufacturing procedures and applications

Nitration is the main reaction used to synthesize nitroaromatic compounds. Nitronium ions (NO_2^+) are generated in a mixed sulfuric and nitric acids and then added onto aromatic substrates via electro philic substitution [4]. Using this method, benzene, toluene, and

phenol are converted into nitrobenzene, nitrotoluenes and nitrophenol. Nitration to the *ortho, meta*, or *para* positions can be achieved by varying manufacturing conditions [5]. For nitrotoluenes, the normal manufacturing process starts with the nitration of toluene [6]. Nitration with nitric acid and sulfuric acid at 10-15 °C produces three isomeric products (*ortho*-, *meta*- and *para*- nitrotoluene). Most industrially-produced MNT is further nitrated to DNT by increasing the temperature to 70 – 80 °C with mixture of nitric acid and sulfuric acid at higher concentration. Subsequent additions of fuming nitric acid and sulfuric acid results in 2,4,6-trinitrotoluene (TNT).

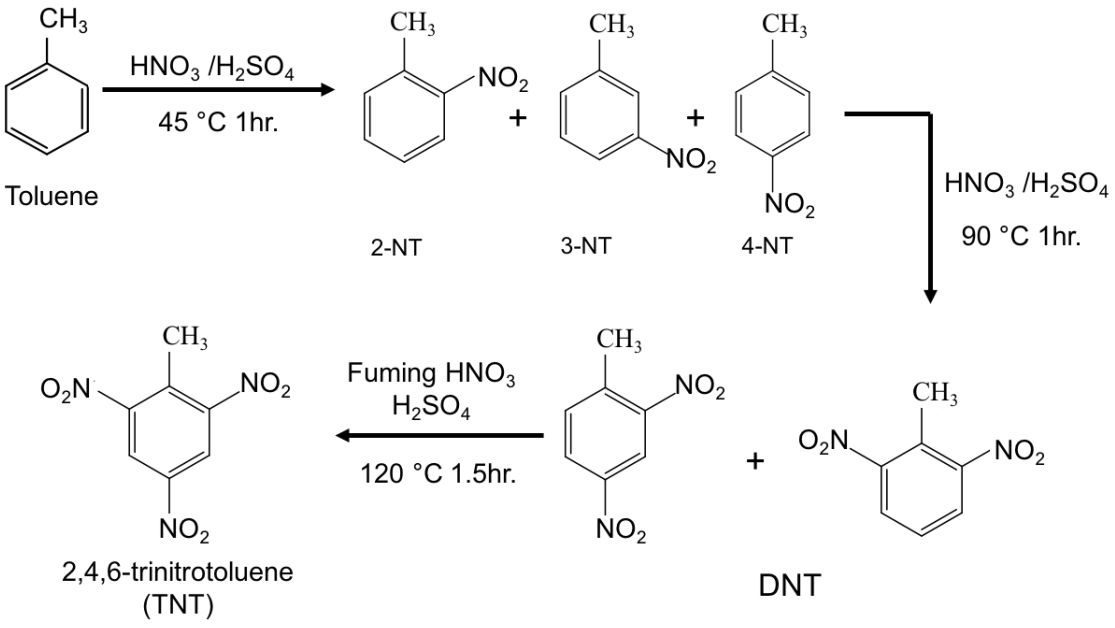

Figure 6. Manufacturing process of TNT.

In addition to DNT production, pure MNT isomers are also being utilized in smaller specialty markets, like the production of dyes, rubber chemicals, and agricultural chemicals. In 1993, the production of MNT in the U.S. was 28,652 tons of which approximately 62% (17764 tons) were the 2-NT, 3% (860 tons) were the 3-NT and 35% (10028 tons) were the 4-NT [7]. The ortho-nitrotoluene (2-NT) is listed as a 'high production volume chemical' according to U.S. Environmental Protection Agency (EPA), and the production of 2-nitrotoluene in the U.S. was between 10 to 50 million pounds for every 4-year's report from 1986 to 2002 [8]. According to the data in 2010, 2-NT is produced by 10 companies in the U.S., seven companies in the China, three companies in the United Kingdom, two companies in Canada, and one company each in the Czech Republic, Germany, India, Italy, Japan and Switzerland [9].

Dinitrotoluene (DNT) is used in the production of toluene diisocyanate (TDI), a component of polyurethane. Also, it can be used for special application markets, such as explosives, dyes, polyure thane foams, agricultural chemicals and solvents. According to the data between 1999 and 2000, around 1.5 million tons of DNT were produced worldwide every year [10] . Air Products and Chemicals have a 500 million pounds per year DNT production facility in Geismar, Louisiana and a billion pounds per year DNT facility in Pasadena, Texas [11].

1.2 Incidents history

Historically, fire and explosion incidents of MNT and DNT occurred due to the thermal decompositions reactions, which resulted in the fatalities and injuries.

Table 1 summarized the main reported MNT & DNT related incidents happened in the past 30 years. The most recent incident related to the MNT/DNT is the Xiangshui chemical plant explosion on March 21, 2019 which killed 78 people already and injured 600 others. Though the cause of the incident is still under investigation, one of the main chemical onsite is the 2,4-dinitrobenzene and MNT/DNT exist during the manufacturing process as the precursor for the fertilizer production. Due to the explosive behavior of the nitroaromatic compounds, once the runaway reaction is triggered, it will cause a tragedy. The explosion related to nitroaromatic compounds mainly happened in three operation units: nitration reactors, distillation columns and transportation pipelines. The direct causes of the incidents can be summarized into two main categories: the incompatible contaminations and the external heating sources. Details of the incidents are discussed based on three operation units – nitration reactors, distillation towers and storage and transportation devices.

Table 1. MNT & DNT related incidents in the past 30 years

Date	Location	Company	Injuries	Fatalities	Units	Causes
03/21/2019	Yancheng, China	Tianjiayi Chemical	600	78	N/A	N/A
05/11/2007	Cangzhou, China	China National Chemical Corporation	80	5	Reactor	Incompatible contamination
10/13/2002	Pascagoula, Mississippi	First Chemical Corporation	3	0	Distillation column	External heat
09/21/1992	United Kingdom	Hickson & Welch Ltd	181	5	Distillation column	Incompatible contamination & External heat
08/07/1972	Institute, West Virginia	Union Carbide Facility	1	0	Pipeline	External heat

6.3.1. Nitration reactors

On May 11, 2007, a fatal explosion occurred in the toluene nitration reactor at China National Chemical Corporation in Cangzhou, China. A large local excess of acid beyond that required for the completion of the nitration from toluene to MNT was added into the reactor due to human errors. The normal operation temperature in the MNT nitration reactor is relatively low (< 100 °C). However, the excess acid lowered the thermal stability of MNT as well as generated the unwanted DNT and even TNT. When the DNT and TNT decomposed, they would release even larger amount of heat at a short period of time. As the result, the accumulated temperature rise triggered the decomposition of the MNT at

relative lower temperature due to the incompatible contaminant. Later on, heat of decomposition from MNT triggered the runaway reactions of DNT and TNT, which leaded to the huge explosion and fire. Duh (1997) et al. [12] found that excess acids can lower the decomposition onset temperatures of MNT and DNT.

6.3.2. Distillation columns

The only satisfactory method of separating the MNT and DNT isomers is distillation. Due to the relatively high boiling points and the narrow boiling range (220-238 °C for MNT and 285-300 °C for DNT [13]) of the isomers, the normal distillation is unable to finish the task. Therefore, it requires the use of an efficient fractionating column, requiring the nitro aromatics to be held at high temperatures for long periods of time which makes the process dangerous due to the potential decompositions of MNT and DNT. A number of explosions (First Chemical Corporation explosion, 2002 [14] and Hickson & Welch Ltd explosion, 1992 [15]) have occurred in the distillation columns of MNT and DNT production in which chemicals have been heated to an excessively high temperature or held at a more moderate temperature for longer period of time [16]. The phenomenon that runaway reactions can occur at lower temperatures if reactive chemicals are exposure to lengthy heating time is called the induction effect.

6.3.3. Storage & transportation devices

During the manufacturing process, MNT and DNT are stored in a tank or transferred pipelines. However, when the chemicals are exposed to elevated temperature, they will

accumulate the heat slowly and once a critical temperature is met, an explosion can happen. When and how the runaway reactions will happen depend on the quantity of stored chemical, temperature, pressure, length of storage time at the specific temperature and also the presence of retardance or promoter behaving contaminants. On August 7, 1972, a pipeline contains Dinitrotoluene (DNT) exploded. This incident happened at a Union Carbide facility located in Institute, West Virginia. According to the incident investigation, the DNT was contained in a transfer line for 10 days before the incident happened. The temperatures of the chemical was about 210 °C, which is lower than the Differential Scanning Calorimeter (DSC) detected onset temperature (250-300 °C) in the lab [12]. Due to the auto-catalytic behavior of the MNT thermal decomposition, this expected incident happened.

The reoccurrence of incidents indicates that a comprehensive understanding of the thermal behavior of MNT and DNT is of vital importance. More experimental tests are needed to avoid underestimation of the hazards of the chemicals.

1.3 Hazards of MNT & DNT

1.3.1. Toxicity

Table 2. Health rating for MNT & DNT

	NFPA Health	IDLH (mg/m3)
2-Nitrotoluene	1	1122
3-Nitrotoluene	2	1122
4-Nitrotoluene	2	1122
2,4-Dinitrotoluene	2	50
2,6-Dinitrotoluene	3	50

Mononitrotoluene and dinitrotoluene are toxic by inhalation, ingestion and skin absorption [17]. Experiments were conducted by Dunnick et al. [18][19] to compare toxicities of 2-NT, 3-NT and 4-NT in 13-week feed studies in rats. It was found that all three chemicals caused toxicity in rats.

Comparing the IDLH (Immediately dangerous to life or health) value, we see that DNT is more toxic than MNT. In fact, in the environment, DNT has been found in at least 122 hazardous waste sites that release DNT. The EPA claims DNT is expected to exist in the water for long periods of time due to moderate water solubility and volubility. [20] Workers who have been exposed to 2,4-DNT showed a higher death rate of heart disease [21].

1.3.2. Flammability

Table 3 shows the heat of combustion for various nitrated aromatics. MNT and DNT have lower heat of combustion than diesel fuel (448×10^2 kJ kg^{-1}) [24]. Also, the auto-ignition temperature for 2-nitrotoluene is 420 °C [25] and it is not easy to be ignited (Diesel fuel auto ignition temperature is 256 °C [26]). All the tests in this document are operated in the nitrogen gas atmosphere, which make sure there are only decomposition reactions happen but not the combustions.

Table 3. NFPA fire and heat of combustion for MNT & DNT

Chemicals	NFPA fire	Heat of Combustion [22][23] (kJ/kg)
2-Nitrotoluene	1	-262×10^2
3-Nitrotoluene	1	-361×10^2
4-Nitrotoluene	1	-375×10^2
2,4-Dinitrotoluene	1	-193×10^2
2,6-Dinitrotoluene	1	-188×10^2

2. LITERATURE REVIEW

2.1 Thermal decomposition of MNT and DNT

The decomposition reactions of MNT and DNT are rapid and highly exothermic. This is due to the following factors [40]:

- The decomposition occurs at relative high temperatures (250-350 °C). Since the activation energy is higher, once the decomposition happens and it will release a lot of heat.
- The heat of decomposition is very high (>1.3 kJ g^{-1}). Consequently, under pseudo adiabatic conditions, or in normal process conditions, the decomposition reaction rate will accelerate due to a rapid increase in temperature.

Gustin (1998) stated that experimental proof of the autocatalytic decomposition behavior is difficult to obtain due to the high app arent activation energy of the nitro aromatic compounds decomposition reactions [27].

Within a series of nitro aromatic compounds, the thermal stability and heat of the decompositions are influenced by the type, the position, and the number of the substituents [28]. There are three different isomers for MNT and six isomers for DNT. Due to the different position and number of nitro groups, their thermal behaviors are slightly different. Table 4 summarized the thermal stability tests' results from the literature for three MNT isomers and six DNT isomers.

Table 4. Summary of experimental values of observed on-set temperature and heat of reaction

Compound	T_{onset} (°C)	$-\Delta H_{rxn}$ ($J \cdot g^{-1}$)	$-\Delta H_{rxn}$ ($kJ \cdot mol^{-1}$)	Calorimeter	References
2-NT	290	2404	330	DSC	[12]
	338	1326	182	DSC	[29]
	250 - 265			ARC	[30]
	317	1710	234	N/A	[31]
3-NT	310	2070	284	ARC	[12]
	361	1088	149	DSC	[29]
	400 - 470	2073	284	N/A	[32]
4-NT	320	2322	318	ARC	[12]
	329	1556	213	DSC	[29]
	380 - 450	2015	276	N/A	[33]
1,2-DNT	280	3310	603	ARC	[12]
1,3-DNT	270	3488	635	ARC	[12]
1,4-DNT	350	3701	674	ARC	[12]
2,4-DNT	250	3574	651	ARC	[12]
	312	3469	632	DSC	[29]
	272-304	2030	370	DSC	[33]
3,4-DNT	280	3987	726	ARC	[12]
	322	3757	684	DSC	[29]
2,6-DNT	290	3451	629	ARC	[12]

From the literature, only two kinds of calorimeters were used to test the MNT and DNT decompositions. One was Differential Screening Calorimeter (DSC) and another was Accelerating Rate Calorimeter (ARC). In the DSC tests, only few milligrams of samples were loaded into the test cells, which would provide the inaccurate results. This is because the sample size is one of the main factors will influence the detectable onset temperatures. Larger the samples sizes will have lower the onset temperature. The ARC is an adiabatic calorimeter, which is designed to measure the rate of heat release associate with a sample volume of 0.5 ml to 7 ml. Due to the relative smaller quantity of the samples, ARC also has the limitations similar to DSC. Other than DSC and ARC, there are many calorimeters who have more advanced testing mechanisms that may yield more accurate results. The Advanced Reactive Screening Tool (ARSST) and Automatic Pressure Tracking Adiabatic Calorimeter (APTAC) in the MKOPS are advanced calorimeters that have been used in this research to make comparison with the current data. The inconsistent experimental data between different researchers also reveals the dilemma of few data.

2.2 Condition dependent decompositions

2.2.1 Induction effect

Induction effect represents that for some chemicals if they are held at elevated temperatures for longer time, they may decompose at lower onset temperature. If MNT and DNT are held at elevated temperatures for a sufficient time, they may decompose at

lower temperatures. Bateman (1974) [34] performed isothermal exposure tests in a closed vessel. Keep isothermal at 150 °C, after 31 days, the decomposition reaction started. Harris (1981) [16] stated that for large quantity of 2-NT that are held between 205 °C and 215 °C, a thermal decomposition reaction will occur within 8 to 25 days. The induction time results showed a linear variation with the reciprocal of temperature in the log scale. Thermal decomposition of 2-NT has autocatalytic nature of the runaway reactions.

2.2.2 Chemical incompatibility

It is of vital importance to study how the trace of impurities may influence the thermal stability. Contamination may largely lower chemical's thermal stability and cause unexpected thermal runaway under normal operation conditions. There is evidence that trace of impurities plays a crucial role in thermal runaway behavior of the nitro aromatics in the previous studies. Multiple studies have been done, using different types of calorimeters, to demonstrate the impact that incompatible substances have on the thermal stability of nitroaromatics. Gustin (2002) [35] proved caustic soda can decrease the onset temperatures of nitromethane and 1,4-dinitrobenzene more than 200 °C. Increase proportions of pure caustic soda in nitrocumene isomer mixture will lower the onset temperature and also lower the maximum heat release rate in DTA (differential thermal analysis). Duh et al. (1997) [12] conducted DSC (differential scanning calorimetry) experiments of MNT, DNT with contaminants and found that HCl and NaOH could lower the detected onset temperature as much as 170 °C. Concentrated acids, such as sulphuric acid, nitric acid, hydrochloric acid, and chlorosulfuric acid have been shown to

significantly lower the decomposition temperature in nitrocompounds. Nitroarenes (including MNT and DNT) are extremely sensitive to acidity [36]. Acids attack the NO_2 group of the nitroaromatics. The acids can lower the activation energy to dissociate it to generate the HNO_2. Bases react with the acidic protons on nitrotoluenes forming Meisenheimer complexes [37]. Metal chlorides, such as calcium chloride, iron (III) chloride, aluminium chloride, and molybdenum(V) chloride can lower 3-nitrobenzoic acid's "onset" temperatures and peak temperatures in DTA [38] [39]. Metallic nitrates may reduce thermal stability of nitroaromatics using nitric oxidation of organics at temperature above 140 °C. (Gustin, 2002 [35], Zhu et al., 2017 [40]). Sodium carbonate was shown to lower the onset temperature of DNT thermal decomposition. (Bateman et al., 1974 [34]).

During the manufacturing process of MNT and DNT, nitric acid and sulfuric acid are added into the reactors as reactants. However, excess existence of acids may threat the safe operation of the reactors. The contaminants may lower the stability of the chemicals and trigger the side reactions to generate unwanted chemicals. This was root cause of the China National Chemical Corporation explosion in 2007. After the nitration step, nitro organic compounds are separated from the acid phase and are washed to remove the extra acids and water-soluble impurities [27]. During the washing process, alkaline substance and caustic soda are added into the system to neutralize the acids. As the result, sodium sulfate and sodium nitrate appears in the system. The large amount of water used in the washing process introduced traces of calcium chloride, sodium chloride, and sodium carbonate. Due to the corrosion of the vessels, traces of ferric oxides may also exist in the

mixture. Table 5 summarized the potential impurities exist during the manufacturing process of MNT and DNT.

Table 5. Traces of impurities exist in the MNT/DNT manufacturing process

Nitration Reaction	Washing Process
Nitric Acid (HNO_3) Sulfuric Acid (H_2SO_4) Rust (Fe_2O_3)	Caustic soda (NaOH), sodium sulfate (Na_2SO_4), sodium nitrate ($NaNO_3$), calcium chloride ($CaCl_2$), sodium chloride (NaCl), sodium carbonate (Na_2CO_3) and rust (Fe_2O_3)

After the First Chemical Explosion happened in 2002, Sachdev and Todd (2005) [30] conducted the ARC tests of 2-NT with stainless steel, wool, packing foulant and the presence of the foulant can accelerate the decomposition, thus enhancing the temperature rise. Oxley et al. (1994) [43] studied the thermal stability of ammonium nitrate and various nitro-aromatic compound mixtures in various mole ratios by using the DSC at isothermal mode in the temperature range 216-360 °C. It was revealed that ammonium nitrate destabilized the nitro-aromatic compounds and increase the rate of decomposition reactions.

2.2.3 Confined space

Confinement can impact the thermal decomposition of nitro aromatic compounds. Lee and Back (1988) [41] studied the runaway behavior of nitroguanidine in both confined and non-confined conditions. The results show that compare to the non-confined, the confined space tests have lower the "onset" temperature, higher self-heating rate, shorter the time to maximum rate is shorter, and higher rate of pressure increase. Furman et al. (2014) [42] used molecular simulated the activation energy of nitro aromatic explosives in the condensed phase using quantum chemical methods. The decomposition of condensed phase TNT is pressure dependent and higher pressure lead to faster decomposition rate. As a conclusion, confinement can significantly affect the behavior of nitroguanidine and TNT decomposition. Nikita et al. [44] studied the pressure influence on the thermal behavior of three energetic chemicals in high pressure DSC in pressures range of 0.1–14 MPa. It is revealed that the thermolysis kinetics are affected by pressure. However, few study reports the impact of confinement on MNT. Therefore, experiments to study the effect of confinement on the MNT is meaningful. This work study the effects of confinement on 2-NT decomposition using a similar method proposed by Lee and Back [41], *i.e.*, varying the N_2 initial gas pressure. Confined space is common for the storage and transportation of MNT/DNT and this work will contribute to safer process design. More works needs to be done on the checking whether confinement will impact and determining how much will impact thermal runaway of 2-NT.

2.3 Possible decomposition pathways and kinetics

The overall energy release of MNT and DNT can be divided into three stages. The first stage is called the induction phase. The temperature will increase very slowly before the observed onset temperature is reached. The second stage is called the acceleration phase. After the observed T_0 is reached, the temperature accelerates very rapidly, auto-catalysis and self-heating dominate the rate of the decomposition during the stage. The last stage is the decay phase. The temperature will slowly de-accelerate and the later stage decomposition products react.

The decomposition pathways for nitro aromatic compounds are very complex. For the MNT, decomposition mechanisms have been studied for many years by experimental or quantum chemical methods. In the review paper by Brill and James (1993) [46] the early thermal decomposition reactions of MNT/DNT have three pathways: C-NO_2 homolysis, nitro-nitrite isomerization and C-H alpha attack as shown in Figure 7. Nikolaeva et al. (2018) [47] investigated the activation energies of the five possible initial decomposition pathways of 2-NT (P1 → P2, P1 → P4, P1 → P6, P1 → P7, P1 → P8, P1 → P11) using quantum chemical methods (Figure 8). The most energetically favorable step is the formation of the 2-NT (P1 → P11) and the least favorable is the radical elimination of the –CH_3 group (P1 → P4). It is believed that the main reaction channel for 2-NT decomposition at low temperature range (300 °C to 800 °C) is the formation of anthranil and water (highlighted in red box) [48][49][50]. The MNT and DNT decomposition mechanisms in solvent has also been investigated [51].

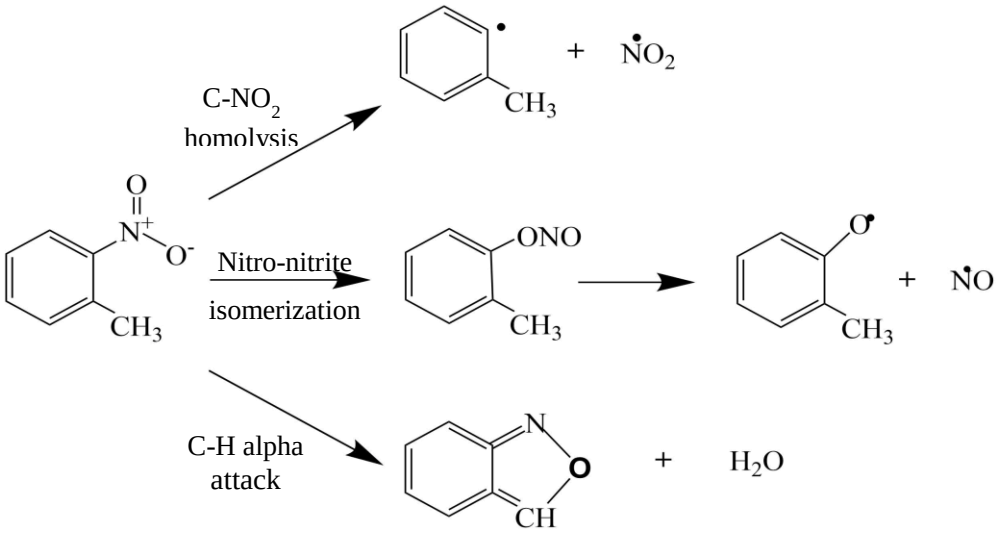

Figure 7. Three main initial decomposition pathways of MNT/DNT/TNT (2-NT as example).

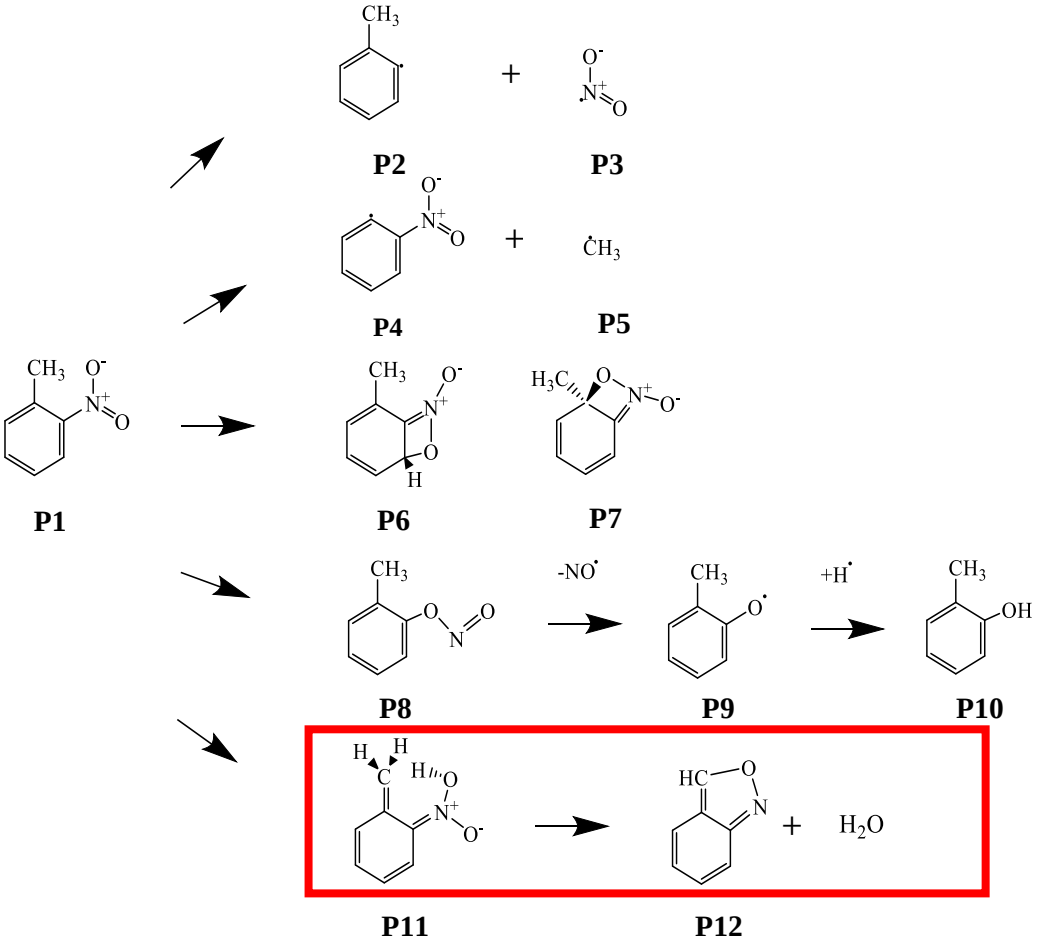

Figure 8. All possible initial decomposition pathways of 2-NT

Many researchers used laser-assisted homogeneous and shock tube to analyze the gas phase, revealing the main initial pathways for MNT and DNT: C-NO2 homolysis, nitro-nitrite isomerization and C-H alpha attack.

a. C-NO_2 homolysis

$C\text{-}NO_2$ homolysis was the dominant decomposition pathway for 2-, 3-, and 4-nitrotoluene [49][52][53]. The Arrhenius data (800-1000 °C) for $C\text{-}NO_2$ homolysis of 2-NT was summarized in Table 6 as first order reaction.

b. NO_2-ONO rearrangement

NO_2-ONO rearrangement was the dominant step presented by for 3-nitrotoluene and 4-nitrotolune rather than $C\text{-}NO_2$ homolysis found by Tsang (1986) [53]. Diez (2013) [54] proposed a subsequent decomposition stage, which removed NOH that then combined with a hydrogen radical resulting the formation of 2-cresol.

c. C-H alpha attack

Several studies proved that C-H alpha attack was primary decomposition pathway for TNT, 2,4-DNT, and 2-NT [55][56][57]. The Arrhenius Data (300-907 °C) for condensation of 2-nitrotoluene to anthranil can be found in the review paper by Brill and James (1993) [46]. The Arrhenius data (300-900 °C) for C-H alpha attack of 2-NT was summarized below in Table 6. In Figure 9, 2-Nitrotoluene is believed to react further (P12 →P16) [46]. For the later stage reactions, anthranil would degrade into 1-Cyano-2,4-cyclopentadien-1-yl by releasing CO [55]. The proposed decomposition mechanisms of anthranil is shown in Figure 8. Lifshitz et al. [58] studied the decomposition of anthranil

diluted in argon in single shock tube between 552-727 °C. Aniline (P15) and cyclopentadiene carbonitrile (P19) are the two main products as well as four other minor products (pyridine, CH_2=CHCN, HCN and CH≡C-CN). The aniline is formed in contact with traces of water.

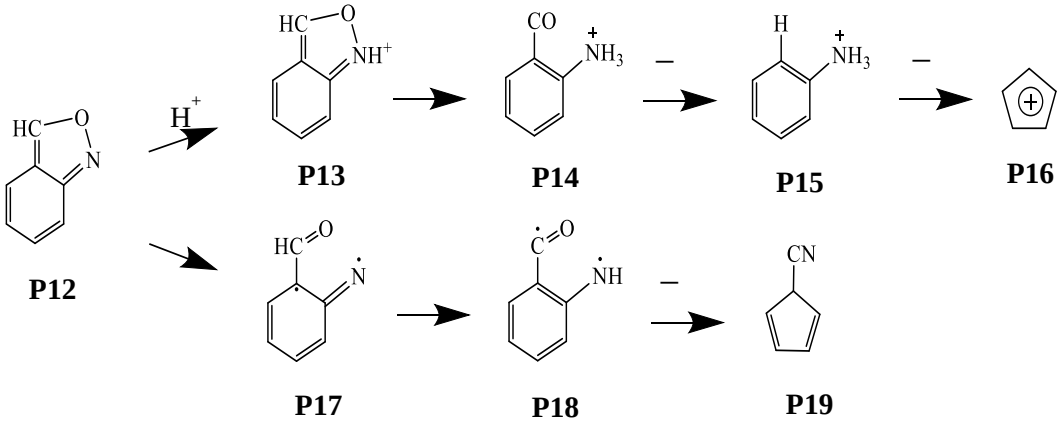

Figure 9. Proposed decomposition mechanisms of anthranil.

Table 6. Arrhenius data for decompositions of 2-Nitrotoluene

Pathway Type	T, [°C]	E_a, [kJ mol^{-1}]	A, [s^{-1}]	References
C-NO_2 Homolysis	797-907	257.19	$10^{14.84}$	[53]
	827-977	280.33 ± 9	$10^{16.4\pm0.8}$	[2]
C-H alpha Attack	300-350	177.82	$10^{10.22}$	[46]
	400-450	207.11±5	$10^{12.4\pm0.4}$	[46]
	797-907	215.60	$10^{13.08}$	[53]

Most thermal decomposition kinetic data of aromatics is obtained at relatively low temperatures (<500 °C), and the overall aromatic decomposition process in the liquid phase of is modeled by a first-order auto-catalytic reaction [59][60].

Qingsheng Wang (2009) [45] used molecular simulation to get the activation energy and adiabatic time to maximum rate for MNT and DNT based on some of the experimental data in Table 4. The kinetic data can be further used for calculation of SADT (Self-Accelerating Decomposition Temperature) and TMR_{ad} (Time to Maximum Rate).

2.4 Molecular simulations and QSPR

Ideally, real-time detection methods would be used to discover the reaction pathways. However, for MNT and DNT, the reaction acceleration stage is so fast that current measurement technology cannot capture the real time detailed information of these reactions. Because of this, simulations are often required to better understand the chemical reaction details.

Chen (1995) [61] calculated the molecular structures of three MNT isomers and their internal rotation isomers using DFT (HF/6-31G). 4-nitrotolune was found the most stable using the calculated relative energy. Fayet (2009) [49] used density functional theory (PBE0/63-31+G(d,p)) to study 2-NT and 20 of its derivatives. They discovered C-H alpha attack was the major decomposition pathway and substituents on the direct dissociation of the carbon nitrogen bond was very important. Chen (2006) [50] studied the kinetics and mechanisms for 2-NT by using DFT (level G2M (RCC, MP2)//B2LYP/6-311G(d, p)). He

revealed 10 decomposition channels of 2-NT and its six isomeric intermediates. Proposed rate expression for the 4 main pathways were also presented. Tanaka (2008) [62] employed DFT (B3LYP/6-31 G(d)) to study three possible decomposition pathways and calculated their energy barriers.

Fayet (2010) [63] used the QSPR to study 22 nitro-aromatic compounds' (including MNT and DNT) decomposition enthalpy to find correlations with their molecular properties. More than 300 descriptors were computed. Saraf (2003) [64] used transition state theory to estimate the decomposition mechanism and DFT and AM1 theory to calculate the bond dissociation energy. Fayet (2011) [65] combined the quantitative structure-property relationship (QSPR) method with DFT (PBE0/6-31+G) to predict heat of decomposition of 77 nitro-aromatic compounds (including MNT and DNT). Not like using the QSPR to predict the T_0 and heat of decomposition by Lu (2010) [66], Baati (2015) [67] combined the DSC's peaks for 20 nitro-aromatic compounds to get a global model.

3. PROBLEM STATEMENT AND OBJECTIVES

MNT is very important intermediates and products in the chemical industries and are precursors of many daily products. Historically, MNT caused many serious incidents, which have led to the severe loss of life and property. These incidents indicate the lack of comprehensive understanding of the thermal behaviors of these reactive chemicals. It is obvious that there is a gap in the literature in the thermal reactivity assessment of MNT. The primary objective was, therefore, to identify the thermal properties of these chemicals under different conditions as well as understanding the reaction mechanisms and kinetics. The thermal properties will be the basis for the design of the safe operation conditions and protection measures in case of runaway reactions. Based on the gaps identified in the literature, study should focus on the following statements.

1) Most calorimeters (DSC and ARC) tests were operated at relatively low temperature with very small quantities. Thus the results cannot precisely predict a massive MNT or DNT decomposition in a distillation tower or storage pipelines.
2) Large data variance of MNT decomposition “onset” temperatures and heat of reactions from literature. Gas generation (pressure) and self-heat rate are missing from the literature.
3) Few research used screening calorimetric ARSST or adiabatic calorimetric APTAC to study the MNT runaway reactions. More tests needed to be done by using these two advanced calorimeters to show comparison results.

4) During the manufacturing process of MNT, some contaminants may exist in the flow. Though some research work has been done using acids and bases, it is still unclear how the other contaminants will influence the thermal behaviors of MNT. Besides, for the additives that could change the "onset" temperatures of 2-NT, how the quantities of the additives will influence is still unknown.
5) The decomposition mechanisms for relatively low temperature is unclear.
6) Different opinions exist for the kinetics of 2-NT runaway reaction.
7) Induction time for 2-NT based on experimental results is unclear
8) Possible decomposition pathways that happen in the liquid phase of MNT and DNT (under high pressure).
9) Lack of data used for the relief-valve sizing design for the MNT vessels in case of fire.
10) The condition dependent factor, such as heating rate, sample sizes, thermal history and confinement effect are not clear for 2-NT decomposition.

Nitro aromatics have many family members and most of them are energetic material and releases a lot of heat in very short time. Due to the limitations of the equipment and laboratory safety requirements, this research's experimental part focus on the MNT, especially the 2-NT. This is because the 2-NT is most widely used products among the three isomers of MNT and it is more reactive than the others. Due to the similar molecular composition, the results from 2-NT can give hints to other MNT isomers as well.

There are four main objectives of the study. First, to get the thermal data of 2-NT, 3-NT and 4-NT's decomposition reactions by using the ARSST to identify most hazardous

one. Second, using DSC, ARSST and APTAC calorimetry to study the kinetics and thermal decomposition pathways. Third, to understand how different contaminants and other condition effects will influence the stability of 2-NT. Last, to generate predictive models and design protective measures for safe storage, handling and transportation of the reactive chemicals.

4. METHODOLOGY

According to the HSE Reaction hazard studies, the reactive chemical study should involve the following activities [68]:

- Preliminary reviews
- Screening tests
- Adiabatic tests
- Basis for safe operation

After identifying the gaps from the literature review, the next step is to do the screening tests. The ARSST will be employed in the research to study the pure MNT decomposition and condition dependent 2-NT's decomposition. Then, selected experiment will be performed in the adiabatic tests in APTAC based on the factorial design. Due to the sample loss during the ARSST test, more DSC tests of 2-NT are performed for the purpose of kinetic data comparison with APTAC. Thermodynamic and kinetic parameters will be estimated based on the test data (DSC and APTAC). 2-NT decomposition with different sample sizes will be performed to build up the scale-up prediction model. Basis for the safe operation, for example the SADT prediction of the 2-NT of UN 25 kg package storage, induction time and emergency relief sizing design will be studied. Figure 10 shows the diagram of the proposed research methodology.

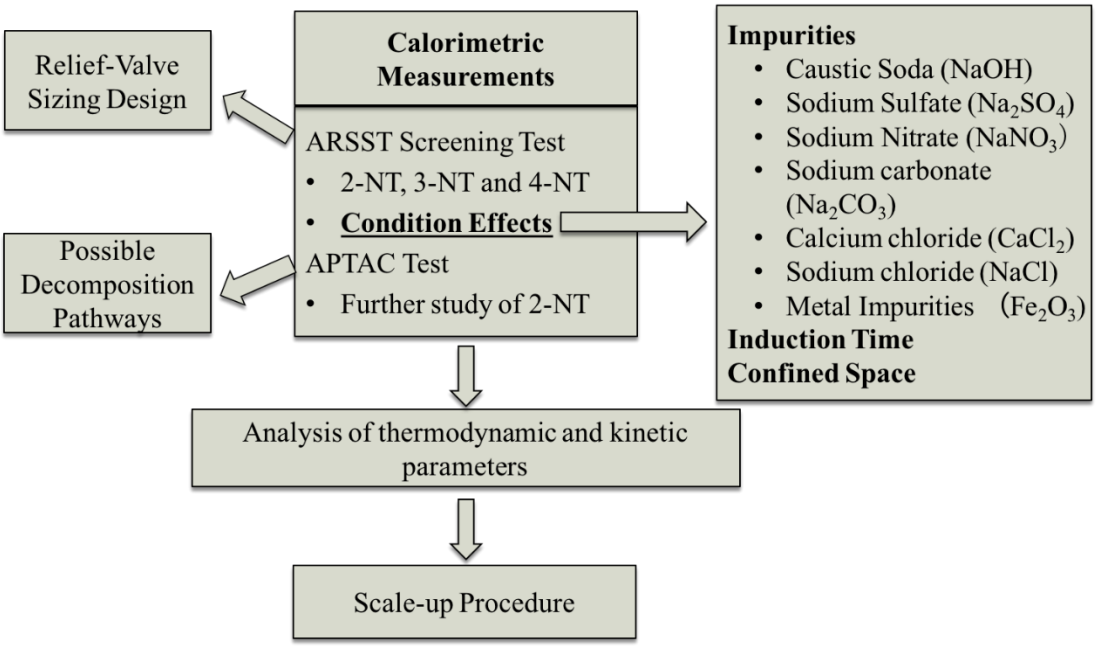

Figure 10. Research methodology for the current study.

4.1 Calorimetry measurements

In this study, calorimetry such as ARSST, DSC and APTAC will be used to study MNT. The results are compared with the other calorimetric tests results from ARC and DSC. This will help to confirm the data reliability and can be combined together with other data to study the mechanism of the 2-NT decomposition.

To analyze the reaction mechanisms of 2-NT decomposition, this research identifies data such as “onset” temperature, “onset” pressure, temperature increase rate, pressure increase rate, heat of reaction, reaction order, activation energy, and pre-exponential factor.

Section 4.2 provides detailed methods to analyze thermodynamic and kinetic parameters based on experimental results.

4.1.1 Differential Screening Calorimeter (DSC)

Differential scanning calorimetry (DSC) is a powerful thermal analysis technique that has been widely used. DSC measure heat flow variations as a function of temperature or time, which help evaluate the thermal hazards of chemicals. [69][70]. In this study, DSC measurements were conducted using Mettler Toledo HP DSC1 equipped with STARe System. HP DSC stand for High Pressure Differential Scanning Calorimetry. It is an excellent instrument for studying the influence of pressure and atmosphere on a sample or for separating an effect that is overlapped by vaporization. The HP DSC1 can measure the temperature range from ambient temperature to 700 °C in one measurement and pressure up to 10 MPa. The accuracy of the measurement is $\pm$ 0.2 K.

Additional devices include a 30 μL gold-plated stainless-steel crucible (51140405) which is capable of standing high pressure, gold-plated copper seals and a sealing tool that enables the crucible to be easily and securely sealed. Approximately 6.0 mg 2-NT was injected and sealed into the crucible. The scanning rates for the temperature-programmed ramp were chosen as 10.0, 8.0, 5.0 K min^{-1} and the examined range of temperature was 150 – 450 °C for all the test.

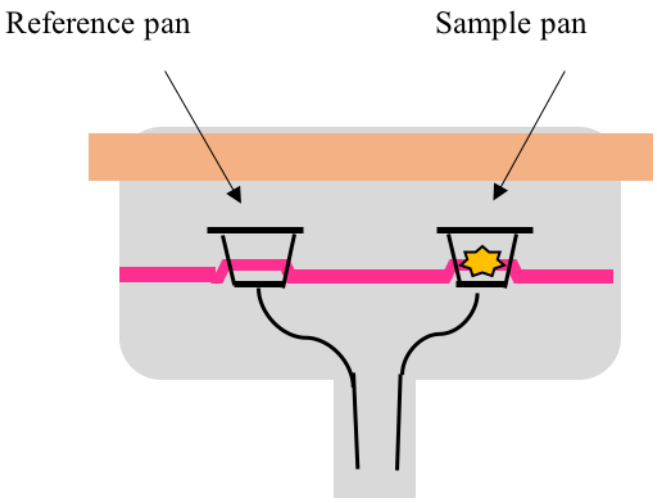

Figure 11. The simplified diagram of the DSC.

4.1.2 Advanced reactive system screening tool (ARSST)

The ARSST is a calorimeter manufactured by Fauske and Associates. It consists of three major components: containment vessel, control box, and computer. It can screen reactive chemical systems for temperatures up to 700 °C and pressures up to 3447 kPa (500 psi). The ARSST is capable of handling larger quantities of sample (approximately 1 g - 10 g) as compared to the DSC which could use only several milligrams of sample. It is a pseudo-adiabatic calorimeter, which can compensate heat losses by adding additional power generated from the electric heater. A sample is usually heated at a constant rate (0.5 °C/min to 5 °C/min). For the polynomial control mode, mathematical polynomial correlations were generated before by using pentadecane at similar initial pressures. The open glass sample cell has volume of 5, 10 ml or 15 ml. The pressure containment vessel

has volume of 350 ml. The thermal inertia factor, namely the φ-Factor (see section 4.2 for definition), can be as low as 1.04 [71][72]. Because the test cell is open to the surrounding atmosphere, vapor loss from the sample may occur. To reduce these, a "pad" pressure of an inert gas (usually nitrogen) can be applied to the containment vessel. The ARSST is recommended by the American Institute of Chemical Engineers (AIChE)'s DIERS [68]. The schematic diagram of the ARSST is shown in Figure 12.

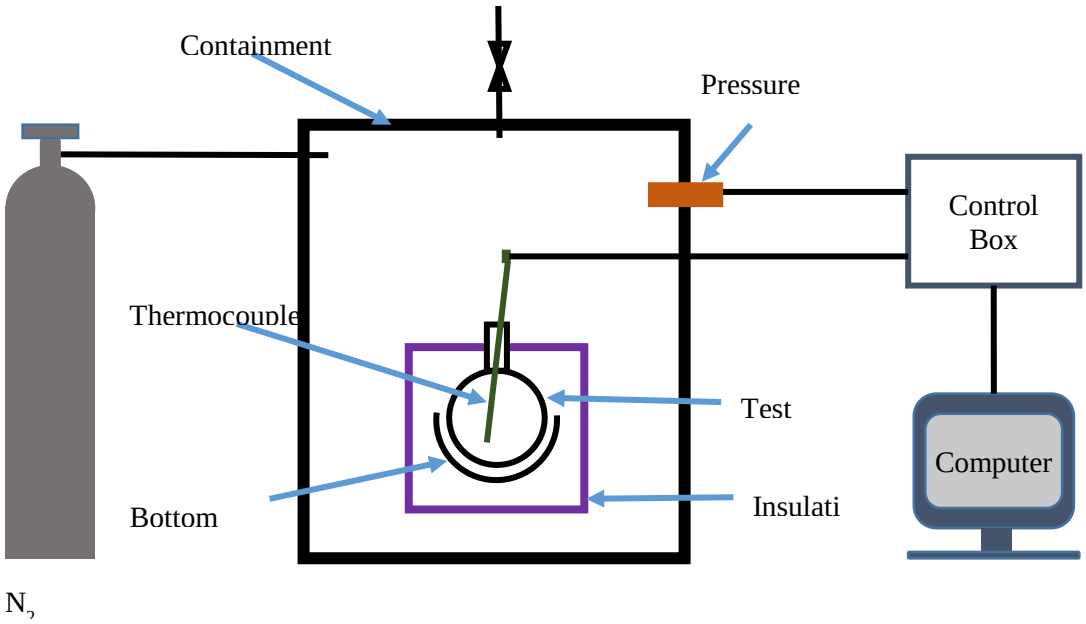

Figure 12. The simplified diagram of the ARSST.

There are seven different control modes for the ARSST [73][74] and the single ramp polynomial control is the most popular one. This method provides a constant power to the

sample over a specific temperature range and can heat the sample smoothly compared to other methods. In this study single ramp-polynomial control was used. The polynomial ramp calibration was performed using 6.5 g (5 ml) of pentadecane under a pad of nitrogen at 220 psig (1.5 MPa), with a heating rate of 4 °C min^{-1}, reaching a maximum temperature of 460 °C. During calibration, the heater operates under PID control, while after calibration the heater is then controlled by the calibration polynomials. The correlation of power input and time from this calibration is used as the baseline for all subsequent measurements reported. In a typical experiment, liquid 2-NT (0.5 ml to 2 ml) was weighed and then injected into the 10 ml glass test cell. All measurements are performed with an initial nitrogen pad pressure of 220 psig (1.5 MPa) in most cases and the calibration polynomial heating ramp is used with a heating rate of 4 $^{\circ}C\ min^{-1}$. The shutdown temperature and pressure limits selected are 460 °C and 460 psig (2.9 MPa), respectively. The ARSST computer records time, temperature(s), pressure, and heater power during a test. Live temperature, pressure, and power histories are displayed simultaneously on the graphical int erface. The heat-up rates for each experiment can differ, due to variation in heat capacity and sample volumes. As a result, samples can experience various initial heat-up ramp, even with the same calibration polynomial. When a decomposition reaction occurs, higher temperature rates are observed, while heater control maintains a constant thermal power. The heat generated by the reaction acts as an additional heating source, resulting in faster heating of the sample. It is worth noting that in this apparatus only the test cell is heated, while the containment vessel remains at ambient temperature.

The maximum data acquisition frequency of the ARSST^{TM} instrument is 500 points/second [Fauske & Associates, LLC. (2007). ARSST user manual], which may not be fast enough to capture the maximum point of the temperature and pressure during the explosive decomposition of 2-NT. Figure 13 shows the temperature profile of 2-NT decomposition reaction, it took less than 0.3 second to increase the temperature from 600 to 610 °C, and only 5 points can be detected. Due to the fast reaction rate of 2-NT decomposition, it is possible that the highest temperature rate cannot be detected. Also, there is only one thermocouple in the ARSST to detect the sample temperature and though the researcher tried to place the thermocouple at same location for all the tests, it is possible that small differences in thermocouple location impact the results because of a non-uniform temperature profile. Therefore, though the detected parameters from the tests have shown the severity of the 2-NT decomposition with additives, the reality may be even worse. To attenuate the resulting error, each 2-NT with additive test was repeated three times. The standard error of the mean was calculated, and it provides an indication of the data dispersion and precision.

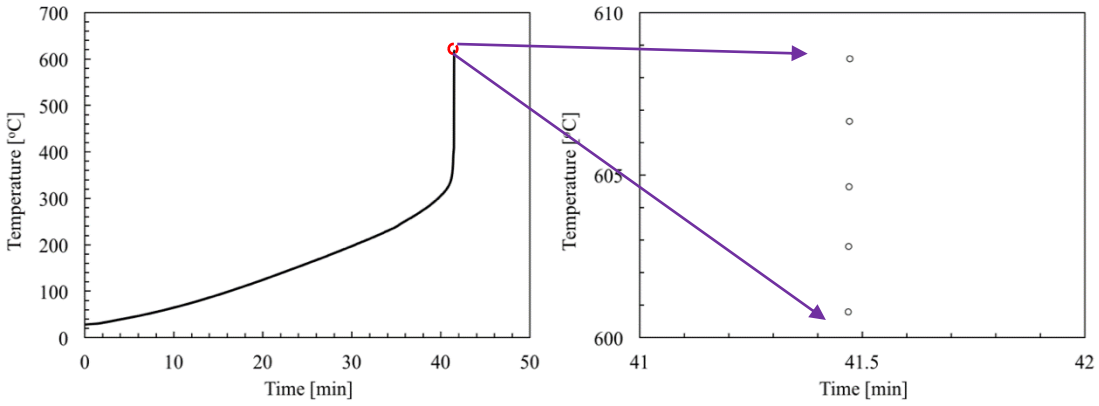

Figure 13. Temperature profile as a function of time for thermal decomposition of 2.35 g 2-NT.

4.1.3 Adiabatic calorimeter (APTAC)

The runaway behavior of 2-NT will be evaluated in the Automatic Pressure Tracking Adiabatic Calorimeter (APTAC) by Netzsch.

It is fully automated, operated by a user friendly control program. The APTAC can be operated at temperatures up to 500 °C and pressures up to 2000 psi in a batch process. During the experiment, sample is loaded to a reaction vessel and then it is placed inside a 500 ml pressure vessel. The reaction vessel is a spherical cell, which can be constructed of various materials including glass, titanium, and stainless steel. The volume of the cell varies from 10 ml, 25 ml, 50 ml to 100 ml, and in most cases the volume of 100 ml is used. For each test, the sample size is typically between 1 g and 5 g. At the bottom of the vessel, a magnetic stirrer bar is used to stir the reactants when needed. There are four main heaters and located on the bottom, top, side, and tube heaters of the pressure vessel. There are

seven Type-N thermocouples measuring the temperatures of the sample, reaction vessel walls, and nitrogen gas within the pressure vessel. The thermocouples help to monitor the temperatures and keep the temperature surrounding the sample as close as possible to that of the sample and maintaining adiabatic conditions. The pressure auto compensation mechanisms are to prevent the reaction cell from bursting due to the internal pressure build up. Nitrogen is injected into the pressure vessel at a rate of up to 20,000 psi min^{-1} to ensure the pressure differential across the wall of the reaction vessel is less than 10 psi [75].

The APTAC has four different operating modes. (1) heat-wait-search (HWS), (2) heat-ramp-search, (3) constant temperature difference ramp, and (4) isothermal. In the isothermal mode, the sample is maintained at a desired constant temperature for a certain period programmed in the software. In HWS mode, the sample is heated up in steps and the equipment is searching for an exotherm at each step. After each temperature rise to a selected point (heat), the system temperature stabilizes and stays constant temperature for 30 minutes (wait), and in the meanwhile it seeks for an exotherm (search). When an exotherm is identified, the APTAC automatically shifts to adiabatic mode and the temperature, pressure, and other variables are tracked and recorded until the reaction finishes or the shutdown criteria is met. If exothermic was not detected between the 30 minutes' window, the sample will be heat up 10 °C (this number may vary), to repeat the heat-wait-search cycle again. In a typical experiment, liquid 2-NT (0.5 ml to 2 ml) was weighed and then injected into the 100 ml or 50 ml glass cells. The shutdown temperature and pressure limits selected are 460 °C and 1078 psi (7.4 MPa), respectively. Figure 14 shows the simplified diagram of APTAC reaction vessel part.

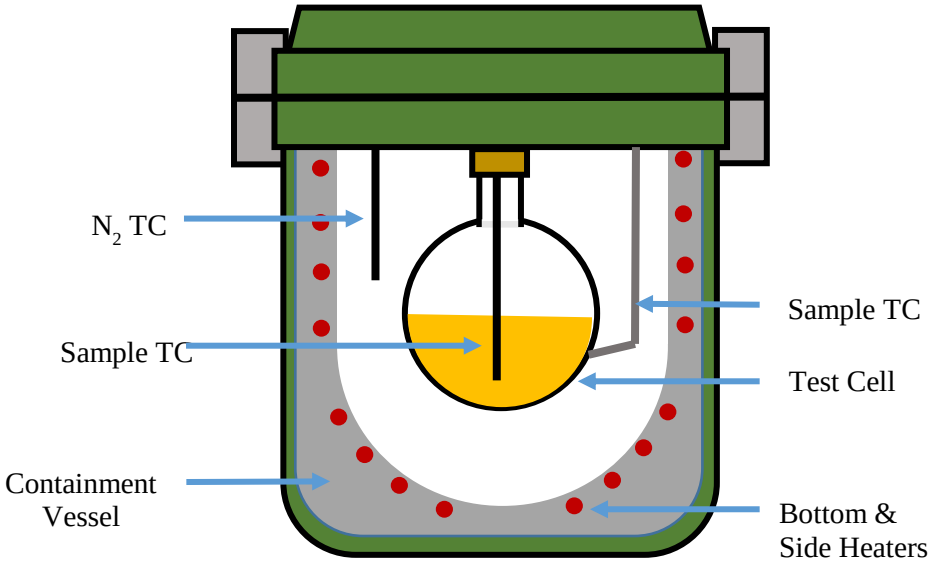

Figure 14. Simplified diagram of the APTAC (reaction vessel part).

4.2 Analysis of Thermodynamic and Kinetic Parameters

4.2.1 Thermokinetic models

In calorimeters, heating the sample cell will use a certain fraction of heat generated by heaters, which is supposed to heat up the sample. Thus, the heat measured based on the temperatures of the sample are not able to represent the heat absorbed by the sample and the cell. Moreover, during the runaway reaction, the heat released by the reaction, not only to heat up the sample, but also heat up the vessel. Therefore, a thermal inertia factor, φ, is

introduced here to correct this deviation. The thermal inertia factor, φ factor, is calculated using Equation (1) [76]:

$$\varphi = \frac{m_s C_{p,s} + m_c C_{p,c}}{m_s C_{p,s}} \qquad \text{(Eq. 1)}$$

Where φ is the PHI factor, m is the mass, and C_p is the heat capacity. The subscript s and c respectively stand for the sample and the cell (glass).

Worth noting is the common use of constant pressure heat capacity for calculating the φ factor in adiabatic calorimeters. Such systems are constant volume rather than constant pressure. In addition, the heat capacity is a function of temperature which makes the φ factor a function of temperature because the heat capacity of the sample and the heat capacity of the container don't change at the same rate or to the same extent. The differences between the constant volume and constant pressure heat capacity are expected to be small and can be estimated as:

$$C_p - C_v = \hat{V} T \frac{a^2}{b_T} \qquad \text{(Eq. 2)}$$

Typical organic liquids have a thermal expansion coefficient, a, on the order of 10^{-4} (K^{-1}), an isothermal compressibility, b, on the order of 10^{-5} (pa^{-1}) and a molar volume of the order 10^{-4} m^3 mol^{-1}. For a low molecular weight material like butane the resulting differences is approximately 6.2 J mol^{-1} K^{-1} or 0.1 J g^{-1} K^{-1} and as molecular weight increases the difference decreases. As most non-halogenated organics have heat capacities near 2 J g^{-1} K^{-1} at 25 ˚C this difference is considered small. The key benefit of a low PHI device like the ARSST is the avoidance of correcting the data for thermal inertia as the experimental data closely represent what is observed at the full scale.

The heat of reaction $-\Delta H_{rxn}$ is the heat generated per mole reacted. If it is assumed that the heat capacity C_p is not the function of temperature, then $-\Delta H_{rxn}$ can be calculated by Equation (3) [76].

$$-\Delta H_{r\times n} = \frac{m\cdot\varphi\cdot C_{p,s}\cdot(\Delta T_{ad})}{n_{r\times n}} \quad \text{(Eq. 3)}$$

In this equation, m is the sample mass, φ is the thermal inertia factor from Eqn. (1), $C_{p,s}$ is the heat capacity of the sample mass, and $n_{r\times n}$ is the moles of chemical reacted. ΔT_{ad} represents the adiabatic temperature rise, which is the difference between the final and initial temperatures over an exothermic period. For the ARSST, ΔT_{ad}=T_f – T_o – $\Delta T_{external}$. $\Delta T_{external}$ stands for the ARSST input power. The heat capacity used for 2-NT is 1.47 J g^{-1} K^{-1}[75].T_o is the observed onset temperature from the calorimetric measurements. APTAC is an adiabatic reactor, therefore $\Delta T_{external}$=0.

Performing appropriate ways of kinetic computations on thermal analysis data is important for the reactive chemicals study, since kinetics deals with measurement and parameterization of the process rates [77]. The rate is related to three parameters: the temperature, T, the extent of conversion, α, and the pressure, P as in equation (4).

$$\frac{d\alpha}{dt} = k(T)f(\alpha)h(P) \quad \text{(Eq. 4)}$$

The majority of kinetic computational methods used thermal hazard analysis ignore the pressure term $h(P)$. The rate of the reaction is a function of temperature and extent of conversion only as in equation (5):

$$\frac{d\alpha}{dt} = k(T)f(\alpha) \quad \text{(Eq. 5)}$$

However, the pressure may have impact on the kinetics of the processes, especially for the reaction including the reactants and/or products are gases. In this case, the pressure influence term can be expressed [78].

$$h(\mathrm{P}) = P^n \quad \text{(Eq. 6)}$$

Fortunately, it is possible to use the normal kinetic computational methods as equation (6) for pressure dependent reactions. the computational methods without the pressure term is still useful when two methods are applied: add much more gaseous reactant into the reaction and /or remove the reactive gaseous products in time [79].

There exist wide varieties of reaction models in the differential form, $f(\alpha)$, some of which are listed in Table 7 [80]. Most of these models were originally designed for solid state reactions so there may be limitations in interpreting kinetics of liquid phase reaction. Whereas large amounts of thermal analyses have also verified their potential application in liquid phase reactions with some difficulty in elucidating kinetics of certain reactions.

Table 7. Kinetic models recommended by ICTAC

No.	Reaction model	Brief description of kinetics	f(α)
1	Parabolic rule	one-dimensional diffusion	$1/2\alpha^{-1}$
2	Valensi function	two-dimensional diffusion	$[-\ln(1-\alpha)]^{-1}$
3	Jander function	two-dimensional diffusion, n=1/2	$4(1-\alpha)^{1/2}[1-(1-\alpha)^{1/2}]^{1/2}$
4	Jander function	two-dimensional diffusion, n=2	$(1-\alpha)^{1/2}[1-(1-\alpha)^{1/2}]^{-1}$
5	Jander function	three-dimensional diffusion, n=1/2	$6(1-\alpha)^{2/3}[1-(1-\alpha)^{1/3}]^{1/2}$
6	Jander function	three-dimensional diffusion, n=2	$3/2(1-\alpha)^{2/3}[1-(1-\alpha)^{1/3}]^{-1}$
7	Z-L-T function	three-dimensional diffusion	$3/2(1-\alpha)^{4/3}[(1-\alpha)^{-1/3}-1]^{-1}$
8	Avrami-Erofeev function	random nucleation and nucleus growth, n=1/4, m=4	$4(1-\alpha)[-\ln(1-\alpha)]^{3/4}$
9	Avrami-Erofeev function	random nucleation and nucleus growth, n=1/3, m=3	$3(1-\alpha)[-\ln(1-\alpha)]^{2/3}$
10	Avrami-Erofeev function	random nucleation and nucleus growth, n=2/5	$5/2(1-\alpha)[-\ln(1-\alpha)]^{3/5}$
11	Avrami-Erofeev function	random nucleation and nucleus growth, n=1/2, m=2	$2(1-\alpha)[-\ln(1-\alpha)]^{1/2}$
12	Avrami-Erofeev function	random nucleation and nucleus growth, n=2/3	$3/2(1-\alpha)[-\ln(1-\alpha)]^{1/3}$
13	Avrami-Erofeev function	random nucleation and nucleus growth, n=3/4	$4/3(1-\alpha)[-\ln(1-\alpha)]^{1/4}$
14	Mampel first order	random nucleation and nucleus growth, n=1, m=1	$1-\alpha$
15	Power law	continuous accelerating, n=1/4	$4\alpha^{3/4}$
16	Power law	continuous accelerating, n=1/3	$3\alpha^{2/3}$
17	Power law	continuous accelerating, n=1/2	$2\alpha^{1/2}$
18	Power law	continuous accelerating, n=3/2	$2/3\alpha^{-1/2}$
19	Reaction order	chemical reaction	$(1-\alpha)^{n}$
20	Contracting sphere	phase boundary reaction, n=1/3	$3(1-\alpha)^{2/3}$
21	Contracting cylinder	phase boundary reaction, n=1/2	$2(1-\alpha)^{1/2}$
22	S-B function	solid decomposition reaction, SB (m, n)	$\alpha^{m}(1-\alpha)^{n}$
23	J-M-A function	random nucleation and nucleus growth	$n(1-\alpha)[-\ln(1-\alpha)]^{1-1/n}$
24	Autocatalytic model	nth order reaction with autocatalysis	$(1-\alpha)^{n}(1+K_{cat}\alpha)$

In this study, multiple methods have been used and can be summarized into three categories: (a) nth order reaction, (b) autocatalytic reaction and (c) Ozawa and Kissinger's methods

(a) n^{th} order reaction

For n^{th} order reaction with a single reactant, assuming the reaction happens in a closed system with constant volume and adiabatic condition. Neglect the pressure change and the reaction rate can be expressed in equation (7) or equation (8) [76]:

$$\frac{dC}{dt} = r = -kC^n \qquad \text{(Eq. 7)}$$

$$C_0 \cdot \frac{d\alpha}{dt} = -r = k \cdot C_0^n \cdot (1-\alpha)^n \qquad \text{(Eq. 8)}$$

Where C is the concentration of the reactant at time t, k is the reaction rate constant, n is the reaction order. α is the fractional conversion, and C_0 is the reactant initial concentration.

When adiabatic, all the heat generated by the decomposition reaction will be used in the heating up of the system and will increase temperature, accelerating the rate of the reaction. However, in the meantime, the reactant concentration will decrease. Therefore, the reaction rate will decrease after reaching the maximum self-heat rate of the decomposition and will decrease to zero at T_f when the reaction finished. Assume the heat capacity C_p is independent of the temperature, then the concentration of the reactant is proportional to the temperature increase as expression below of Equation (9).

$$\alpha = \frac{T-T_0}{\Delta T_{ad}} = \frac{T-T_0}{T_f-T_0} \qquad \text{(Eq. 9)}$$

In this equation, T_o is the onset temperature of the adiabatic reaction, ΔT_{ad} is the adiabatic temperature rise, T_f is the max temperature of the adiabatic reaction.

Differentiating Equation (9) by t and then substituting into Equation (8), the following Equation (10) is obtained.

The self-heat rate $\frac{dT}{dt}$ of the adiabatic system is:

$$\frac{dT}{dt} = k \cdot \Delta T_{ad} \left(\frac{T_f - T}{\Delta T_{ad}}\right)^n \cdot C_0^{n-1} = Aexp(-\frac{E_a}{RT})\Delta T_{ad} \left(\frac{T_f - T}{\Delta T_{ad}}\right)^n \cdot C_0^{n-1} \quad \text{(Eq. 10)}$$

Rearranging Equation (10), the Equation (11) is derived:

$$k^* = k \cdot C_0^{n-1} = \frac{dT}{dt} \cdot \frac{(\Delta T_{ad})^{n-1}}{(T_f - T)^n} \quad \text{(Eq. 11)}$$

Where k^* is a pseudo zero order rate constant at temperature T.

Based on the self-heat rate $\frac{dT}{dt}$, T_f and ΔT_{ad}, k* can be obtained from calorimetry tests.

Assume relation between the kinetic rate coefficient and the temperature follows the Arrhenius equation Arrhenius equation:

$$k = A \cdot exp\left(\frac{E_a}{RT}\right) \quad \text{(Eq. 12)}$$

Where A is the constant frequency factor, E_a is the activation energy, and R is the gas constant.

Substituting Equation (12) into Equation (11), the Equation (13) is obtained.

$$\ln(k^*) = \ln(\frac{\frac{dT}{dt}}{\Delta T_{ad}\left(\frac{T_f - T}{\Delta T_{ad}}\right)^n}) = \ln(A \cdot C_0^{n-1}) - \frac{E_a}{R} \cdot \frac{1}{T} \quad \text{(Eq. 13)}$$

The plot of $\ln(k^*)$ versus 1/T yields a straight line, and the Arrhenius parameters A and E_a can be determined. The slope of the straight line is represented by E_a/R, and the intercept is determined by $\ln(A \cdot C_0^{n-1})$.

The method above is called the Townsend and Tou [76] method and can be applied for the thermokinetic study based on data from the adiabatic calorimetry. However, the following assumptions are made in this method:

A single reaction, n^{th} order kinetics; the kinetic rate coefficient and the temperature follows the Arrhenius equation; sample heat capacity is independent of temperature; and reactant conversion is in terms of the adiabatic temperature rise.

(b) Autocatalytic reaction

Autocatalytic reactions are reactions that the reaction rate expression depends on the concentration of one or more products. To simplify the model, in this study, the model is as follows,

where B is the product as well as the reactant.

$A \rightarrow B + \cdots$ initial stage

$A + B \rightleftharpoons 2\ B$ autocatalytic stage

For further simplification, assume the single-stage reactions, then the reaction model is [81]:

$$\frac{d\alpha}{dt} = k(1-\alpha)^{n_1}(\alpha^{n_2} + z) \quad \text{(Eq. 14)}$$

Where, α is the fractional conversion, n_1 and n_2 are reaction orders, and z is a constant.

（c）Ozawa and Kissinger's methods

International Confederation for Thermal Analysis and Calorimetry (ICTAC) Kinetics Committee recommendations recommends the multiple heating rate programs for computation of kinetic parameters. In the meanwhile, methods that only use a single heating rate is not appropriate [82][83]. Multi-scan methods of Kissinger and Ozawa is more suitable to be used [84]. It came from the basic kinetics of heterogeneous chemical reactions.

In the ASTM standard E698 which is the test method determining Arrhenius activation energies and pre-exponential factors using Differential Scanning Calorimetry (DSC), they use the Ozawa and Kissinger's methods. The model equations are given below.

$$E_a = \frac{R}{0.457}\frac{d(\log\beta)}{d(1/T_p)} \qquad \text{(Eq. 15)}$$

$$\frac{d(\ln\beta/{T_p}^2)}{d(1/T_p)} = -\frac{E_a}{R} \qquad \text{(Eq. 16)}$$

Where β is the heating rate (K min^{-1}) and T_p is the peak temperature of a DSC scan at that rate in Kelvin.

Calculate and construct a least square "best fit" line through these points. First plotting the curve between log β vs. $1/T_p$, log (β/T_p), log $(\beta/{T_p}^2)$ vs. $1/T_p$. Then the slope of the curve is the activation energy. The pre-exponential factor (A) is following equation 17 assuming the first order reaction:

$$\mathrm{A} = \frac{\beta\cdot E\cdot \mathrm{e}^{(-\mathrm{E}/(\mathrm{R}T_p))}}{R\times {T_p}^2} \qquad \text{(Eq. 17)}$$

4.2.2 SADT and TMR

Self-Accelerating Decomposition Temperature (SADT) is the temperature at which the heat generation rate equals the heat loss rate, under adiabatic conditions. SADT is used to determine safe storage temperature for chemicals. United Nations included the SADT in its 'Recommendations on the Transport of Dangerous Goods, Manual of Tests and Criteria' (TDG) [85]. The Globally Harmonized System (GHS) [86] uses SADT as a classification method for self-reactive substances.

When calculating SADT, it is assumed that in low temperature range (i.e., low conversion):

$$\frac{dT}{dt} = Aexp(-\frac{E_a}{RT}) \quad \text{(Eq. 18)}$$

Where A is the pre-exponential factor (°C min^{-1}) and E_a is the activation energy (kJ mol^{-1}). The values of A and E_a are calculated based on the model fitting.

Referring to the Semenov model [87] which assumes uniform temperature distribution and the heat release to the environment all happens on the surface, then the heat release rate to the environment is

$$q_L = \mathrm{US(T - T_e)} \quad \text{(Eq. 19)}$$

Where U is the heat transfer coefficient J/(s·m^2·K), S is the wetted surface area, m^2 and T_e is the ambient temperature.

Combine the Equation (18) and (19) and according to the system energy balance, then

$$mC_p \frac{dT}{dt} = \Delta H_{r\times n} m^n Aexp\left(-\frac{E_a}{RT}\right) - \mathrm{US(T - T_e)} \quad \text{(Eq. 20)}$$

When the temperature T equals to T_{NR} (T_{NR} is the temperature of no return [K], at which the rate of heat generation of a reaction or decomposition is equal to the maximum rate of cooling available [88].

$$mC_p \frac{dT}{dt} = 0 \quad \text{(Eq. 21)}$$

Therefore,

$$\Delta H_{r\times n} m^n A exp\left(-\frac{E_a}{RT_{NR}}\right) = US(T_{NR} - T_e) \quad \text{(Eq. 22)}$$

Differentiating both sides of Eq. 23 regarding T_{NR},

$$\frac{\Delta H_{r\times n} \cdot m^n E_a A exp[-E_a/(RT_{NR})]}{RT_{NR}^2} = \text{US} \quad \text{(Eq. 23)}$$

Then

$$T_{\text{SADT}} = T_{NR} - \frac{RT_{NR}^2}{E_a} \quad \text{(Eq. 24)}$$

T_{SADT} is the self-accelerating decomposition temperature, in Kelvin.

Assuming a zero order reaction, the following expression for TMR_{ad}, t_{mr} can be derived [89][76]:

$$t_{mr} = \frac{C_p \cdot R \cdot T^2}{\dot{q} \cdot E_a} \quad \text{(Eq. 25)}$$

$$t_{mr} = \frac{R \cdot T^2}{\varphi \cdot \frac{dT}{dt} \cdot E_a} \quad \text{(Eq. 26)}$$

where, t is time in min, C_p is the reactant specific heat (J kg^{-1} K^{-1}), T is temperature in K, $\dot{q}$ is the corresponding heat release rate (W kg^{-1}), dT/dt is the corresponding self-heat rate in K min^{-1}, and E_a is the activation energy (kJ mol^{-1}).

Based on adiabatic model, Eq. (27), critical temperature for 7 days or 24 hr. TMR (ADT24) can be determined:

$$T = \frac{-\frac{E_a}{R}}{\ln\left(t_{mr} \cdot A \cdot \left(-\frac{E_a}{RT}\right)\right)} \quad \text{(Eq. 27)}$$

Where, A is the pre-exponential factor (°C min^{-1}), E_a is the activation temperature (K), t_{mr} is the time to maximum rate (min).

4.2.3 Non-condensable Gas Generation (NCG)

The non-condensable gas generated from the thermal decomposition is an important parameter to obtain for the reactive chemical study. The non-condensable gas can lead the system pressure increase. The overpressure is one of the main reasons for the explosion. The Antoine equation is used during the calculation[90]. However, in terms of the overall pressure of the system, other factors play a more dominant role than the vapor pressure, such as thermal expansion and gas production. In the ARSST open system test, the initial and final pressure at the same temperature can be compared to calculate the non-condensable gas generated, following Eq. (27) (assume ideal gas):

$$\Delta n = n_{final} - n_{initial} = \frac{P_{final} \cdot V}{R \cdot T_{ambient}} - \frac{P_{initial} \cdot V}{R \cdot T_{initial}} \quad \text{(Eq. 28)}$$

where Δn is the moles of non-conde nsable gases generated, n_{final} is the final moles of non-condensable gases (initial gas + Δn); $n_{initial}$ is the moles of non-conde nsable gases at the beginning of the test; $P_{initial}$ and $T_{initial}$ are the in itial (at the beginning of the experiment) pressure and temperature, respectively, and $T_{initial}$ is the temperature at 40 °C; P_{final} is the pressure after cooling, i.e., the pressure at temperature 40 °C; V is the volume (assume 350 ml in ARSST); and R is the universal gas constant (8.314 J mol^{-1} K^{-1}).

4.2.4 Thermal Inertia Factor Correction

The definition of the thermal inertia φ factor has been introduced in the session 4.2.1. The φ factor is used to correct the fact that the heat capacity of the cell lowers the measured temperature of the reaction and increases the time maximum rate. Therefore, ΔT_{ad}, t_{mr}, the experimental values of T_o and (dT/dt) should also be corrected to φ=1 [91].

The correction method used in this work is based on the standard method and the method from Fisher in the DIERS manual [92]. The equation (29) is for the adiabatic temperature rise; the equation (30) is for the time of the reaction; the equation (31) is for the adiabatic "onset" temperature; the equation (32) is for the adiabatic temperature; the equation (33) is for the adiabatic temperature rise rate (self-heat rate).

$$\Delta T_{\text{ad,actual}} = \Delta T_{\text{ad,measured}} \cdot \varphi \quad \text{(Eq. 29)}$$

$$t_{\text{actual}} = \frac{t_{\text{measured}}}{\varphi} \quad \text{(Eq. 30)}$$

$$\frac{1}{(T_0)_{\varphi=1}} = \frac{1}{T_0} + \frac{R}{E_a} \cdot ln\varphi \quad \text{(Eq. 31)}$$

$$(\text{T})_{\varphi=1} = (T_0)_{\varphi=1} + \varphi \cdot (T - \text{T}_0) \quad \text{(Eq. 32)}$$

$$\left(\frac{dT}{dt}\right)_{\varphi=1} = \varphi \cdot exp\left[\frac{E_a}{R}\left(\frac{1}{T} - \frac{1}{(T)_{\varphi=1}}\right)\right] \cdot \left(\frac{dT}{dt}\right)_{\varphi>1} \quad \text{(Eq. 33)}$$

Where $\left(\frac{dT}{dt}\right)_{\varphi>1}$ is the experimental self-heat rate (K s^{-1})

4.3 Methods and Procedures

4.3.1. Chemicals

2-Nitrotoluene (Sigma–Aldrich, 438804, ≥99%), Sodium hydroxide (Sigma-Aldrich, 221465, ACS regent, ≥97%, pellets), Sodium Nitrate (Sigma–Aldrich, 221341, ACS reagent, ≥99%), Calcium chloride (Sigma–Aldrich, 793639, anhydrous, ≥96%), Sodium sulfate (Sigma-Aldrich, 239313, anhydrous, granular, ≥99%, ACS Reagent), Sodium chloride (Sigma-Aldrich, 746398, anhydrous, ≥99%, ACS Reagent), Sodium carbonate (Sigma-Aldrich, 791768, anhydrous, ≥99.5%, ACS Reagent), Iron(III) oxide (Sigma-Aldrich, 310050, powder, <5 μm, ≥96%) and Sodium hydroxide (Sigma-Aldrich, 795429, anhydrous, pellets, ≥97%, ACS Reagent) were used as received. Nitrogen (Praxair) was used to pressurize the containment vessel before each test.

4.3.2. Experimental Procedures

In ARSST, 2-NT with or without contaminates was loaded into the 10 ml glass test-cell. After shaking vigorously the cell for 1 minute, it was put into the 350 ml stainless-steel containment vessel for the measurement. A thermocouple was inserted inside the sample to monitor the temperature while a pressure transducer on the containment vessel was measuring the pressure during each test (open cell test). A backpressure was applied to the ARSST containment vessel by means of nitrogen in order to prevent liquid boiling, thus minimizing material loss during heating. The system was purged three times with nitrogen (set pressure at 200 psi) before each test to minimalize the amount of air present.

There are different heating modes available in ARSST; Single Ramp – Polynomial Control mode and isothermal hold are the most commonly used testing modes that used in the experiment.

In APTAC, 2-NT with or without contaminates was loaded into the 100 ml or 50 ml glass test-cell. Sample was weighted and placed into the test cell. In order to mix well, the sample was shaken for 1 minute in all directions. The Heat-Wait-Search (HWS) mode was used for all the tests. Initial pad pressure of nitrogen is in both the test cell and containment vessel. The initial heat up rate was 10 °C min^{-1} from ambient temperature to 200 °C, and the exothermic limit was 0.05 °C min^{-1}. The shutdown temperature and pressure criteria are 460 °C and 1078 psig (7.4 MPa), respectively. Once the shutdown criteria are exceeded, the heater power supply will be automatically stopped, and the system will keep recording the data until the temperature drops to the cool down temperature of 40 °C.

5. THERMAL DECOMPOSITION OF MONONITROTOLUENES*

MNT is an important family member of nitro aromatic compounds and have been widely used in the industry. However, current study for the pure MNT decomposition study is not enough to fully understand the runaway behavior and predict the potential hazardous related to MNT. This chapter focus on the MNT thermal decompositions from the fundamental point of view using both experimental and analytical analysis, to fully understand the reactive hazards related to MNT. The temperature pressure related parameters, decomposition mechanisms, thermo kinetics and safe storage and transportation criteria are discussed.

---

*Part of this section is reprinted with permission from "Effect of temperature and selected additives on the decomposition "onset" of 2-nitrotoluene using Advanced Reactive System Screening Tool." by Zhu, W., Papadaki, M. I., Han, Z., & Mashuga, C. V., 2017. *Journal of Loss Prevention in the Process Industries*, 49, 630-635, Copyright 2017 by Elsevier.

5.1 MNTs thermal decomposition in ARSST

Mononitrotoluenes (MNT) have three isomers, which are 2-NT (*ortho*-nitrotoluene), 3-NT (*meta*-nitrotoluene) and 4-NT (*para*-nitrotoluene). All the three isomers are widely used in the industry and may under thermal decomposition with external heat, shock or conditional impacted factors. No previous study use ARSST (open-cell pseudo adiabatic calorimetry) to investigate the thermal decomposition of MNTs.

In a typical experiment, 2.35 g (0.017 mole) pure sample was weighed and then loaded into the 10 ml glass test cell. At ambient temperature, 2-NT is liquid (melting point = -10.4 °C / 262.8 K)), 3-NT is liquid (melting point = -15.5 °C / 288.6 K), and 4-NT is solid (melting point = -51.63 °C / 324.78 K) [93]. 2-NT and 3-NT are loaded using pipette and 4-NT is loaded using the disposal spoons. To keep experiment consistent, no stir bar is used since the 4-NT is solid. The other tests in this study also don't have stir bar to keep initial condition are the same. All measurements are performed with an initial nitrogen pad pressure of 220 psig (1.5 MPa) and the calibration polynomial heating ramp is used with a heating rate of 5 °C min^{-1}. The shutdown temperature and pressure limits selected are 460 °C and 500 psig (3.4 MPa), respectively. Each chemical has three repeated tests to minimize the systematic errors (i.e. potential data collection failure of the maximum values in ARSST). With the time, temperature and pressure data from ARSST, 4 classic profiles (temperature vs. time, pressure vs. time, self-heat rate vs. temperature and pressure rate vs. temperature) are shown below for 2-NT, 3-NT and 4-NT. In this work, the onset temperature is calculated from the self-heat rate graph. The T_{max} is the temperature for the maximum self-heat rate. T_f is the temperature when the reaction

completes. The temperature and pressure rate data for ARSST tests has been treated by using the moving average method with a 5-point window.

5.1.1. Define the detected “onset” temperature in ARSST

In ARSST measurement, the detected “onset” temperature can be defined from either the temperature or pressure-time profile, or from the temperature or pressure rate-time profile. For this reaction the measured “onset” lies between 200 °C and 330 °C, depending on the selected method of identification. Figure 15 (a) and (b) shows the “onset” temperature defined from the temperature or pressure rate profile is around 200 °C, while if defined from the self-heating rate profile Figure 15 (c) is 310 °C. Finally, if the pressure rate profile is used, the calculated “onset” is 330 °C Figure 15(d). These differences are similar to the discrepancies reported in the literature Table 4, which are discussed further in a later section and an attempt is made to justify the deviations. Nevertheless, repeatability was good for all identically performed measurements of this study. The self-heat rate was selected as the most reliable method of the detected decomposition “onset” as will be discussed later.

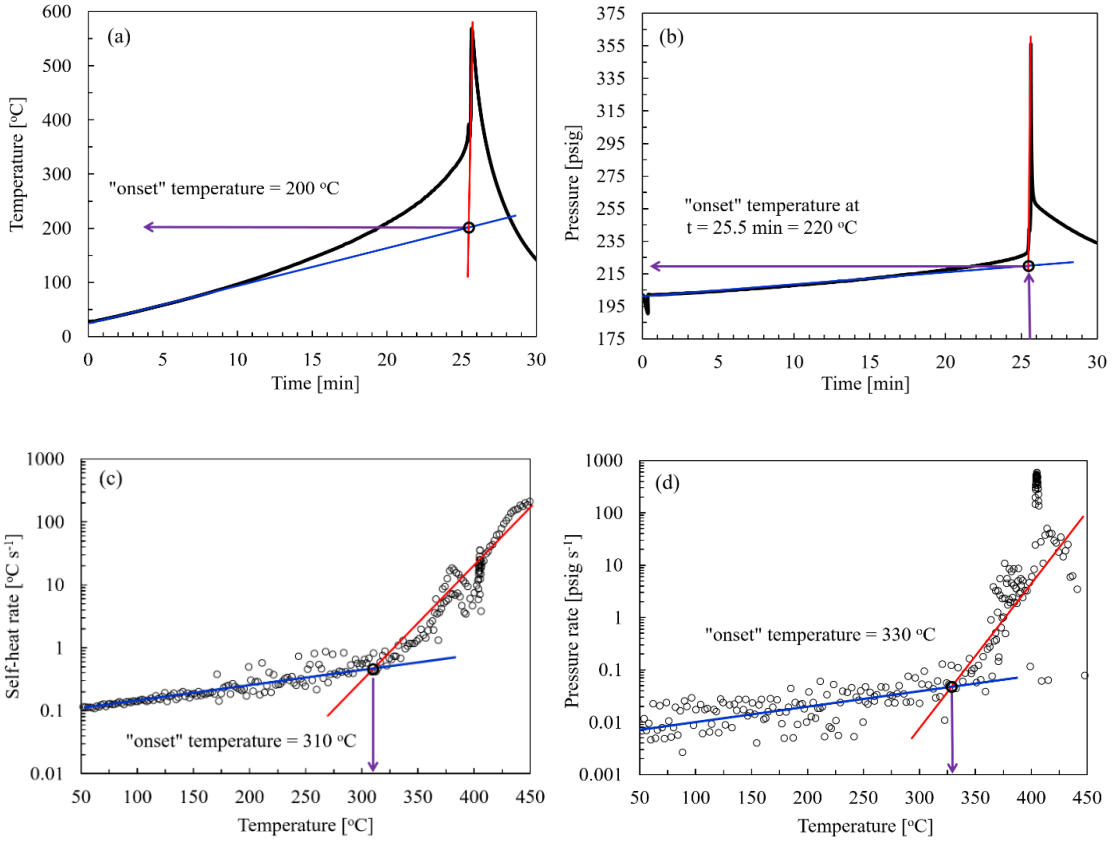

Figure 15. Thermal decomposition of 2-NT (a) “onset” temperature calculated from the temperature profile as a function of time (b) “onset” temperature calculated from the pressure profile as a function of time (c) “onset” temperature calculated from the self-heat

In this study, the onset temperature is defined from the self-heat rate profile for all the ARSST tests. Two tangents were drawn, the first one is at the self-heat rate starting point, the second one is drawn from the end of the self-heat rate.

5.1.2. 2-NT thermal decomposition in ARSST

Figure *16* (a) and (b), the graph of the temperature vs. time and pressure vs. time, for the three repeated tests, starting from the temperature at around 300 °C, both the temperature and pressure started to increase much faster. The similar trend can be told from the Figure *16* (c) and Figure 16 (d). The logarithmic plot of the self-heating rate profile and pressure-rise rate profile respectively. The exothermic reaction started very rapidly, generating gas and vapor accordingly. The key parameters are summarized in and Table *8*. For 2-NT, the observed onset temperature was 310 (±2) °C based on three duplicated tests. The maximum self-heat rate is as high as 229 (±35) °C s^{-1} and the maximum pressure rate is 5880 (±457) kPa s^{-1} for the 350 cm^3 containment vessel. T_{max} is 441 (±7) °C and T_f could be as high as 566 (±27) °C. However, the max values are still conservative since they happened after the shut-down criteria of the experiment was reached (460 °C). After 460 °C, the heater will stop heating the sample and the heat loss to the environment will be significant. The corresponding heat of reaction is 74 (±8) kJ mol^{-1} which is smaller than the DSC and APTAC tests results from the literature. This is due to the mass loss of the 2-NT in the ARSST and it is impossible to measure the ratio of the mass loss of sample in the ARSST, the heat of reaction should be larger than this value. Therefore, 2-NT decomposition can cause even more severe consequences in the adiabatic conditions.

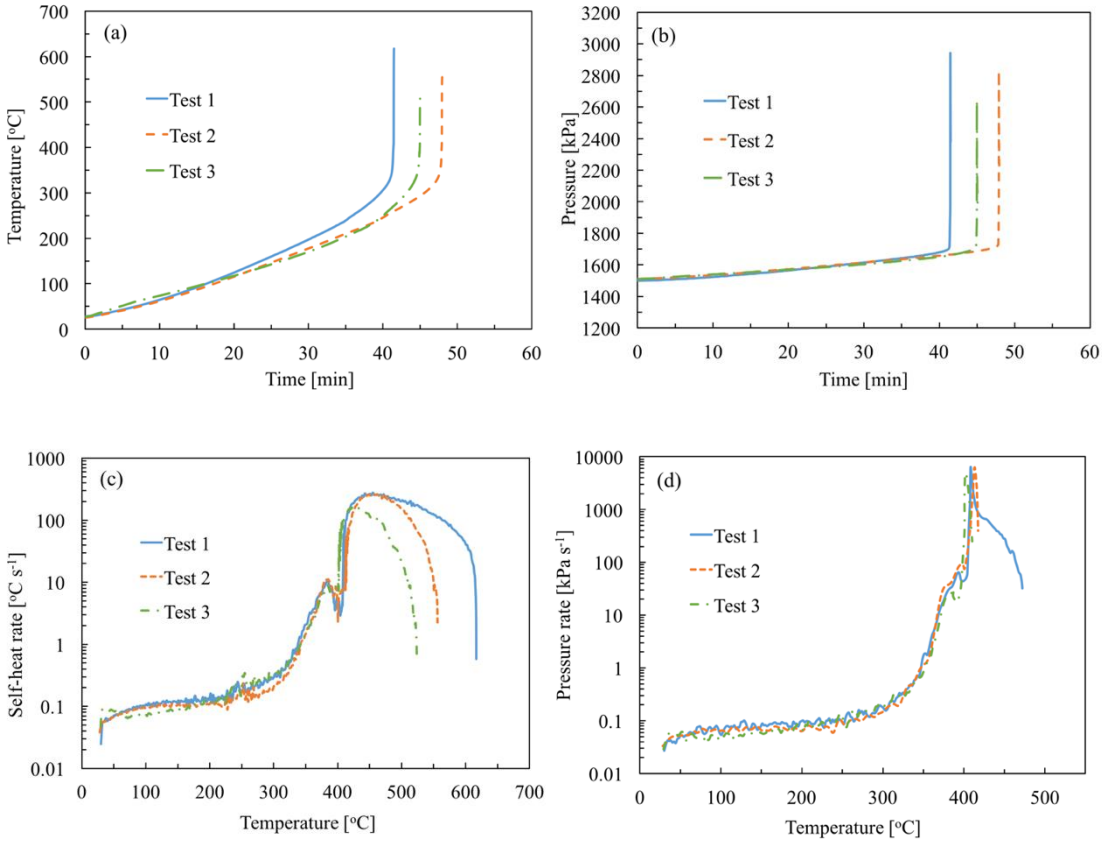

Figure 16. Thermal decomposition of 2-NT for three identical measurements (a) Temperature profile as a function of time (b) Pressure profile as a function of time (c) Self-heat rate as a function of temperature and (d) Pressure rate as a function of temperature.

Table 8. Pure 2-NT experimental data in the ARSST

Test No.	1	2	3	Avg.
T_o (°C)	313	305	311	310 (±2)
T_f (°C)	617	556	524	566 (±27)
T_f-T_o (°C)	314	251	213	256 (±26)
$(dT\ dt^{-1})_{max}$ (°C s^{-1})	262	266	160	229 (±35)
T_{max} (°C)	451	446	427	441 (±7)
$(dP\ dt^{-1})_{max}$ (kPa s^{-1})	6348	6327	4967	5880 (±457)
φ	1.44	1.42	1.44	1.42 (±0.01)
NCG (moles)	0.0190	0.0140	0.0147	0.0159 (±0.0016)
Heat of Reaction (kJ mol^{-1})	88	72	62	74 (±8)

5.1.3. 3-NT thermal decomposition in ARSST

3-nitrotoluene (3-NT) have the nitro group on the *meta* position and the initial decomposition pathways mainly are: C-NO2 homolysis and NO_2-ONO rearrangement. Similar to 2-NT, based on Figure 17 (a) and (b), the graph of the temperature vs. time and pressure vs. time, for the three repeated tests, starting from the temperature at around 300 °C, both the temperature and pressure started to increase much faster. The similar trend can be told from the Figure 17 (c) and Figure 17 (d). The logarithmic plot of the self-heating rate and pressure-rise rate. The exothermic reaction started very rapidly, generating gas and vapor accordingly. The key parameters are summarized in Table 9.

For 3-NT, the observed onset temperature was 302 (±3) °C from the three duplicated tests which is slightly lower than the onset temperature of 2-NT. The maximum self-heat

rate is as high as 228 (±4) °C s^{-1} and the maximum pressure rate is 1934 (±364) kPa s^{-1} for the 350 cm^3 containment vessel. T_{max} is 434 (±7) °C and T_f could be as high as 615 (±17) °C. However, the max values are still conservative since they happened after the shut-down criteria of the experiment was reached (460 °C). After 460 °C, the heater will stop heating the sample and the heat loss to the environment will be significant. The calculated heat of reaction is 92 (±5) kJ mol^{-1} which is smaller than the DSC and APTAC tests results from the literature. This is due to the mass loss of the 2-NT in the ARSST and it is impossible to measure the ratio of the mass loss of sample in the ARSST, the heat of reaction should be larger than this value. Therefore, 2-NT decomposition can cause even more severe consequences in the adiabatic conditions.

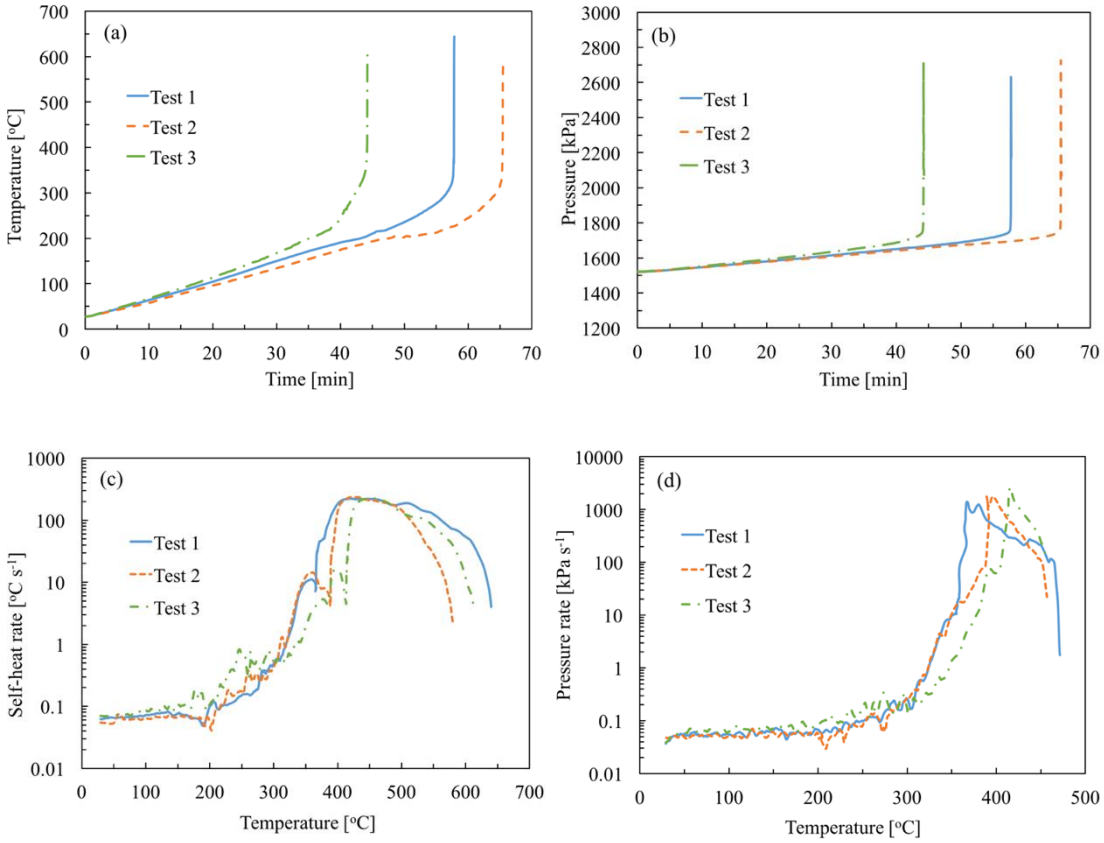

Figure 17. Thermal decomposition of 3-NT for three identical measurements (a) Temperature profile as a function of time (b) Pressure profile as a function of time (c) Self-heat rate as a function of temperature and (d) Pressure rate as a function of temperature.

Table 9. Pure 3-NT experimental data in the ARSST

Test No.	1	2	3	Avg.
T_o (°C)	299	300	307	302 (±3)
T_f (°C)	644	584	618	615 (±17)
T_f-T_o (°C)	346.00	284.00	311.00	314 (±18)
$(dT\ dt^{-1})_{max}$ (°C s^{-1})	224	235	226	228 (±4)
T_{max} (°C)	423	432	448	434 (±7)
$(dP\ dt^{-1})_{max}$ (kPa s^{-1})	1396	1777	2628	1934 (±364)
PHI Factor	1.46	1.46	1.45	1.46 (±0.01)
NCG (moles)	0.011	0.006	0.006	0.019 (±0.001)
Heat of Reaction (kJ mol^{-1})	101	83	91	92 (±5)

5.1.4. 4-NT thermal decomposition in ARSST

Based on Figure 18 (a) and (c), for all the three tests, at 50 °C, an endotherm appears where the temperature reached flat, and then it starts to increase again to the temperature where the exothermic reaction occurs. Since the melting point of 4-NT is 51 °C, and this endotherm may due to the phase change of 4-NT from solid to liquid. The key parameters are summarized in Table 10. For 4-NT, the observed onset temperature was 300 (±2) °C

with three repeated tests. The maximum self-heat rate is 239 (±49) °C s^{-1} and the maximum pressure rate is 2358 (±239) kPa s^{-1} in the 350 cm^3 containment vessel. T_{max} is 404 (±29) °C and T_f could be as high as 632 (±56) °C. For 4-NT, the max values are conservative as well since they are higher than the shut-down criteria of the experiment (460 °C).

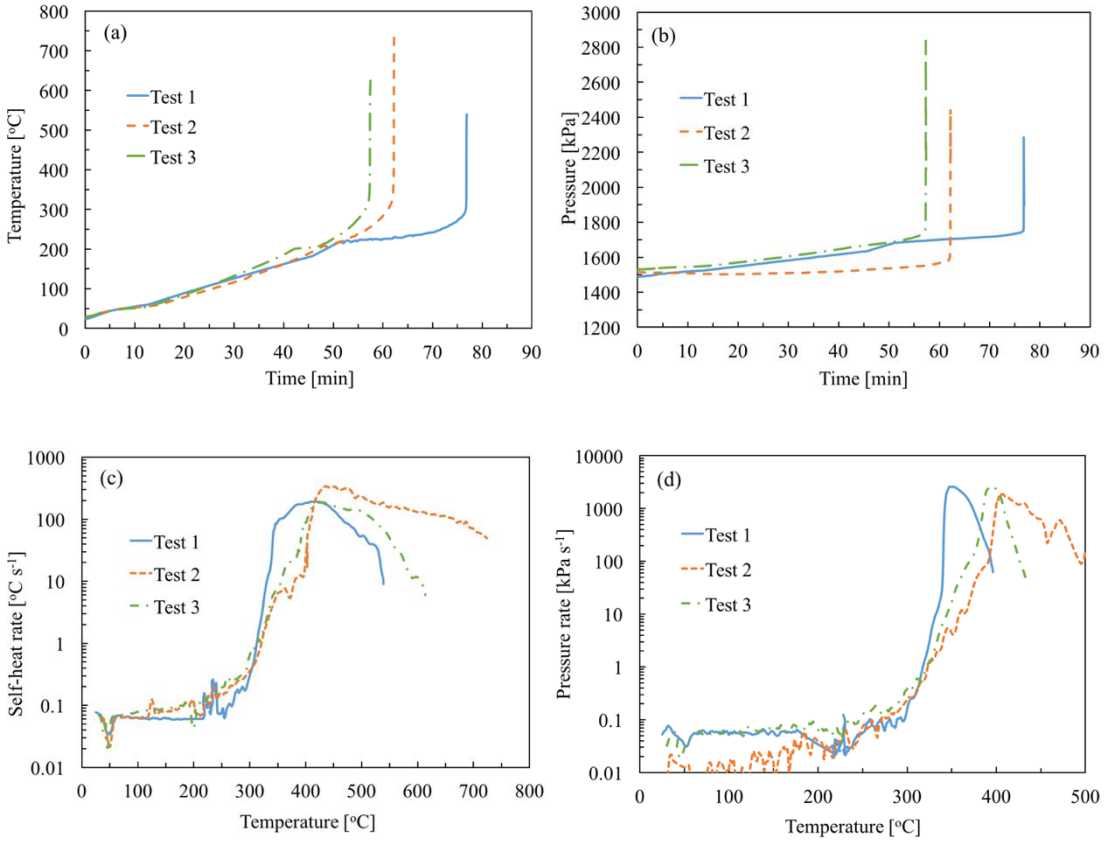

Figure 18. Thermal decomposition of 4-NT for three identical measurements (a) Temperature profile as a function of time (b) Pressure profile as a function of time (c) Self-heat rate as a function of temperature and (d) Pressure rate as a function of temperature.

Table 10. Pure 4-NT experimental data in the ARSST

Test No.	1	2	3	Avg.
T_o (°C)	295	301	303	300 (±2)
T_f (°C)	539	734	624	632 (±56)
T_f-T_o (°C)	244	433	321	335 (±53)
$(dT\ dt^{-1})_{max}$ (°C s^{-1})	192	338	188	239 (±49)
T_{max} (°C)	346	431	404	404 (±29)
$(dP\ dt^{-1})_{max}$ (kPa s^{-1})	2570	1880	2623	2358 (±239)
PHI Factor	1.40	1.40	1.45	1.42 (±0.01)
NCG (moles)	0.0096	0.0081	0.0184	0.012 (±0.003)
Heat of Reaction (kJ mol^{-1})	69	122	94	95 (±15)

5.1.5. Compare three MNT isomers thermal decomposition in ARSST

The thermal decomposition experiment of three isotherms of nitrotoluenes were conducted in ARSST. The PHI factor for the tests are similar (around 1.45) and therefore, the comparisons of three isomers thermal properties are made by using the detected data from ARSST directly without corrections. Six key performance indicators are summarized in Table 11. They are detected "onset" temperature (T_o), maximum temperature (T_f),

adiabatic temperature rise (T_f-T_o), maximum self-heating rate ($(dT\ dt^{-1})_{max}$), maximum pressure rise rate ($(dP\ dt^{-1})_{max}$), and the non-condensable gas generated (NCG).

Table 11. Comparisons between the three nitrotoluenes isomers.

Chemical	T_o (°C)	T_f (°C)	T_f-T_o (°C)	$(dT\ dt^{-1})_{max}$ (°C s^{-1})	$(dP\ dt^{-1})_{max}$ (kPa s^{-1})	NCG (moles)
2-NT	310 (±2)	566 (±27)	256 (±26)	229 (±35)	5880 (±457)	0.016 (±0.0016)
3-NT	302 (±3)	615 (±17)	314 (±18)	228 (±4)	1934 (±364)	0.019 (±0.001)
4-NT	300 (±2)	632 (±56)	335 (±53)	239 (±49)	2358 (±239)	0.012 (±0.003)

(Note: each test contains 2.35 g nitrotoluene with same initial pressure at 1517 kPa)

Among the three isomers, 4-NT has the lowest detected "onset" temperatures and the highest temperature which leads to largest adiabatic temperature rise. The definition of the adiabatic temperature rise is the temperature increase in case of adiabatic decomposition. This value represents the damage potential in case of decomposition. The differences of the adiabatic temperature rise between the three isomers are not quite different. Though there is huge discrepancy of the detected "onset" temperature in the literature, the 2-NT

has the lowest “onset” temperature among the isomers in general. Though the three isomers have similar maximum self-heat rate, the pressure rise rates are quite different. 2-NT shows the largest pressure rise rate which is three times of 3-NT and two times of 4-NT within the same container. The pressure rise rate during the runaway reaction is one of the most important indicators for the system safety evaluation. In case of the explosion of the nitroaromatic compounds in the industry, though the high temperature may lower the robust of the structure, the main reason behind the explosion is pressure. The high pressure rate not only fasten the speed of explosion to happen but also worse the incident consequences by hurting people of the blast and flying pieces of the equipment. The inconsistence of the NCG generation indirectly indicates different thermo decomposition pathways that three isomers followed. In summary, the hazardous sequences are proposed as follows:

$$\text{2-NT} > \text{4-NT} > \text{3-NT}$$

As the most thermal hazardous nitrotoluene, more studies have been conducted to further analysis the thermokinetics and the condition dependent decomposition of 2-NT in this study.

5.2 Thermokinetic analysis of 2-NT

The thermodynamic and kinetic parameters associated with 2-NT decomposition are calculated based on the equations give in Session 4.2. The Confederation for Thermal Analysis and Calorimetry (ICTAC) suggested plotting characteristic reaction profiles which describe the dependence of α or $d\alpha/dt$ on t or T under isothermal conditions, in order

to reduce various reaction models to most popular types: accelerating, decelerating, and sigmoidal. Models of accelerating type, decelerating type and sigmoidal type can be exemplified by three class of models, which are power law, reaction order and Avrami-Erofeev [82]. However, in view of the drawbacks of isothermal measurements like the difficulty in isothermal temperature selection, incompleted signal detection under high temperature and tediously long induction time when heated at low temperature [94], nonisothermal measurements were conducted to investigate the kinetc model. Different calorimeters have their own advantages and limitations. In order to better understand the thermokinetics of the 2-NT runaway reactions, three identical calorimeters have been used. They are the screening calorimetry (HP DSC), pseudo-adiabatic calorimetry (ARSST), and adiabatic calorimetry (APTAC). Furthermore, the comparison between the three popular calorimetry based on same chemical runaway reaction can help better understanding the potential limitations of the calorimetry for thermokinetic analysis which can benefit the other reactive chemicals study.

5.2.1. 2-NT thermokinetic analysis in DSC

The HP DSC was used to conduct the 2-NT non-isothermal thermal decomposition. Various amount of 2-NT was injected and sealed into the crucible. Three scanning rates for the temperature-programmed ramp were used are 10.0, 8.0, 5.0 K min^{-1}. The examine range of temperature was 150-450 °C for all the test. The tests were in nitrogen atmosphere.

Figure 19 shows decomposition of 2-NT at three selected heating rates (10.0, 8.0, 5.0 K min^{-1}) in DSC. From the result, it was found that the decomposition temperature peaks of the 2-NT shifted to higher temperatures with higher heating rate.

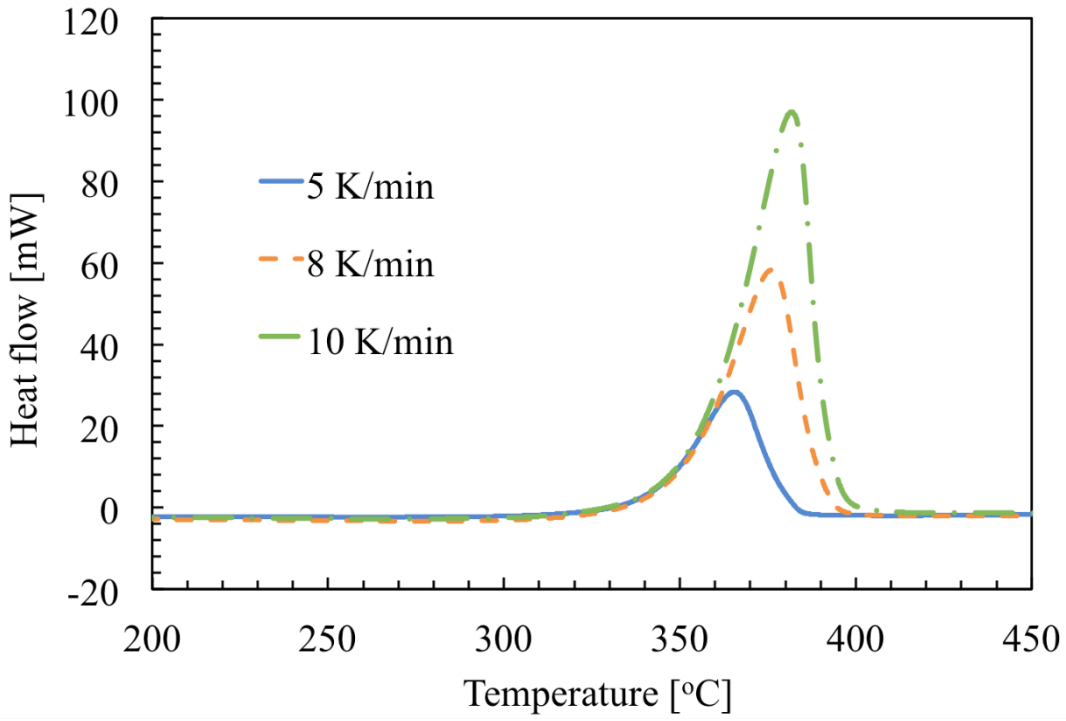

Figure 19. The effect of heating rates on decomposition of 2-NT.

Table 12 displays the exact values of significant calorimetric data derived from DSC measurements, where the average values of T_0 (apparent exothermic onset temperature), T_p (peak temperature), T_f (final temperature) and ΔH_d (heat of decomposition) are approximately 343.31 ℃, 375.27 ℃, 390.52 ℃ and -2433.54 J·g^{-1} (-333 kJ mol^{-1}). The

calorimetric data expressed in Table 12 reveal that T_o, T_p and T_f are delayed when the heating rate is higher.

Table 12. Significant calorimetric data derived from nonisothermal DSC measurements.

β / ℃·min^{-1}	mass (mg)	T_o / ℃	T_p / ℃	T_f / ℃	$-\Delta H_d$ / J·g^{-1}
10.0	6.0	336.97	366.10	383.41	2473.89
8.0	5.1	343.54	377.31	392.97	2326.09
5.0	3.7	349.41	382.41	395.18	2500.65
Avg.	5.1	343.31	375.27	390.52	2433.54

This study used the ASTM method E698 [95] to predict the Arrhenius parameters for thermal decomposition of 2-NT.

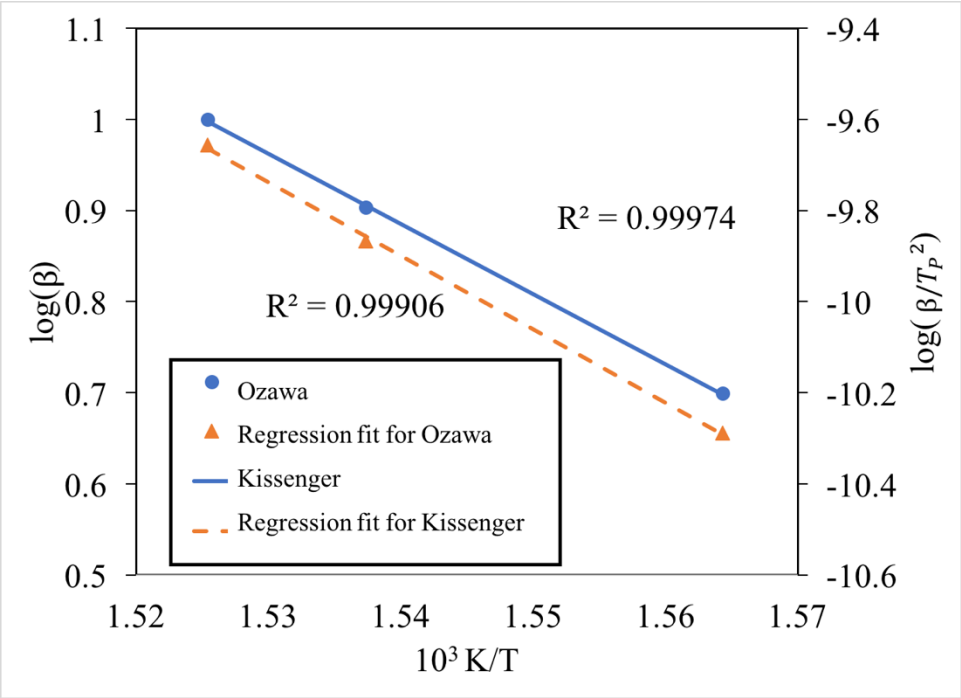

Figure 20. Arrhenius kinetic fitting using Ozawa and Kissenger methods

The plot lines of $\log \beta$ against $1/T$ and $\ln \beta/{T_p}^2$ against $1/T_p$ were straight lines. Therefore, the mechanism of thermal decomposition of this energetic material is independent with various heating rates. The original data is shown in Table 13 and Table 14. Using Ozawa's method, the calculated value of E_a is 172.481 kJ mol^{-1} and the pre-exponential constant (A) is $10^{11.68}$ s^{-1}. The coefficient of determination (R^2) is 0.999. Using Kissinger's method, the calculated value of E_a is 174.578 kJ mol^{-1} and the pre-exponential constant (A) is $10^{11.85}$ s^{-1}. The coefficient of determination (R^2) is also as high as 0.999 which shows good correlations.

Table 13. Thermokinetic parameters by Ozawa method

Heating Rate (°C min^{-1})	log(β)	(1/T)× 10^3	E_a (kJ mol^{-1})	Log (A/s^{-1})
5	0.6990	2.5542	172.481	11.72
8	0.9031	2.5389	172.481	11.67
10	1.0000	2.5305	172.481	11.65

(Note: coefficient of determination R^2 is 0.999)

Table 14. Thermokinetic parameters by Kissinger method

Heating Rate (°C min^{-1})	$\ln(\beta/T_p^2)$	(1/*T*)× 10^3	E_a (kJ mol^{-1})	Log (A/s^{-1})
5	-10.3306	2.5542	174.578	11.90
8	-9.8726	2.5389	174.578	11.84
10	-9.6561	2.5305	174.578	11.82

(Note: coefficient of determination is 0.999)

The results show very good agreement of activation energy respectively by Ozawa and Kissinger's methods. This confirms that the methods discussed here can be satisfactorily used to assess the kinetics of the 2-NT initial decomposition stage. Combine

these two methods together, average $E_a = 174$ kJ mol^{-1} and Log (A s^{-1}) is 11.77 for the 2-NT decomposition at low temperature range in DSC.

5.2.2. 2-NT thermokinetic analysis in ARSST

Unlike the DSC, ARSST is a pseudo adiabatic calorimetry with larger sample sizes. 2.35 g 2-NT were loaded into the 10 ml test cells and heated up by the polynomial control. The tests were repeated three times. For the ARSST results shown here, there are two peaks in the self-heat rate graphs. This is likely due to distinct reactions happening during the thermal decomposition process. The first reaction happens at a lower temperature and releases less heat while the second reaction happens at a higher temperature but release much more heat. The first reaction might be the C-H alpha attack and the second reaction maybe the combination of C-NO_2 homolysis and nitro-nitrite rearrangement. From the self-heat rate vs. temperature graph (Figure 21), 2-NT thermal decomposition can be divided into three phases: induction phase (T_o to 400 °C), accelerating phase (400 °C to 440 °C) and decay phase (440 °C to T_f).

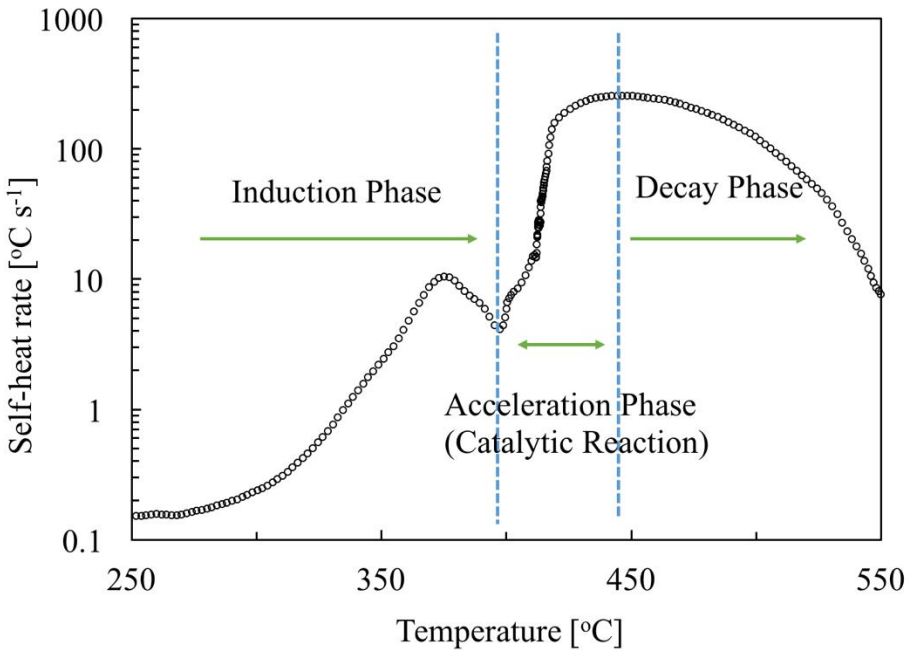

Figure 21. The energy release trace for 2-NT decomposition at a relatively low temperature.

a) Induction phase

The induction phase from T_0 to 400 °C draws great interest since it may represent the initial decomposition reaction, for 2-NT, the rate limiting step is C-H attach generate anthranil and water). To further understand the mechanisms behind, this work employ the n^{th} order reaction model by Townsend and Tou [76] to study the decomposition of pure 2-NT during the induction phase. Assuming the 2-NT decomposition reaction was a zero order reaction which was also reported by the literature [99], and the reaction occurred in a closed system with constant volume at adiabatic condition. Assume there is no pressure change during the reaction. Plot the ln(dT/dt) vs. $-\frac{1000}{T}$ for the three tests, and the slop of

the linear regression is the ($\frac{E_a}{R}$) respectvely. The Gibbs activation energy (E_a) has been calculated as summarized in Table 15.

One thing worth noting that, a lot of reactive chemical study didn't correct the φ factor during the thermokinetic study. However, the heat lost to the container vessel can take decrease the observed self-heat rate during the test and therefore may largely impact the values of the activation energy. The sensitivity analysis has been conducted by not applying the φ correction and applying the φ correction, the results are summarized in Table 15 and Figure 22. Without doing the φ correction, the detected "onset" temperature is higher and the activation energy is lower with larger deviation and smaller R^2. After applying the φ correction, the results are closer to the literature values with smaller deviation. Our study evidenced the importance of φ correction for thermokinetic study of reactive chemicals.

Table 15. Comparison of the kinetic parameters with and without φ corrections

Test No.	1	2	3	Avg.
T_o (°C)	313	305	311	311 (±2)
Corrected T_o (°C)	307	300	305	304 (±2)
E_a(kJ mol^{-1})	159	175	142	159 (±10)
R^2	0.993	0.984	0.978	0.985 (±0.004)
Corrected E_a(kJ mol^{-1})	163	177	152	164 (±7)
R^2	0.997	0.992	0.989	0.993 (0.0023)

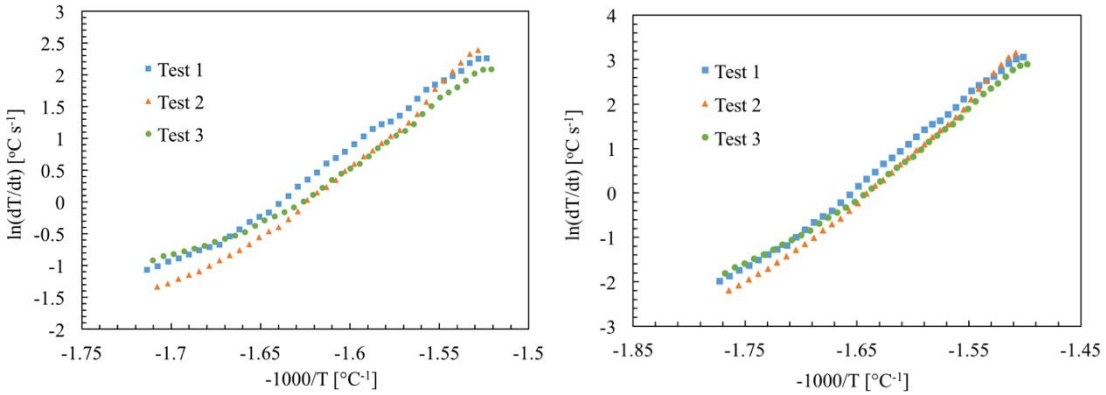

Figure 22. ln(dT/dt) vs. -1000/T for 2-NT thermal decomposition during induction phase without PHI correction (left) and with PHI correction (right) in ARSST.

All the three tests show good linear fitting (figure and the initial decomposition reactions follow the zero order reaction. The average Ea is 164 (±8) kJ mol^{-1},

b) Acceleration phase and decay phase

The acceleration phase is autocatalytic reaction with complex reaction mechanisms behind. It is not clear which autocatalytic models can accurate present the thermal behavior during this phase. In session 4.2.1, Table 7 the commonly used kinetic model suggested by the ICTAC (International Confederation for Thermal Analysis and Calorimetry) are introduced. However, aforementioned prejudgment methods can only tell the reaction model roughly, exact expressions of reaction models require more work to acquire. As long as adequate data is used into the a model-free iso-conversional methods,

the model fitting methods are apocopate to use [83]. What's more, model fitting methods have been widely used for multi-step reaction models identification, which can compensate the disadvantages of model-free methods. Activation energy E_a and pre-exponential factor A calculated with previous model-free methods can be exploited as the initial estimates for nonlinear curve fitting, which is suggested by ICTAC.

With the assumption of ignore the impact of the pressure, the rate of the reaction is a function of temperature and extent of conversion as shown in equation (4):

$$\frac{d\alpha}{dt} = k(T)f(\alpha) \quad \text{(Eq. 4)}$$

To calculate the E_a and A, it is required to first figure out the expression of $f(\alpha)$.

The alternative forms of the $f(\alpha)$ summarized from the possible models suggested by the ICTAC are listed in Table 16.

Table 16. Alternative forms of reaction model for determination of $f(\alpha)$

Number	Expression of $f(\alpha)$	Number	Expression of $f(\alpha)$
1	α^m	6	$(1-\alpha)^n[-\ln(1-\alpha)]^p$
2	$(1-\alpha)^n$	7	$(1-\alpha)^m[1-(1-\alpha)^n]^p$
3	$[-\ln(1-\alpha)]^p$	8	$(1-\alpha)^m[(1-\alpha)^n-1]^p$
4	$\alpha^m(1-\alpha)^n$	9	$n(1-\alpha)[-\ln(1-\alpha)]^{1-1/n}$
5	$\alpha^m[-\ln(1-\alpha)]^p$	10	$(1-\alpha)^n(1+k\alpha)$

The ARSST test data were simulated using the 10 models based on two fitting models (lsqcurvefit and nlinfit), however the results showed no good correlations can be achieved. This may indicate the ARSST tests data are not useful for the thermokinetics analysis due to the mass loss. Another reason probably due to the pressure influence for autocatalytic phase which current models have ignored.

5.2.3. 2-NT thermokinetic analysis in APTAC

APTAC is a powerful equipment for the decomposition reaction study under adiabatic condition. Since it is a closed cell system, and all the chemicals are maintained inside the container during the runaway reaction. It is a powerful tool to make accurate predictions for the thermokinetic and the safe operation conditions in the industry. As proved by the previous study of ARSST (session 5.1.2), there are three stages for the 2-NT decomposition. The induction phase is at low temperature range (T_o to 410 °C), the

acceleration phase and decay phase is at high temperature range (410 °C to T_f). Since there is mass loss in the ARSST test and small sample sizes used in the DSC tests, therefore, further tests were conducted in APTAC to better understand the thermo behavior and thermokinetics of 2-NT at different stages. The temperature limit of the calorimeter is 500 °C and the system cannot maintain the adiabatic scenarios. Though the reaction speed during the acceleration phase of 2-NT is quite fast, the heat loss influence to the reaction rate is negligible and it has been proved in the previous session using ARSST data. Three repeated tests have been done during the low temperature range (for induction phase) study only.

1 ml (1.2 g) 2-NT was loaded into the 100 ml glass cell and tested in the APTAC equipment with the HWS mode. The shutdown criteria were 410 °C and 1000 psi (7000 kPa), above which the system loss the adiabatic condition. The tests have been repeated for three times.

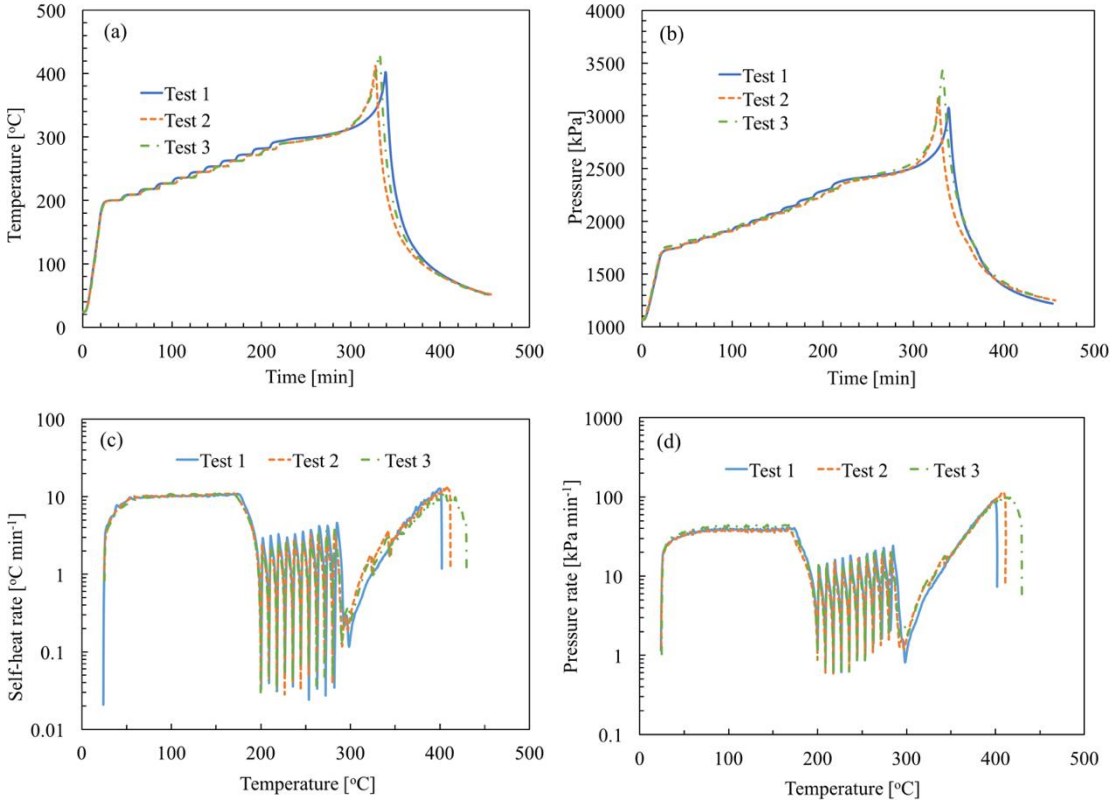

Figure 23. Thermal decomposition of 2-NT for three identical measurements in APTAC (a) Temperature vs. time (b) Pressure vs. time (c) Self-heat rate vs. temperature and (d) Pressure rate vs. temperature.

Figure 23 shows the sample was first heated up to 200 °C at the heating rate of 10 °C min^{-1}, then the HWS starts with 30 minutes waiting time for each step. When the system detected the exothermic reaction from the sample, it automatically changed to the adiabatic mode. The onset temperature detected by the APTAC is 289 (±1) with the φ factor of 20 (±0.3) as summarized in Table 17. With the high φ factor, it is required to do the corrections with the method introduced in Session 4.2.4 for the "onset" temperature,

temperature and the self-heat rate. After the φ correction, the n^{th} order reaction model [76] was employed with n=0.

Table 17. Thermal Decomposition of 2-NT in APTAC (without φ corrections)

Test No.	1	2	3	Avg.
T_o (°C)	291	288	289	289 (±1)
T_f (°C)	402	412	430	415 (±8)
T_f-T_o (°C)	111	124	141	125 (±9)
$(dT\ dt^{-1})_{max}$ (°C min^{-1})	13	14	11	13 (±1)
T_{max} (°C)	400	407	404	404 (±2)
$(dP\ dt^{-1})_{max}$ (kPa s^{-1})	92	112	99	101 (±6)
PHI Factor	29	30	30	30 (±0.3)
NCG (moles)	0.004	0.004	0.005	0.004 (±0.0002)

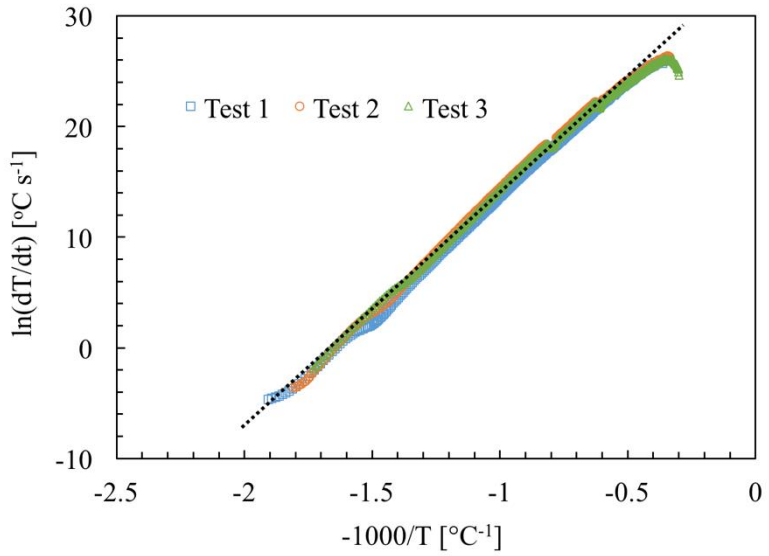

Figure 24. ln(dT/dt) vs. -1000/T for 2-NT thermal decomposition in APTAC

Table 18. Kinetic parameters for the 2-NT decomposition calculated in APTAC

Test No.	E_a (kJ mol^{-1})	Log (A/s^{-1})	R^2
1	175	11.85	0.998
2	169	11.57	0.993
3	165	11.43	0.993
Avg.	170 (±3)	11.60 (±0.1)	0.995 (±0.002)

Average $E_a = 170$ kJ mol^{-1} and Log (A s^{-1}) is 11.60 for the 2-NT decomposition at low temperature range in APTAC.

5.2.4. Discussions

Thermokinetics of 2-NT thermal decomposition during the low temperature range (induction phase) have been reported by using three different calorimetry with various amount of sample. The calculated activation energy (E_a) and log (A/s^{-1}) are similar from the DSC and APTAC with high correlation coefficient as shown in Table 19. However, the results from the ARSST shows much higher pre-exponential factor value. This is due to the nature of the equipment is open cell. During the test, sample was escaping from the test cell all the time. Therefore, the real time PHI factor increase together with the heating up rate caused by the power of the calorimetry increase. Another reason as the sample escape from the test cell, it will take away the heat, and the system is pseudo adiabatic and not fully adiabatic system. The n^{th} order reaction method by Townsend and Tou required the adiabatic system without heat loss. Therefore, the calculated kinetic parameters from the ARSST are not as reliable as the result from DSC and APTAC.

Table 19. Comparison of the thermokinetic parameters calculated by DSC, ARSST and APTAC

	DSC	ARSST	APTAC
E_a (kJ mol^{-1})	174	164	170
Log (A/s^{-1})	11.77	22.2	11.60
R^2	0.999	0.993	0.995

One interesting finding is that the calculated E_a value of 2-NT thermal decomposition at low temperature range is within the range of literature value (167-184 kJ mol^{-1})[49] of the 2-nitrotoluene condensed to anthranil and water. This study not only proved the reaction activation energy using experimental methods but also indirectly evidenced the main reaction of the 2-NT decomposition during the induction phase is the reaction:

$$C_6H_4(CH_3)(NO_2) \rightleftharpoons C_6H_4CHNO + H_2O \quad Ea = 167 - 184 \text{ kJ mol}^{-1}$$

The key parameters in the reactive chemical study are shown in Table 20. The pressure relate data is only available for the APTAC and ARSST tests. As we can see, the APTAC has lowest detected "onset" temperature, and DSC has the largest. The non-condensable gas generated per mole of 2-NT is quite different for APTAC and ARSST. This is due to the thermal kinetics are strongly depend on the temperature. The adiabatic temperature rise in ARSST is about twice the amount in APTAC, and the linear correlation between the temperature rise and NCG generation may exist.

Table 20. Comparison of thermal decomposition parameters by DSC, ARSST and APTAC

Test No.	DSC	ARSST	APTAC
2-NT Mass	4-6 mg	2.35 g	1.20 g
T_o (°C)	343	310	289
T_f (°C)	391	566	415
NCG / 2-NT (mole/mole)	N/A	0.93	0.46
Heat of Reaction (J g^{-1})	2434	693	2674

5.2.5. SADT and TMR

For a specified commercial package, the self-accelerating decomposition temperature (SADT) is the lowest ambient temperature when the chemicals can increase 6 °C less or equal to 7 days (by United Nations, 1999). It is not an intrinsic property of a reactive chemical. It is a complex system considering different factors such as influences of the ambient temperature, kinetics of reaction, size of the package and the heat transfer rates of the substance and its packaging [96]. Above the temperature of no return (T_{NR}), the rate of heat of the reaction is larger than the cooling capacity that the runaway reactions cannot be avoided.

For the UN 25 kg standard package, U= 2.83 J/(s·m^2·K), S=0.4812 m^2 [97]. Using Matlab nonlinear least-squares (lsqnonlin) function to solve the T_{NR} from Equation (24)

and further calculate the T_a using Equation (25). The calculated results of the T_{NR} and SADT for DSC and APTAC are listed in Table 21. The results for APTAC and DSC are very similar that has T_{NR} around 237 to 229 °C and the SADT temperature around 225 to 217 °C.

Table 21. TNR and SADT calculation of two types of calorimeters for UN 25 kg package

Test No.	DSC	APTAC
T_{NR} (°C)	237	229
T_{SADT} (°C)	225	217

The time to maximum rate under adiabatic conditions can be determined using the Equation (26). In other words, for an arbitrarily selected starting temperature, it can be predicted that a runaway reaction will occur assuming ideal adiabatic conditions. After solving the kinetics, the thermal stability diagram was obtained, describing the starting temperature. One important assumption is the heat capacity of 2-NT is independent of composition and temperature (1.47 J g^{-1} K^{-1}). A TMR_{ad} of 24 hr. is got for initial temperatures of 218 °C and TMR_{ad} of 7 days is reached at 196 °C. The data used for the calculations were: activation energy from the APTAC test, E_a = 170 kJ mol^{-1} with pre-exponential factor A = $10^{11.6}$ s^{-1}. The simulation of the sample temperature under adiabatic conditions at initial temperature is represented in Figure 25.

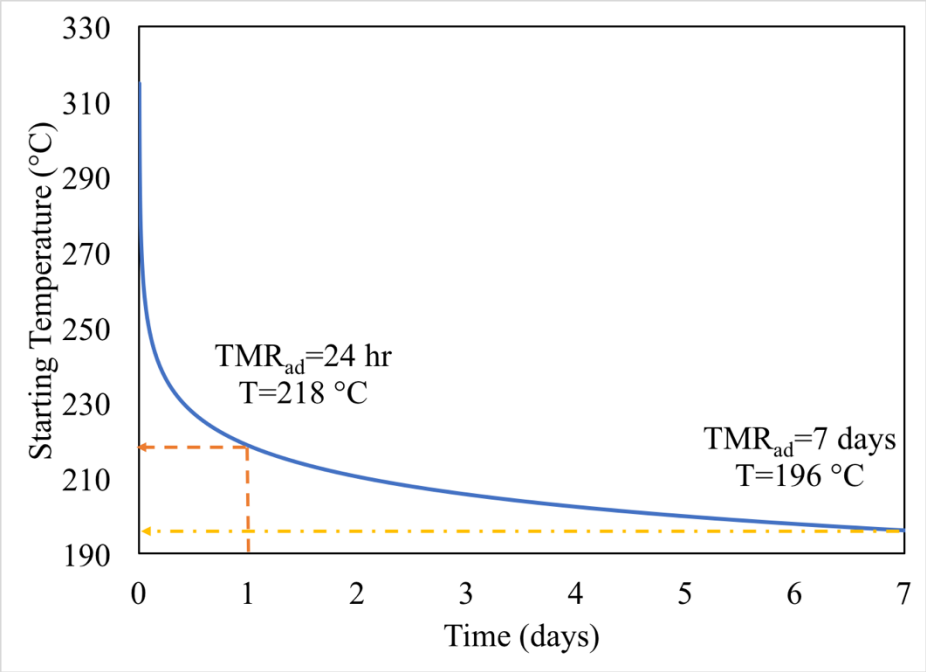

Figure 25. Thermal safety diagram of the 2-NT: dependence of adiabatic induction time TMR_{ad} on starting temperature.

5.3 Conclusions

Based on DSC, ARSST and APTAC tests of nitroaromatics under non-isothermal, pseudo adiabatic and adiabatic conditions, the following conclusions can be drawn.

1. From ARSST tests, the three isomers of nitrotoluenes (2-NT, 3-NT and 4-NT) have similar detected "onset" temperatures and the maximum self-heat rates. 2-NT has the largest pressure rise rate (twice the 4-NT's and triple the 3-NT's) which may lead much more severe consequences (more powerful explosions) than the other two isomers. The 4-NT shows largest adiabatic temperature rise indicates the energy it released is higher than the other two under the same temperature and pressure condition. The differences in the NCG for the three isomers indicates the decomposition mechanisms of the three isomers are different in the initial stage. Based on the key parameters from the experiment and the literature values, the reactive hazards among the three isomers are:

   2-NT > 4-NT > 3-NT

2. For 2-NT, a detected "onset" temperature of 289 °C was observed using APTAC calormeter. Although it is difficult to have this relative high temperature during normal operations niroatomatics. The temperature can be achieved in abnormal conditions such as ignition of unknown sources (external fire). Under such situations, the nitrotoluenes may runaway.
3. The decomposition of nitrotoluenes have three stages which are the induction phase, acceleration phase and the decay phase. The induction phase was further studied for the thermokintics using DSC, ARSST and APTAC by different models. The induction phase of the 2-NT decomposition follows the zero order reaction kinetics. The Arrhenius parameters such as activation energy (E_a) and pre-

exponential factor (A) determined emphasized the potential severe threat of the 2-NT decomposition.

4. The calculated activation energy of 2-NT (164-174 kJ mol^{-1}) at low temperature range (300 °C to 410 °C) shows agreement with the literature value of the reaction 2-nitrotoluene condensed to anthranil and water (167-184 kJ mol^{-1})[49]. Though there are multiple possible reaction pathways competing during the runaway reaction (as shown in Figure 8), the main reaction happened during the low temperature is the pathway of P1-P11-P12 which generate the water and anthranil.
5. The heat of the decomposition of the 2-NT decomposition was 2674 J g^{-1} which equivalent to 0.57 g of TNT (1 g TNT yielding 4686 J of energy) [1]. The impact of shockwave explosion and propagation during the decomposition of 2-NT decomposition under adiabatic conditions may be half that of TNT under similar circumstances. Besides, the of 2-NT decomposition was found to be less severe under pseudo adiabatic condition (693 J g^{-1}) compared to adiabatic conditions (2674 J g^{-1}).
6. For the UN 25 kg standard package, U= 2.83 J/(s·m^2·K), S=0.4812 m^2, the temperature of no return (T_{NR}) is 502 to 510 K and the self-accelerating decomposition temperature (SADT) is 490 to 498 K.
7. From the thermal safety diagram of 2-NT (induction time), TMR_{ad} of 24 hr. and TMR_{ad} of 7 days are reached for starting temperatures of 218 °C and 196 °C respectively.

6. CONDITION-DEPENDENT THERMAL DECOMPOSITION OF ORTHO-NITROTOLUENE

In order to the advance the understanding of the effect of conditions on the decomposition of 2-NT and use this knowledge to mitigate these risks to make 2-NT storage and use inherently safer, it is important to study the conditions which affect the 2-NT thermal decomposition. The conditions that were studied in this section include the presence of additives, confinement, heating rate, temperature, thermal history, and sample size. Those conditions were studied using the heating ramp mode (polynomial) in the ARSST and the HWS mode in the APTAC. The thermodynamic and kinetic parameters were analyzed, and the data were corrected based on thermal inertia factor to provide more accurate results. In addition, the ARSST isothermal mode was used to study the thermal decomposition of 2-NT. Thus, safe storage conditions for 2-NT were identified.

---

*Part of this section is reprinted with permission from "Calorimetric studies on the thermal stability of 2-nitrotoluene explosives with incompatible substances." by Zhu, W., Papadaki, M. I., Horsch, S., Krause, M., & Mashuga, C. V., 2019. *Industrial & Engineering Chemistry Research,* Copyright 2019 by American Chemical Society.

6.1 Incompatible component tests in ARSST

The possible contaminants exist during the manufacturing process of 2-NT is summarized in Table 5. After the nitration process, nitrated compounds are separated washed to remove the water-soluble impurities and acids. During the washing process, incompatible compounds such as sodium hydroxide, sodium nitrate, sodium sulphate, sodium carbonate, sodium chloride, calcium chloride, and rust (hydrated iron (III) oxide and iron (III) oxide-hydroxide) may enter in the system. More importantly, if after the washing the mixture is treated thermally (such as drying for the removal of the solvent and water or distilled for the separation of nitrotoluene isomers) or exposed to higher temperatures runaways may be unexpectedly triggered. This research work addresses the effects that sodium hydroxide, sodium sulphate, sodium carbonate, sodium chloride, calcium chloride or rust (iron (III) oxide) have on the thermal stability of 2-NT. 2-NT (2.35 g) with contaminates in a molar proportion 5:1 have been tested in ARSST. The employed contaminates were sodium hydroxide (0.15 g), calcium chloride (0.38 g), sodium sulphate (0.51 g), sodium chloride (0.20 g), sodium carbonate (0.36 g) and iron (III) oxide (0.54/ 0.27/ 0.14 g). The key performance parameters ("onset" temperature T_0, maximum temperature reached during the reaction T_f, adiabatic temperature rise ($T_f - T_0$), maximum self-heat rate $(dT/dt)_{max}$, maximum pressure rise rate $(dP/dt)_{max}$, thermal inertia factor (φ) and moles of non-condensable gas generated NCG. This work aims to compare the thermal decomposition behavior of 2-NT with contaminates at the same conditions. Since the values of PHI factors are similar for the tests, the temperature and temperature

rate data shown in this chapter are not corrected by the PHI factors. All the experiments performed in the ARSST were repeated 3 times.

6.1.1. Sodium Hydroxide

Sodium hydroxide is a strong base that can split up into metal ions and hydroxide ions in solution. Strong bases can lower the stability of the nitro aromatic compounds due to the attack to the NO2 group.

Figure 26 (a) is the temperature vs. time from where to tell the heating up rates, maximum temperature. Figure 26 (b) is the pressure vs. time, from where to get the onset pressure, maximum pressure. Figure 26 (c) is the enlarged self-heating rate vs. temperature to get the observed 'onset' temperature and Figure 26 (d) is the pressure rise rate vs. temperature. The experimental data obtained from the ARSST tests of 2-NT with NaOH are summarized in Table 22. The detected "onset" temperature of 2-NT with NaOH is 127 (±6) with PHI factor of 1.4. The pure 2-NT has the detected "onset" temperature at 310 °C (±2), but while the 2-NT mixed with NaOH, the "onset" temperature were reduced by as much as 183 °C.

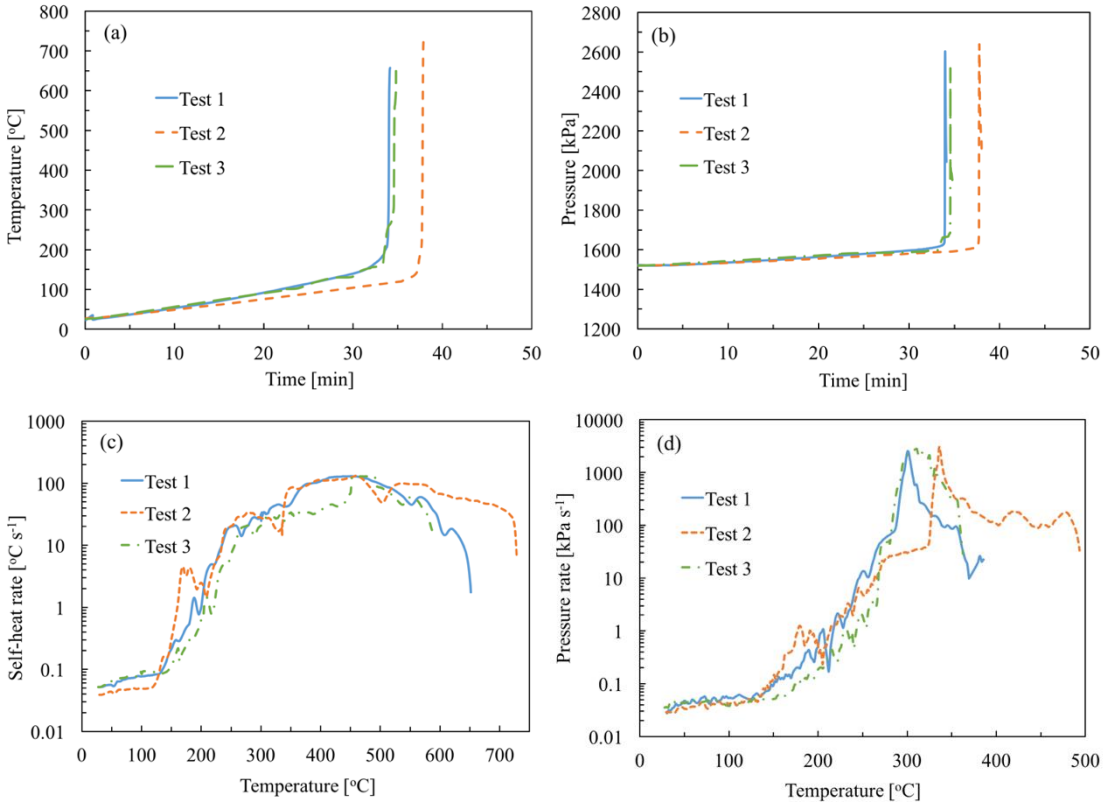

Figure 26.Thermal decomposition of 2-NT with NaOH for three identical measurements (a) Temperature profile as a function of time (b) Pressure profile as a function of time (c) Self-heat rate as a function of temperature and (d) Pressure rate as a function of temperature.

Table 22. 2.35 g 2-NT with 0.51 g NaOH thermal decomposition in ARSST

Test No.	1	2	3	Avg.
T_o (°C)	131	116	134	127 (±6)
T_f (°C)	657	733	649	680 (±27)
T_f-T_o (°C)	526	617	515	553 (±32)
$(dT\ dt^{-1})_{max}$ (°C s^{-1})	130	131	134	132 (±1)
T_{max} (°C)	450	461	480	464 (±9)
$(dP\ dt^{-1})_{max}$ (Pa s^{-1})	2544	3090	2772	2802 (±158)
PHI Factor	1.41	1.40	1.41	1.41 (±0.01)
NCG (moles)	0.026	0.026	0.025	0.026 (±0.003)
Heat of Reaction (kJ mol^{-1})	149	175	146	156 (±9)

The mechanisms of the hydroxide ion lower the "onset" temperature is the attack of strong diatomic anion OH^- on the nitro group of 2-NT and other nitro aromatics. It is generally associated with the reduction of nitrogen when the base is a reducing agent. Unlike the carboxylate ion (b), the nitro group has positive charge on the nitrogen (a). The nitro nitrogen atom is more reactive toward bases due to the positive charge [98].

(a) (b)

6.1.2. Sodium Sulfate

Sodium sulfate (Na_2SO_4) is inorganic compound that is highly soluble in water. Figure 27 shows the key parameter's graphs. The experimental data obtained from the ARSST tests of 2-NT with sodium sulfate are summarized in Table 23.

The detected "onset" temperature of 2-NT with sodium sulfate is 291 (±1) with PHI factor of 1.38. The 2-NT has the "onset" temperature at 310 °C (±2), but while the 2-NT mixed with Na_2SO_4, the "onset" temperature were slightly reduced by 19 °C.

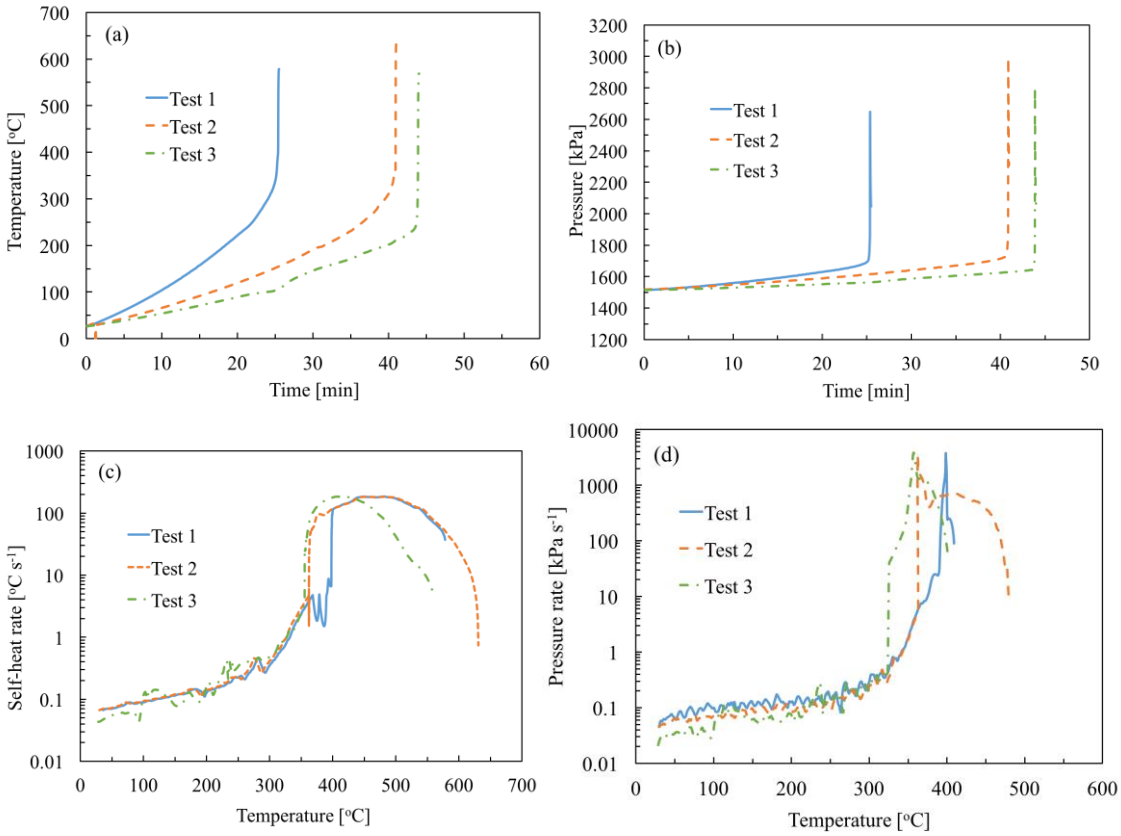

Figure 27. Thermal decomposition of 2-NT with Na_2SO_4 for three identical measurements (a) Temperature profile as a function of time (b) Pressure profile as a function of time (c) Self-heat rate as a function of temperature and (d) Pressure rate as a function of temperature.

Table 23. 2.35 g 2-NT with 0.51 g Na_2SO_4 thermal decomposition in ARSST

Test No.	1	2	3	Avg.
T_o (°C)	292	290	291	291 (±1)
T_f (°C)	576	632	570	593 (±20)
T_f-T_o (°C)	284	342	279	302 (±20)
$(dT\ dt^{-1})_{max}$ (°C s^{-1})	140	185	180	168 (±14)
T_{max} (°C)	448	484	416	449 (±20)
$(dP\ dt^{-1})_{max}$ (Pa s^{-1})	3759	3460	3807	3675 (±109)
PHI Factor	1.36	1.39	1.38	1.38 (±0.01)
NCG (moles)	0.019	0.025	0.022	0.022 (±0.002)
Heat of Reaction (kJ mol^{-1})	78	96	78	84 (±6)

6.1.3. Sodium Carbonate

Sodium carbonate (Na_2CO_3) is inorganic compound that is water soluble. Figure 28 shows the key parameter's graphs. The experimental data obtained from the ARSST tests of 2-NT with sodium sulfate are summarized in Table 24. The detected "onset" temperature of 2-NT with sodium carbonate is 277 (±6) with φ factor of 1.40. The pure 2-NT has the detected "onset" temperature at 310 °C (±2), but while the 2-NT mixed with Na_2CO_3, the "onset" temperature were slightly reduced by 33 °C.

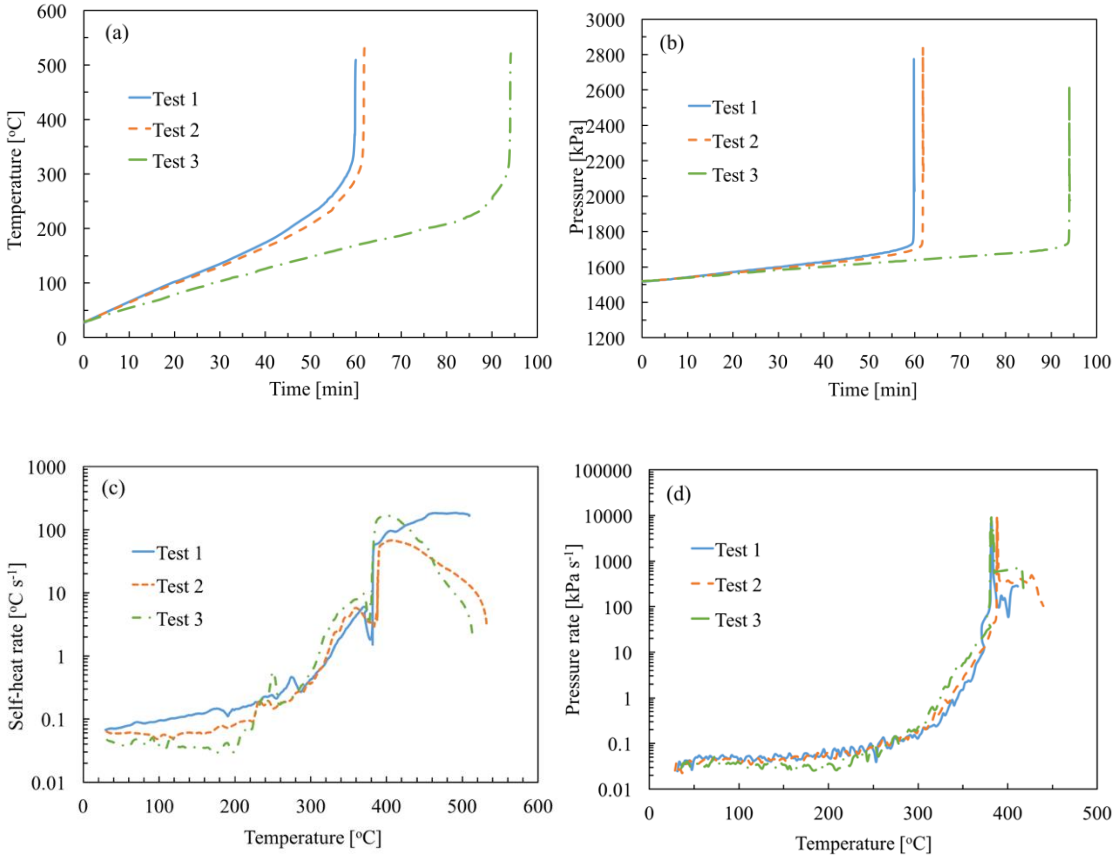

Figure 28. Thermal decomposition of 2-NT with Na_2CO_3 for three identical measurements (a) Temperature profile as a function of time (b) Pressure profile as a function of time (c) Self-heat rate as a function of temperature and (d) Pressure rate as a function of temperature.

Table 24. 2.35 g 2-NT with 0.36 g Na_2CO_3 thermal decomposition in ARSST

Test No.	1	2	3	Avg.
T_o (°C)	290	270	272	277 (±6)
T_f (°C)	509	532	521	521 (±7)
T_f-T_o (°C)	219	262	249	243 (±13)
$(dT\ dt^{-1})_{max}$ (°C s^{-1})	185	166	170	174 (±6)
T_{max} (°C)	490	406	399	432 (±29)
$(dP\ dt^{-1})_{max}$ (Pa s^{-1})	3461	4009	4264	3911 (±237)
PHI Factor	1.40	1.40	1.39	1.40 (±0.01)
NCG (moles)	0.021	0.026	0.017	0.021 (±0.003)
Heat of Reaction ($kJ\ mol^{-1}$)	62	74	70	68 (±4)

6.1.4. Sodium Chloride

Sodium chloride (NaCl) is ionic compounds that is water soluble. Figure 29 shows the key parameter's graphs. The experimental data obtained from the ARSST tests of 2-NT with sodium chloride are summarized in Table 25. The calculated "onset" temperature of 2-NT with sodium sulfate is 305 (±3) with PHI factor of 1.40. The pure 2-NT has the detected "onset" temperature at 310 °C (±2), but when the 2-NT mixed with NaCl, the "onset" temperature does not change much.

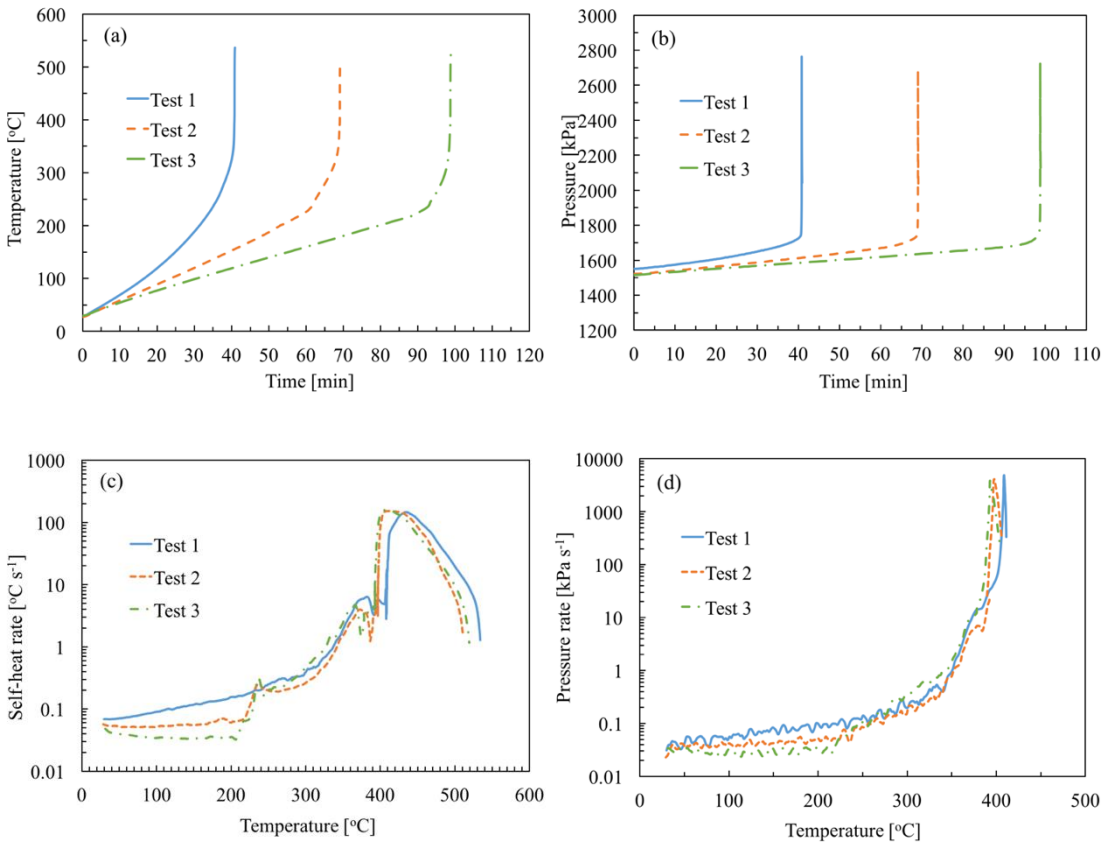

Figure 29. Thermal decomposition of 2-NT with NaCl for three identical measurements (a) Temperature profile as a function of time (b) Pressure profile as a function of time (c) Self-heat rate as a function of temperature and (d) Pressure rate as a function of temperature.

Table 25. 2.35 g 2-NT with 0.20 g NaCl thermal decomposition in ARSST

Test No.	1	2	3	Avg.
T_o (°C)	311	303	300	305 (±3)
T_f (°C)	537	515	523	525 (±6)
T_f-T_o (°C)	226	212	223	220 (±4)
$(dT\ dt^{-1})_{max}$ (°C s^{-1})	147	152	161	153 (±4)
T_{max} (°C)	410	412	409	410 (±1)
$(dP\ dt^{-1})_{max}$ (Pa s^{-1})	4847	4133	3811	4264 (±306)
PHI Factor	1.39	1.41	1.40	1.40 (±0.01)
NCG (moles)	0.016	0.018	0.021	0.018 (±0.001)
Heat of Reaction (kJ mol^{-1})	62	60	63	62 (±1)

6.1.5. Calcium Chloride

Calcium chloride ($CaCl_2$) is an inorganic compound that highly water soluble. Figure 30 shows the key parameter's graphs. The experimental data obtained from the ARSST tests of 2-NT with calcium chloride are summarized in Table 26. The detected "onset" temperature of 2-NT with sodium sulfate is 276 (±5) with PHI factor of 1.42. The pure 2-NT has the "onset" temperature at 310 °C (±2), but while the 2-NT mixed with $CaCl_2$, the "onset" temperature decreased as much as 34 °C.

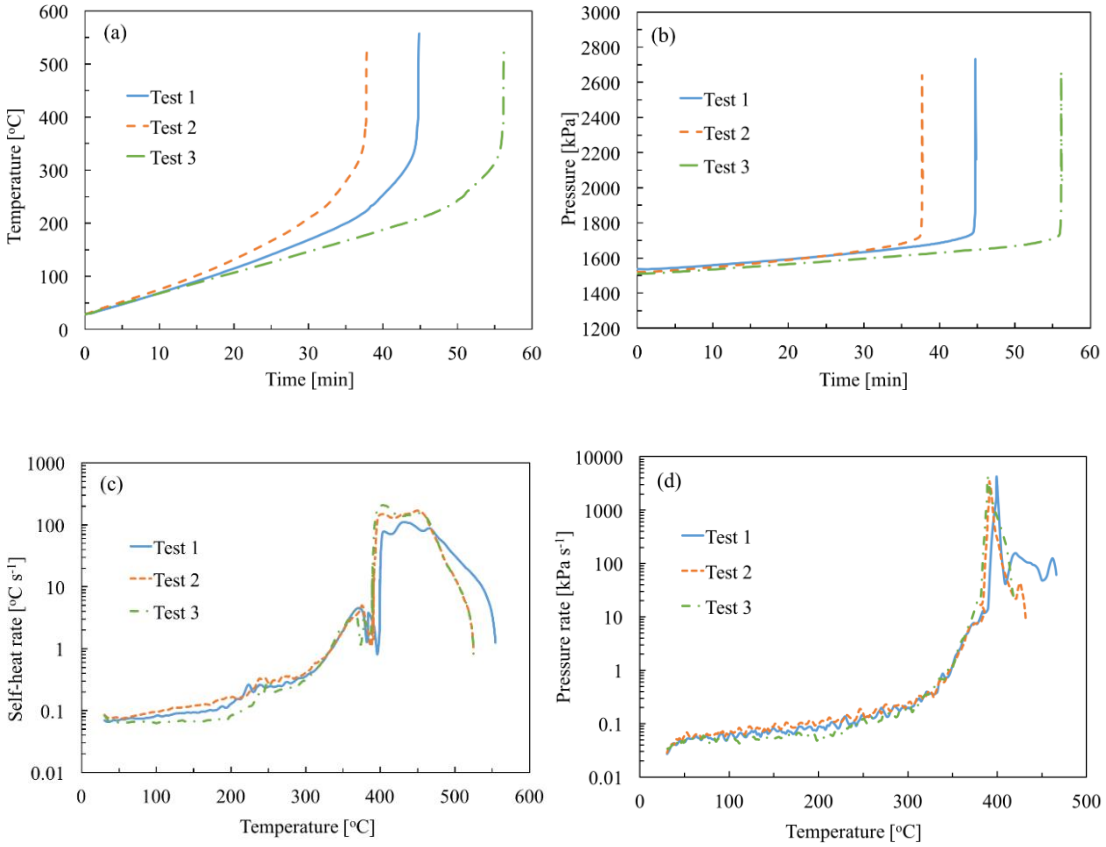

Figure 30. Thermal decomposition of 2-NT with $CaCl_2$ for three identical measurements (a) Temperature profile as a function of time (b) Pressure profile as a function of time (c) Self-heat rate as a function of temperature and (d) Pressure rate as a function of temperature.

Table 26. 2.35 g 2-NT with 0.38 $CaCl_2$ thermal decomposition in ARSST

Test No.	1	2	3	Avg.
T_o (°C)	272	285	271	276 (±5)
T_f (°C)	557	528	527	537 (±10)
T_f-T_o (°C)	285	243	256	261 (±12)
$(dT\ dt^{-1})_{max}$ (°C s^{-1})	151	168	208	176 (±17)
T_{max} (°C)	432	450	404	429 (±13)
$(dP\ dt^{-1})_{max}$ (Pa s^{-1})	4262	3437	4159	3953 (±260)
PHI Factor	1.42	1.42	1.43	1.42 (±0.01)
NCG (moles)	0.022	0.018	0.018	0.019 (±0.001)
Heat of Reaction (kJ mol^{-1})	81	70	74	75 (±3)

6.1.6. Hazard analysis by ARSSTTM for 2-NT with various amounts of iron (III) oxide

Owing to the increased complexity in hazard evaluation of 2-NT contaminated with iron (III) oxide more tests were conducted to understand its influence on the thermal decomposition severity. The study involved experiments with three different mole ratios of the iron (III) oxide in 2-NT. More precisely mole ratios 20:1, 10:1 and 5:1 were performed. Each test was repeated three times.

a) Mole ratio of 2-NT and iron (III) oxide (5:1)

2.35 g 2-NT with 0.54 g iron oxide (III) thermal decomposition were tested three times in ARSST. Figure 31 shows the key parameter's graphs. The experimental data obtained from the ARSST tests of 2-NT with calcium chloride are summarized in Table 27.

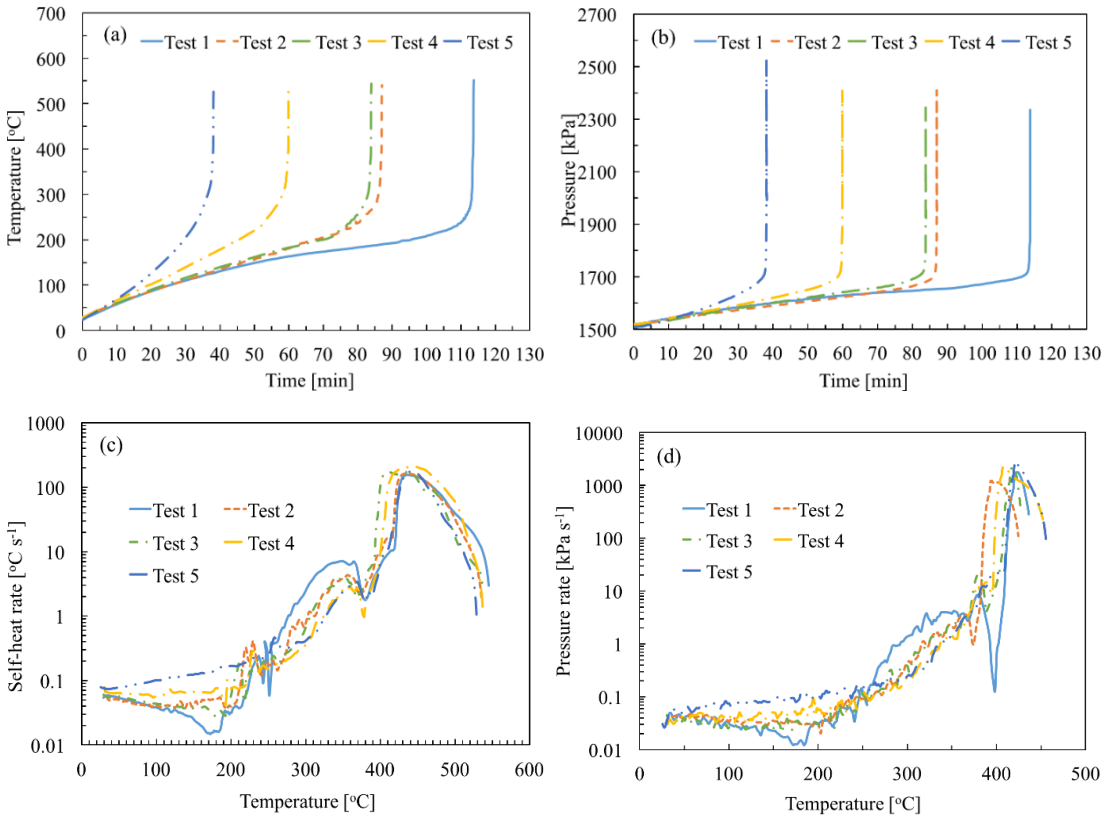

Figure 31. Thermal decomposition of 2.35 g 2-NT with 0.54 g iron oxide (III) for three identical measurements (a) Temperature profile as a function of time (b) Pressure profile as a function of time (c) Self-heat rate as a function of temperature and (d) Pressure rate as a function of temperature.

Table 27. 2.35 g 2-NT with 0.54 g iron oxide (III) thermal decomposition in ARSST

Test No.	1	2	3	4	5	Avg.
T_o (°C)	267	266	269	267	278	269 (±1)
T_f (°C)	551	540	544	540	532	541 (±3)
T_f-T_o (°C)	284	274	275	273	254	268 (±3)
$(dT\ dt^{-1})_{max}$ (°C s^{-1})	156	162	172	210	175	175 (±5)
T_{max} (°C)	436	434	437	443	421	434 (±4)
$(dP\ dt^{-1})_{max}$ (Pa s^{-1})	1776	2230	1623	1221	2850	1940 (±279)
PHI Factor	1.39	1.38	1.36	1.39	1.37	1.38 (±0.01)
NCG (moles)	0.010	0.010	0.014	0.011	0.015	0.012 (±0.001)
Heat of Reaction (kJ mol^{-1})	80	76	76	76	70	77 (±2)

b) Mole ratio of 2-NT and iron (III) oxide (10:1)

2.35 g 2-NT with 0.27 g iron oxide (III) thermal decomposition were tested three times in ARSST. Figure 32 shows the key parameter's graphs. The experimental data

obtained from the ARSST tests of 2-NT with calcium chloride are summarized in Table 28.

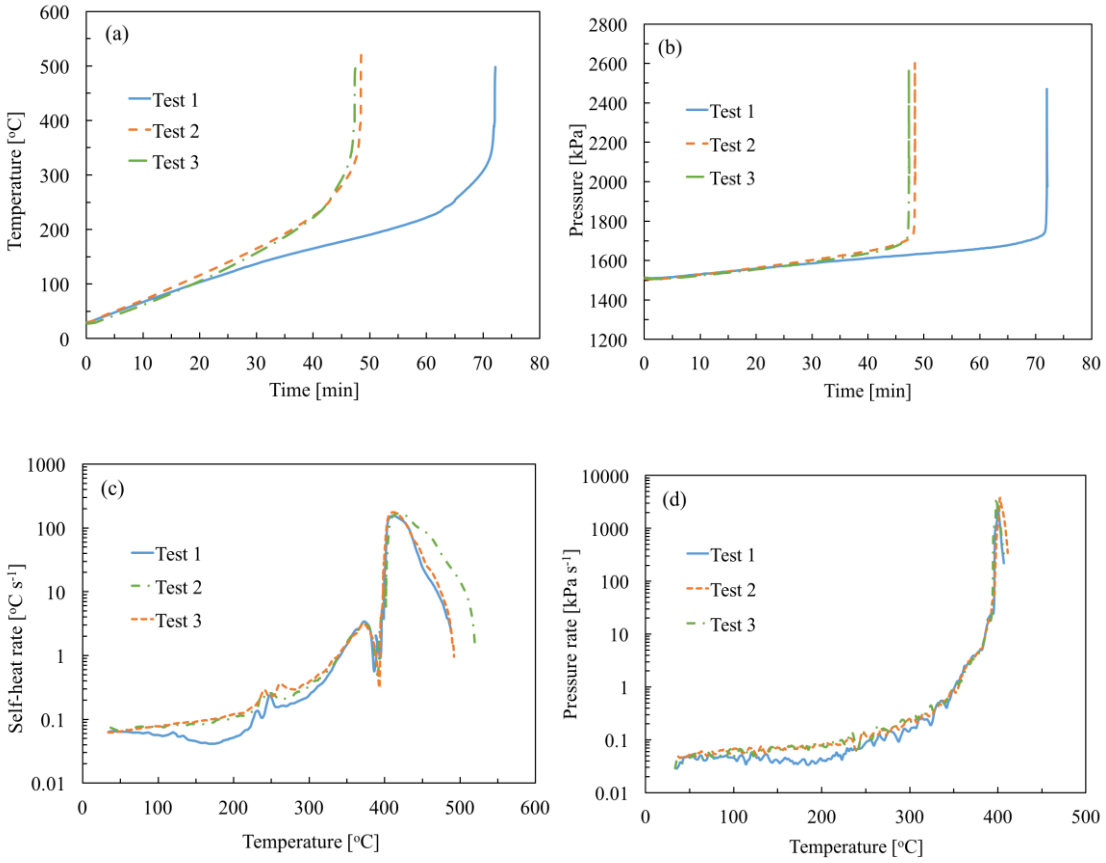

Figure 32. Thermal decomposition of 2.35 g 2-NT with 0.27 g iron oxide (III) for three identical measurements (a) Temperature profile as a function of time (b) Pressure profile as a function of time (c) Self-heat rate as a function of temperature and (d) Pressure rate as a function of temperature.

Table 28. 2.35 g 2-NT with 0.27 g iron oxide (III) thermal decomposition in ARSST

Test No.	1	2	3	Avg.
T_o (°C)	280	277	272	276 (±2)
T_f (°C)	498	523	499	507 (±8)
T_f-T_o (°C)	218	246	227	230 (±8)
$(dT\ dt^{-1})_{max}$ (°C s^{-1})	255	171	177	201 (±27)
T_{max} (°C)	413	421	411	415 (±3)
$(dP\ dt^{-1})_{max}$ (Pa s^{-1})	2873	3752	3910	3512 (±323)
PHI Factor	1.41	1.41	1.41	1.41 (±0.00)
NCG (moles)	0.014	0.015	0.014	0.014 (±0.0002)
Heat of Reaction ($kJ\ mol^{-1}$)	81	70	74	75 (±3)

c) Mole ratio of 2-NT and iron (III) oxide (20:1)

2.35 g 2-NT with 0.14 g iron oxide (III) thermal decomposition were tested three times in ARSST. Figure 33 shows the key parameter's graphs. The experimental data obtained from the ARSST tests of 2-NT with calcium chloride are summarized in Table 29.

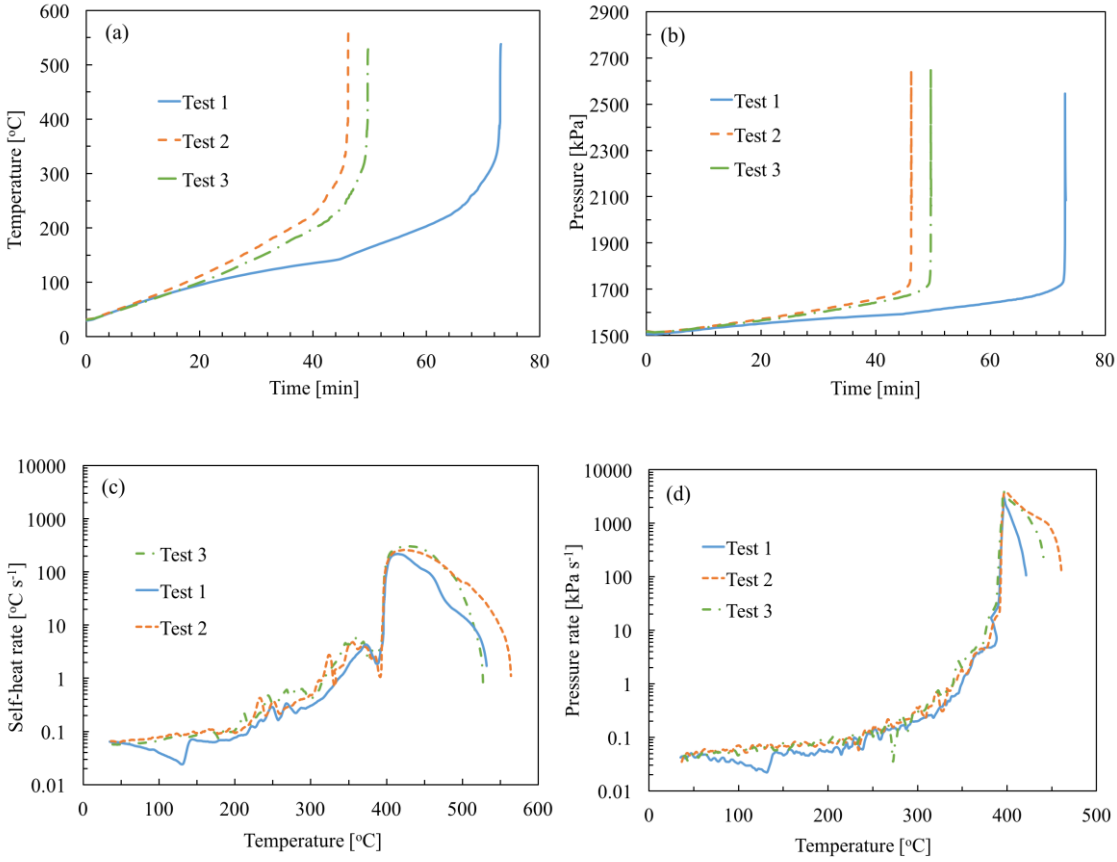

Figure 33. Thermal decomposition of 2.35 g 2-NT with 0.14 g iron oxide (III) for three identical measurements (a) Temperature profile as a function of time (b) Pressure profile as a function of time (c) Self-heat rate as a function of temperature and (d) Pressure rate as a function of temperature.

Table 29. 2.35 g 2-NT with 0.14 g iron oxide (III) thermal decomposition in ARSST

Test No.	1	2	3	Avg.
T_o (°C)	283	285	288	285 (±1)
T_f (°C)	538	566	528	544 (±11)
T_f-T_o (°C)	255	281	240	259 (±12)
$(dT\ dt^{-1})_{max}$ (°C s^{-1})	303	333	226	287 (±32)
T_{max} (°C)	427	430	427	428 (±1)
$(dP\ dt^{-1})_{max}$ (Pa s^{-1})	4013	2904	2370	3096 (±484)
PHI Factor	1.40	1.42	1.41	1.41 (±0.00)
NCG (moles)	0.015	0.014	0.015	0.016 (±0.0006)
Heat of Reaction (kJ mol^{-1})	72	81	70	73 (±4)

Increasing the amount of the iron (III) oxide resulted in a respective drop of the "onset" temperature, maximum self-heat rate, maximum pressure rise rate and the moles of NCG (Table 30). The heat of reactions with or without iron (III) oxide are similar.

Table 30. Thermal decomposition of 2-NT with various amount of iron (III) oxide (each experiment contains 2.35 g of 2-NT).

Mass (g) (mol%)	0 (0)	0.14 (4.9%)	0.27 (9.1%)	0.54 (16.7%)
T_o (°C)	310 (±2)	285 (±1)	276 (±2)	269 (±1)
T_f (°C)	566 (±13)	544 (±11)	503 (±10)	541 (±3)
T_f-T_o (°C)	266	259	227	268
$(dT\ dt^{-1})_{max}$ (°C s^{-1})	246 (±14)	287 (±32)	201 (±27)	175 (±5)
T_{max} (°C)	441 (±7)	428 (±1)	415 (±3)	434 (±4)
$(dP\ dt^{-1})_{max}$ (Pa s^{-1})	5881 (±457)	3096 (±484)	3512 (±323)	1940 (±279)
PHI Factor	1.43 (±0.009)	1.42 (±0.007)	1.41 (±0.002)	1.38 (±0.008)
NCG (moles)	0.016 (±0.001)	0.016 (±0.001)	0.014 (±0.0002)	0.012 (±0.001)
Heat of Reaction (kJ mol^{-1})	74 (±8)	77 (±2)	75 (±3)	73 (±4)

The polynomial relation between the "onset" temperature of 2-NT with the moles of iron (III) oxide in mixture is (Figure 34, left):

$$T_o=0.19x^2 - 5.63x + 309.45$$

Where T_o is the "onset" temperature and x is the mole fraction of additive iron (III) oxide. The R-squared value is 99.5% which shows good correlation between the model and the data.

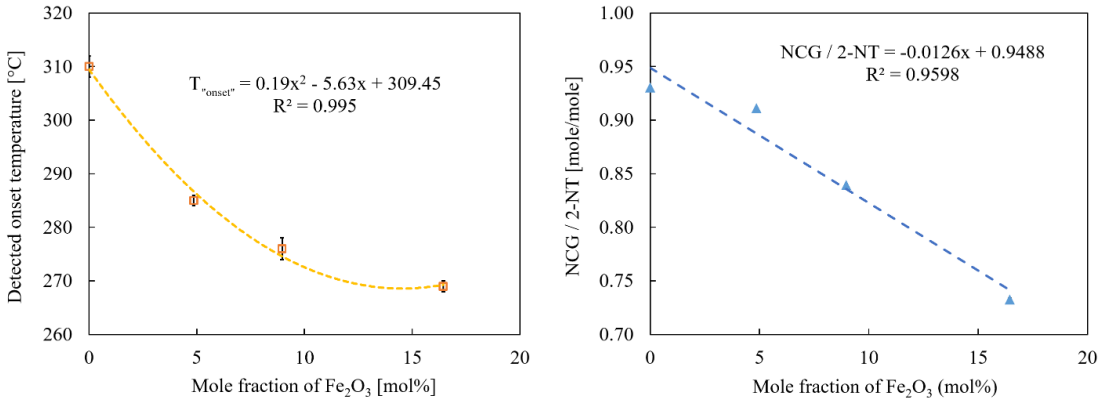

Figure 34. The detected "onset" temperature of the thermal decomposition of 2-NT with various amount of iron (III) oxide (left figure). The mole ratio of NCG vs. 2-NT with various amount of iron (III) oxide (right figure).

The polynomial correlation between the NCG per 2-NT and the moles of iron (III) oxide in mixture is (Figure 34, right):

$$y=-0.0126x + 0.9488$$

Where y is the moles of the NCG per mole of 2-NT and x is the mole fraction of additive iron (III) oxide. The R-squared value is 96.0% which is a good correlation between the model and the data.

6.2 Discussions of effects from incompatible substances

2-NT (2.35 g) with contaminates in a molar proportion 5:1 have been tested in ARSST**.** The employed contaminates were calcium chloride (0.38 g), sodium sulphate (0.51 g), sodium chloride (0.20 g), sodium carbonate (0.36 g) and iron (III) oxide (0.54 g). Each test was repeated for 3 times. The key performance parameters ("onset" temperature T_o, maximum temperature T_f, adiabatic temperature rise (T_f - T_o), maximum self-heat rate $(dT/dt)_{max}$, maximum pressure rise rate $(dP/dt)_{max}$, thermal inertia factor (φ) and moles of non-condensable gas generated NCG are summarized in Table 31.

6.2.1. Influence of incompatible substances on "onset" temperature (T_o), maximum temperature (T_f) and adiabatic temperature increase ($T_f - T_o$)

From the temperature vs. time curves, we readily acquired the "onset" temperature, maximum temperature and temperature increase. The values of the pseudo-adiabatic temperature rise are directly proportional to the energy release and represent the damage potential in case of decomposition. The "onset" temperature of pure 2-NT is 310 (±2) °C and all six contaminants result in a lower the "onset" temperature from as little as 5 °C (NaCl) to as much as 183 °C (NaOH). This illustrates the incompatible effect on 2-NT of the mixtures containing of hydroxide, sulfate, carbonate, ferric, and chloride ions, respectively. Sodium hydroxide and sodium sulfate contaminates tested which resulted in an increase in the maximum temperature of 2-NT decomposition and more importantly a larger pseudo-adiabatic temperature rise (Figure 35). Ammonia nitrate shows very

different behavior after adding the sodium sulfate. Zhe et al.[100] [101] studied the impact of sodium sulfate on ammonium nitrate decomposition. For ammonia nitrate, sodium sulfate behaves as an inhibitor that caused an increase in the "onset" temperature and the maximum self-heating rate.

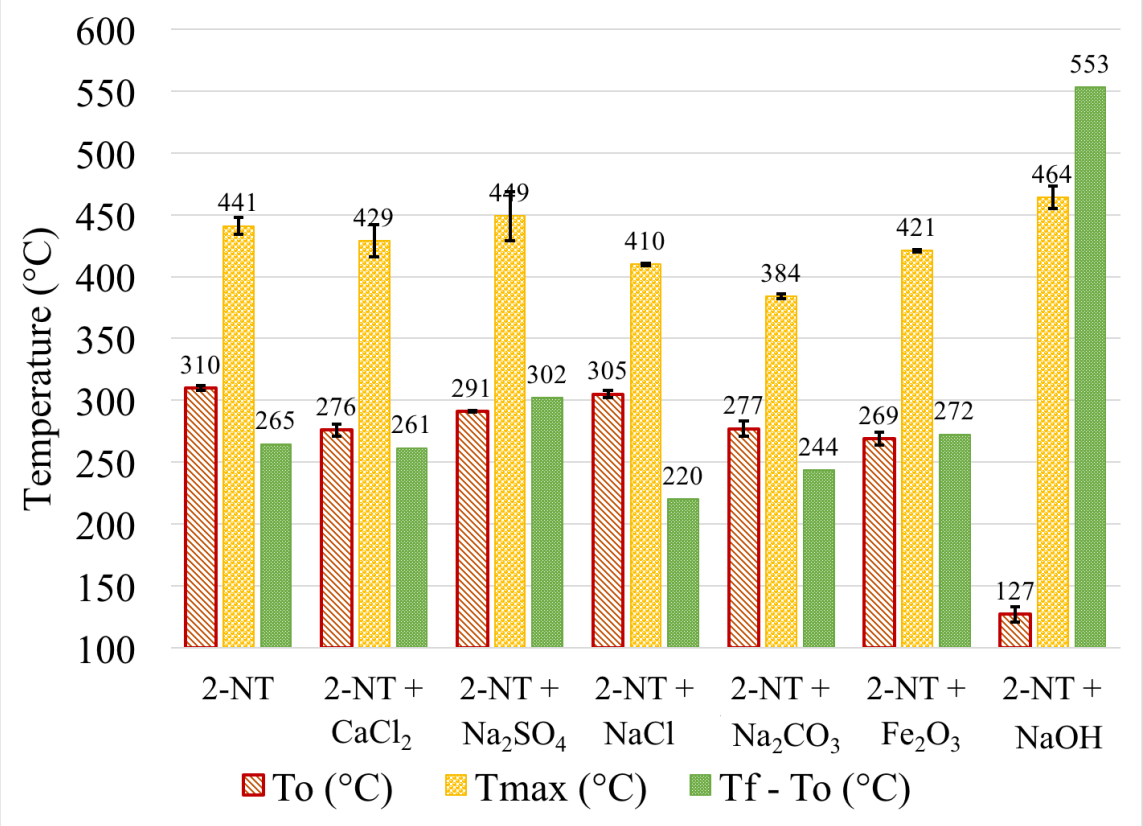

Figure 35. Comparison of 2-NT with and without additives. "onset" temperature (T_o), temperature at maximum self-heating rate (T_{max}), and maximum temperature (T_f) (2-NT : additive molar ratio = 5:1)

Table 31. Summary- key parameters of thermal decomposition of 2-NT with six different incompatibilities

Substance	T_o (°C)	T_f (°C)	T_f-T_o (°C)	$(dT\ dt^{-1})_{max}$ (°C s^{-1})	T_{max} (°C)	$(dP\ dt^{-1})_{max}$ (kPa s^{-1})	φ	NCG (moles)
2-NT	310 (±2)	566 (±13)	266	246 (±14)	441 (±7)	5881 (±457)	1.43 (±0.009)	0.016 (±0.001)
2-NT + NaOH	127 (±6)	680 (±27)	553	132 (±1)	464 (±9)	2802 (±158)	1.41 (±0.01)	0.026 (±0.003)
2-NT + $CaCl_2$	276 (±5)	537 (±10)	261	176 (±17)	429 (±13)	3953 (±260)	1.42 (±0.004)	0.019 (±0.001)
2-NT + Na_2SO_4	291 (±1)	593 (±20)	302	168 (±14)	449 (±20)	3675 (±109)	1.38 (±0.008)	0.022 (±0.002)
2-NT + NaCl	305 (±3)	525 (±6)	220	153 (±4)	410 (±1)	4264 (±306)	1.40 (±0.005)	0.018 (±0.001)
2-NT + Na_2CO_3	277 (±6)	521 (±7)	244	174 (±6)	384 (±2)	3911 (±237)	1.39 (±0.003)	0.021 (±0.003)
2-NT + Fe_2O_3	269 (±1)	541 (±3)	272	175 (±5)	434 (±4)	1940 (±279)	1.38 (±0.008)	0.012 (±0.001)

6.2.2. Influence of incompatible substances on maximum self-heating rate ((dT/dt)max) and maximum pressure rise rate ((dP/dt)max)

Maximum self-heat rate and maximum pressure rise rate are also very important parameters in reactive chemicals study to estimate the worst consequences the runaway reactions may lead to. As shown in Figure 36, all six contaminants can lower both the maximum self-heat rate and maximum pressure rise rate during the runaway reactions. The iron (III) oxide demonstrates the largest decrease in maximum pressure rate. T_{max} represents the temperature at the maximum self-heat rate, and it is in all cases but with sodium carbonate above 400 °C. Though the system is pressurized (initial pressure of 1.5 MPa), at high temperature, a significant portion of the 2-NT and volatile products vaporize and the decomposition mainly happens in the gas phase. In the meantime, the additives such as sodium sulfate, sodium chloride, iron oxide and calcium chloride are stable solid salts and few will react with 2-NT at $T_{max.}$ However, since the incompatible substances lower the "onset" temperature of the 2-NT decomposition reaction, the initial reaction mechanisms changed and more 2-NT was consumed before the T_{max}. Therefore, the heat release rate of 2-NT decomposition with additives was slower than that of pure 2-NT and the respective detected maximum self-heat rate and pressure rate decreased.

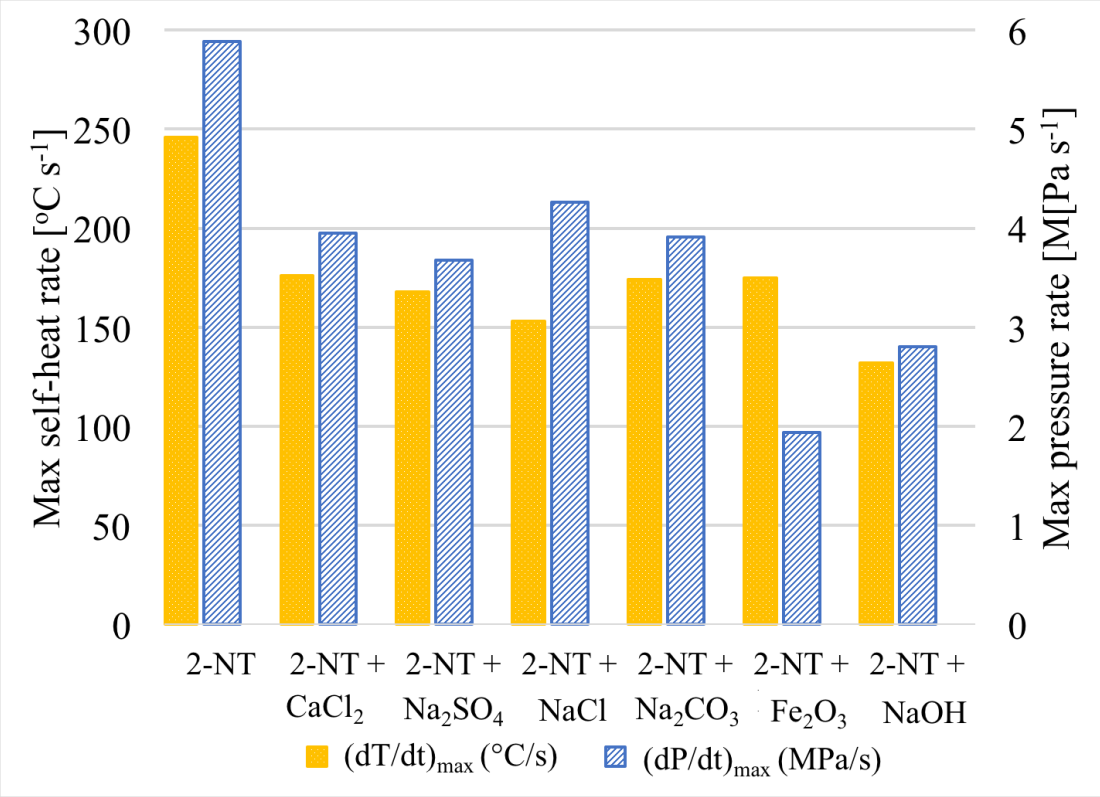

Figure 36. Comparison of 2-NT with and without additives. Maximum self-heating rate ($(dT/dt)_{max}$) and maximum pressure rise rate ($(dP/dt)_{max}$) (2-NT：additive molar ratio = 5:1).

6.2.3. Influence of incompatible substances on non-condensable gas generation (NCG)

The NCG in the 2-NT decomposition includes but is not limited to small molecules, such as CO, CO_2, NO, NO_2, CH_3, and HCN. The moles of NCG generation with pure 2-NT was very repeatable experimentally. As such, the moles of non-condensable gas may

indirectly reflect whether adding the contaminants can influence the original decomposition reaction of 2-NT. Three of the contaminants (iron (III) oxide, sodium carbonate and sodium sulfate) clearly changed the moles of NCG generated (as shown in Figure 37). The same moles of 2-NT were present in each test, as such, a decrease in the total moles, like was seen with the iron (III) oxide, supports a different decomposition pathway or that the decomposition products reacted to form larger condensable molecules. The typical pathway for the decomposition of sodium carbonate is to produce one mole of sodium oxide and one mole of CO_2 for every mole of sodium carbonate decomposing. A total of 0.021 moles of NCG was generated in the presence of 0.0034 moles of sodium carbonate. If the standard decomposition pathway was followed the maximum gas generation should have been 0.0194 moles (the combination of 0.016 moles 2-NT and 0.0034 moles of CO_2). The difference measured is outside the standard deviation of the experiment and supports a different decomposition pathway for 2-NT in the presence of sodium carbonate. In the case of sodium sulfate contamination, under the right conditions, it is expected that 91.2% will decompose to one mole of SO_2 (g) and one mole of O_2 (g) [102]. Therefore, of the 0.0034 moles present, 0.0031 moles will decompose forming 0.0062 moles of non-condensable gas bringing the total moles in the mixture to 0.022 moles (the combination of 0.016 moles from 2-NT and 0.0062 moles from sodium sulfate) which is in good agreement with the results in the experiment. The result is inconclusive in determining if the decomposition pathway for 2-NT has changed in the presence of sodium sulfate. The chloride salts are stable and in the case of sodium chloride contamination the difference in NCG is within the standard deviation in the experiments

and in the case of calcium chloride it is slightly beyond the standard deviation. These results are inconclusive toward determining if the decomposition mechanism is altered. In hazard evaluation, understanding the moles of NCG generated is critical. Regardless of whether the reaction mechanism changed, the presence of sodium carbonate and sodium sulfate result in a significant rise in NCG generation which increases the hazard. These two compounds also appear to reduce the "onset" temperature and to increase the temperature rise when normalized to mass of 2-NT. Consequently, their overall effect on the runaway causes a serious concern and their presence should be screened for when processing 2-NT. Among the six contaminants studied in the paper, the additive that draws great interest for further study is the main component for the dust - iron (III) oxide. It can significantly lower the "onset" temperature (gas generation and heat release occurring faster at lower temperatures) but also lowers the maximum self-heat rate, the maximum pressure rise rate and the moles of the NCG making it more challenging to analyze hazard scenarios. Specifically, the presence of iron (III) oxide can likely induce a thermal runaway at a lower temperature but the overall consequences from a thermal runaway may be less severe.

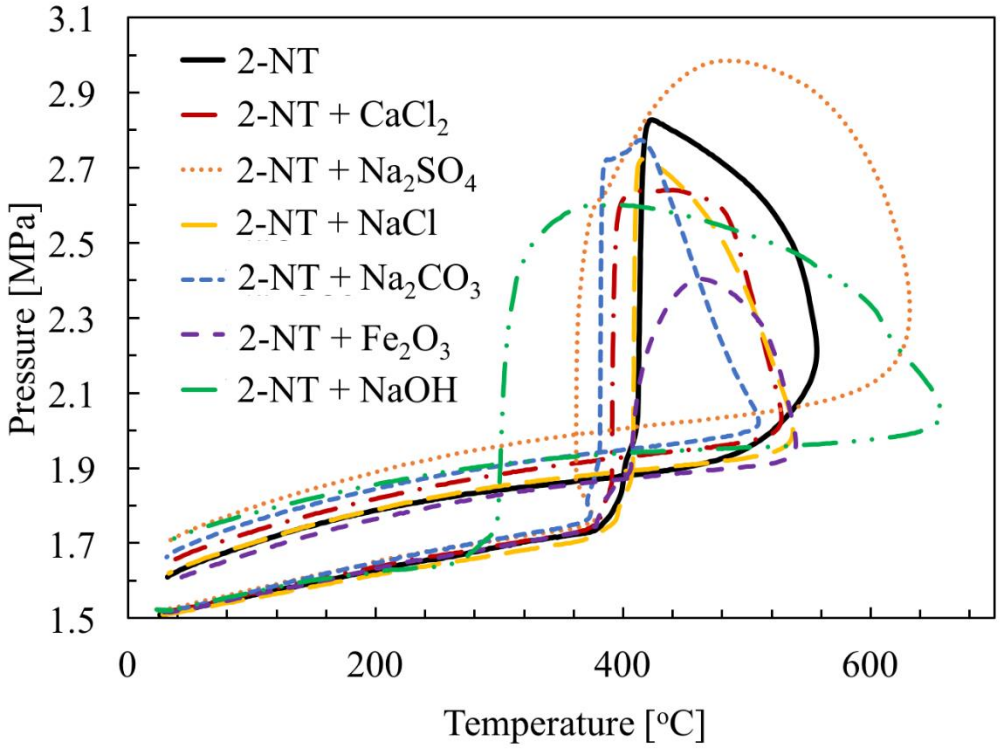

Figure 37.The pressure vs. temperature profile of the thermal decomposition of 2-NT with different additives (2-NT：additive molar ratio = 5:1).

6.3 Possible mechanisms of 2-NT decomposition with incompatible substances

As mentioned earlier, previous research has indicated that the main decomposition pathway for 2-NT in the temperature range employed in this research is the formation of anthranil (P12) and water (reaction I). When sodium hydroxide, sodium sulfate, sodium carbonate, calcium chloride or sodium chloride respectively is mixed with 2-NT, the salt is partially or totally dissolved in the water generated by the reaction. The salt which is

dissolved is fully dissociated to its constituent ions. When one or both of them are ions of a weak base or a weak acid, they cause water hydrolysis thus liberating hydrogen cations or hydroxyl anions, respectively.

$C_6H_4(CH_3)(NO_2) \rightleftharpoons C_6H_4CHNO + H_2O$ (I)

6.3.1. Generation of OH^-

The sodium carbonate and sodium sulfate consume water to generate hydroxyl anions, the former (being the anion of a weaker acid), more than the latter, which shift the main initial reaction of 2-NT thermal decomposition (I) to the right.

Sodium sulfate fully dissociates in water according to reaction ($Na_2SO_4 \rightarrow 2Na^+ + SO_4^{2-}$). Subsequently SO_4^{2-} provokes hydrolysis to produce HSO_4^- and OH^- ions. However, HSO_4^- is amphiprotic that is capable of acting as an acid or a base. Via hydrolysis, addition of Na_2SO_4 can slightly increase the pH during the initial stage of the decomposition.

$Na_2SO_4 \rightarrow 2Na^+ + SO_4^{2-}$ (II)

$SO_4^{2-} + H_2O \rightleftharpoons HSO_4^- + OH^-$ $K_b = 9.8 \times 10^{-8}$ (III)

Where K_b is the base-dissociation constant at 25 °C [103].

Sodium carbonate is the dis odium salt of carbonic acid with al kalinizing property due to hydrolysis as shown below. When dissolved in water, sodium carbonate forms carbonic acid and hydroxyl radicals. At high temperatures the CO_2 escaped [104]. CO_2 may explain the reason larger NCG is generated for 2-NT thermal decomposition with sodium carbonate.

$Na_2CO_3 \rightarrow 2Na^+ + CO_3^{2-}$ (IV)

$CO_3^{2-} + H_2O \rightleftharpoons HCO_3^- + OH^-$ $K_b = 1.8 \times 10^{-4}$ (V)

$HCO_3^- + H_2O \rightleftharpoons H_2CO_3 + OH^-$ $K_b = 2.3 \times 10^{-8}$ (VI)

$[H_2CO_3] = K_h [CO_2]$ $K_h = 1.7 \times 10^{-3}$ (VII)

$PCO_2 = [CO_2]_{aq} / k_H$ $k_H = 29.76$ atm/(mol/L) (VIII)

Where K_b is the base-dissociation constant at 25 °C [105] and K_h the hydration equilibrium constant at 25 °C in pure water [106], PCO_2 is the partial pressure of carbon dioxide above the solution and k_H is the Henry constant at 25 °C.

Generation of OH^- (increase the pH) is another possible reason for the lower "onset" temperature. Previous studies provided that bases such as caustic soda can decrease the "onset" temperature of 2-NT thermal decomposition by more than 100 °C [12][40]. To prove that caustic soda's impact, the ARSST test with 2.35 g 2-NT and 3 g of anhydrous NaOH was performed in this study. The addition of NaOH can decrease the "onset" temperature substantially but also to decrease the maximum pressure during the decomposition of 2-NT accordingly. Figure 38 shows a comparison between the decomposition of 2-NT and the decomposition of its mixture with anhydrous NaOH. The self-heat rate vs. temperature curves revealed two exothermic reaction regions. This agrees with the three stages of the 2-NT decomposition, the induction phase, acceleration phase and the decay phase [46]. NaOH shifted the two exothermic reaction regions left to lower temperature. It also lowered the maximum self-heat rate for both regions. The same happened to the pressure rise rate profile. Similarly, for hydroxylamine decomposition, hydroxide ion (OH^-) was found to decrease the "onset" temperature and generate more gas products [107][124].

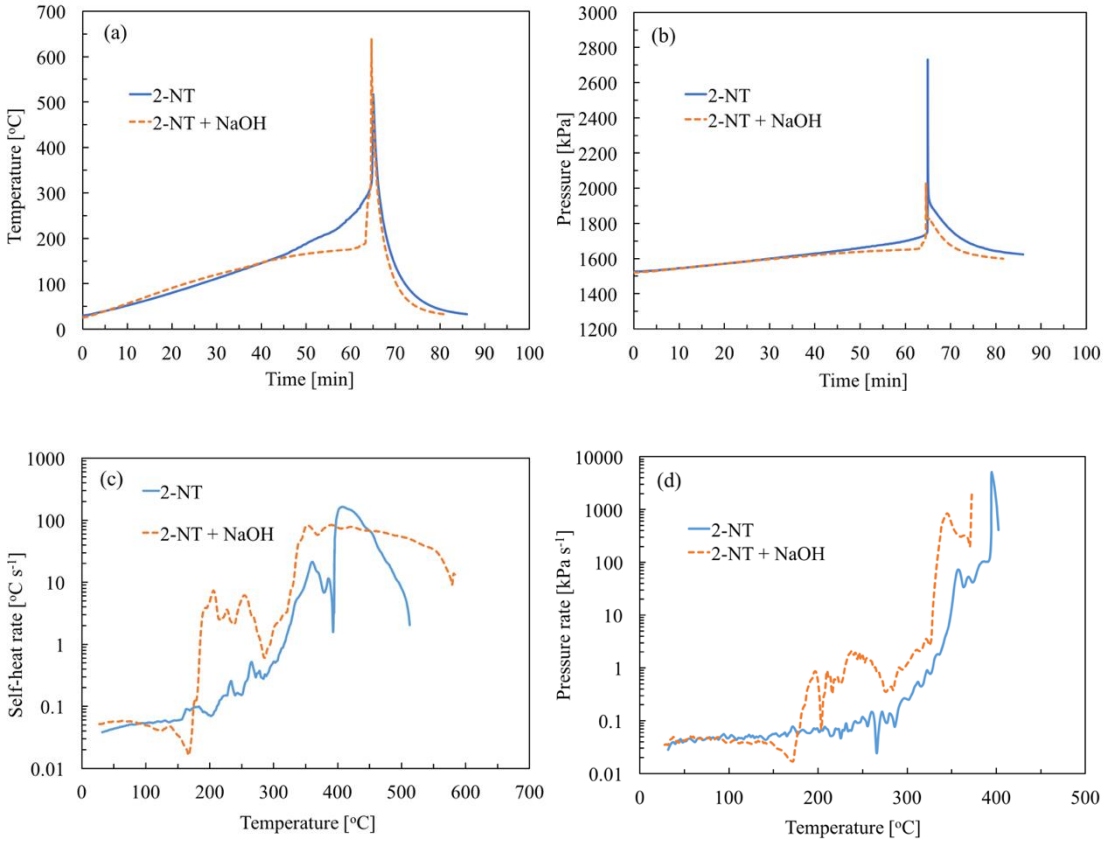

Figure 38. Thermal decomposition of 2-NT with NaOH (a) temperature as a function of time (b) pressure as a function of time (c) self-heat rate as a function of temperature and (d) pressure rate as a function of temperature.

The mechanisms of the hydroxide ion lower the "onset" temperature is the attack of strong diatomic anion OH^- on the nitro group of 2-NT and other nitro aromatics. It is generally associated with reduction of the nitrogen where the base is a reducing agent. Unlike the carboxylate ion, the nitro group has positive charge on the nitrogen (P1). Because of this charge, the nitro nitrogen atom is more reactive toward bases [108].

6.3.2. Impact of chloride ions

Metal chlorides can lower the "onset" temperature for some nitro aromatic compounds [35][39] In this study, sodium chloride and calcium chloride lower the "onset" temperature of the 2-NT by 5 °C and 34 °C, respectively. The calcium chloride contributes twice the amount of chloride irons than sodium nitrate and this may be the reason that their impact on "onset" temperature was different.

The second possible reason is that the dissolution of calcium chloride in the water is exothermic and the standard enthalpy of solution is -81.3 kJ/mol [109].

Table 23 summarizes the enthalpy change of solution at 25 °C. Not like calcium chloride, solution enthalpies of sodium sulfate, sodium chloride and sodium carbonate are negligible; therefore, their addition is not expected to cause any measurable thermal effects. However, the $CaCl_2$ species containing 0.3 equivalent of water is stable [110]. The third possible reason is that the calcium chloride consumes traces of water which makes the reaction (I) shift right which caused lower detected "onset" temperature.

$$CaCl_2(s) + 0.3\ H_2O(g) \rightleftharpoons\ CaCl_2 \cdot 0.3H_2O(s) \qquad \text{(IX)}$$

Table 32. Standard Enthalpy of solution of additives [109][123]

Chemicals	ΔH (kJ mol^{-1})
Sodium Hydroxide	-44.2
Calcium Chloride	-81.3
Sodium Sulfate	+2.4
Sodium Chloride	+3.9
Sodium Carbonate	-26.7

6.3.3. Iron (III) oxide catalyzed nitroarenes reduction

Hydrogenation of nitroarenes is catalyzed by iron [111][112][113], zero valent iron [114][115], iron oxide [116][117][118][119][120] have been studied for the environmental treatment and the production of anilines, hydroxylamines, and azo compounds. Factors such as substrate properties, iron surface, pH and mixing rate also have been discussed by Agrawal and Tratnyek [114]. The thermal decomposition of 2-NT with iron (III) oxide was shown in this paper. 2-NT decomposition is possibly catalyzed by the iron (III) oxide for the formation of the 2-toluidine as the mechanisms shown in Figure 39. Further study of 2-NT thermal decomposition with iron (III) oxide and trace amounts of acids which provide the hydrogen atoms may provide useful data for the elucidation of the reaction mechanisms.

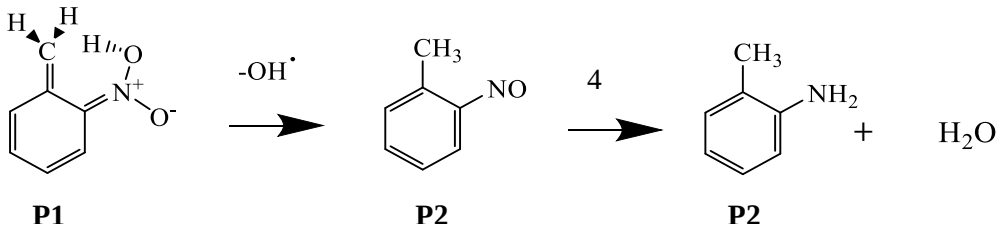

Figure 39. Proposed decomposition pathways for 2-toluidine formation.

6.4 Effect of Confinement

In the typical ARSST test, top open test cells are used. Therefore, for liquid reactive chemicals, especially the low boiling point liquids, it is possible to reach the boiling points during the heating up processes. If the chemicals reach the boiling points earlier than the "onset" temperature, then it is very likely that no runaway reaction can be detected. Or the decomposition reaction will happen in the gas phase but not the liquid phase, and this is what happened during the test C. Therefore, the initial pressure is a very important parameter. For better understanding of the pressure effects on the 2-NT decomposition. Three tests with different initial pressures (1517 kPa, 869 kPa and 345 kPa respectively) but same sample quantities were performed (2.35 g). Tests results are shown in Figure 40.

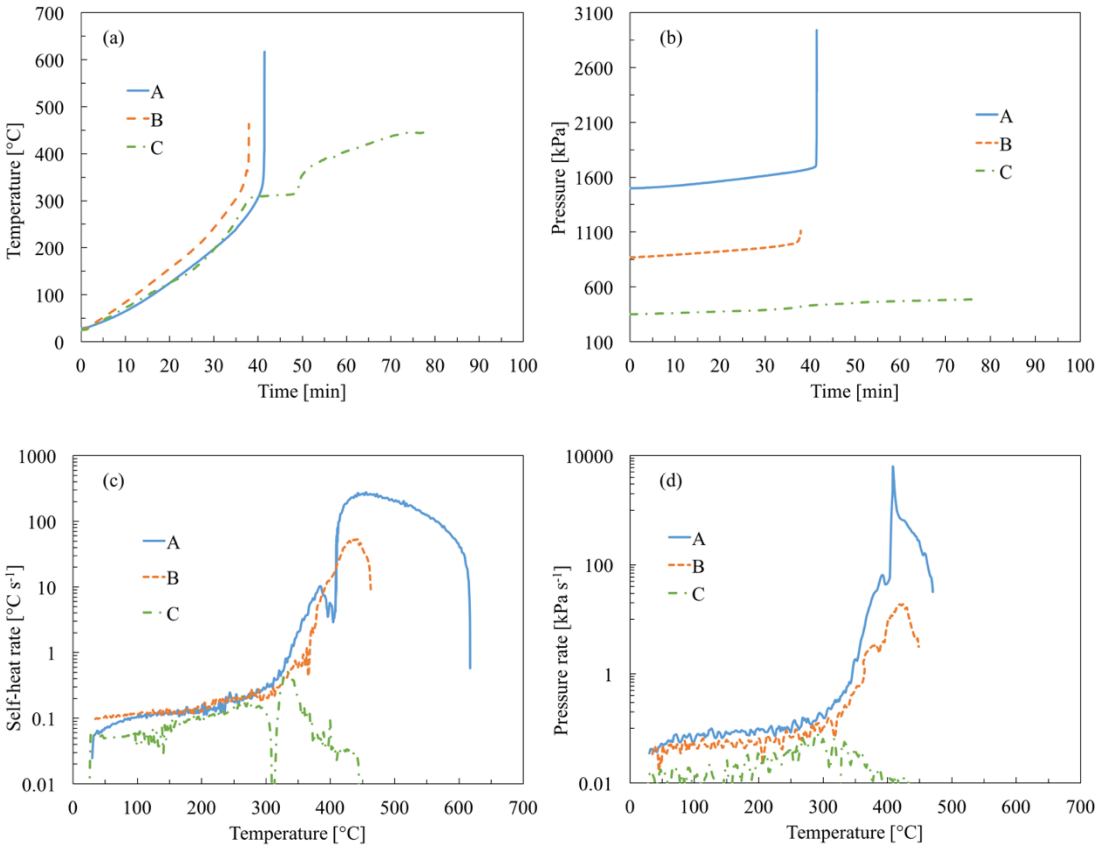

Figure 40. Thermal decomposition of 2-NT for three different initial pressures (a) Temperature profile as a function of time (b) Pressure profile as a function of time (c) Self-heat rate as a function of temperature and (d) Pressure rate as a function of temperature

Table 33 summarized the thermal properties of each test. Lower initial pressure increases the onset temperature, and lowers the self-heat rate. ARSST tests are open cell, thus sample phase shift from liquid to vapor will occur during heat up. This latent heat

will lower the observed onset temperature. For the test C, there was a flat stage at 305 °C, which lasted for about 15 minutes then the temperature suddenly increased. The flat stage means that the liquid 2-NT reached the boiling point of 305 °C at 60 psig. After a while, unclear amount of vapor 2-NT suddenly decomposed and released heat and gases. There were black substances exist in the test cell after the test (2-NT is yellow clear liquid). Also the non-condensable gases were released during the test, which caused the pressure increase before and after the test at same temperature.

Table 33. Pure 2-NT ARSST experimental data at different initial pressures

Test No.	A	B	C
Initial Pressure (kPa)	1517	869	345
T_o (°C)	313	320	326
T_f (°C)	617	463	445
T_f-T_o (°C)	314	137	115
$(dT\ dt^{-1})_{max}$ (°C s^{-1})	262	53	0.5
T_{max} (°C)	451	443	451
$(dP\ dt^{-1})_{max}$ (kPa s^{-1})	6348	324	0.1
PHI Factor	1.44	1.40	1.41
NCG (moles)	0.0190	0.0055	0.0048

6.5 Effect of Thermal History

After the dynamic heating decomposition studies, isothermal tests were conducted. Measurements were performed using 2.35 g of 2-NT in each isothermal test. In three tests, the samples were heated at an identical rate (3 °C min^{-1}) up to 180 °C, 250 °C and 270 °C, where they are to remain for 50, 90 and 90 minutes respectively. The color remained constant for the sample which was kept at 180 °C for 50 minutes. This is an indicator that minimal self-decomposition occurred. However, the sample held at 250 °C had substantial color change, indicating the presence of self-decomposition without a thermal runaway. Additional heating was provided to the sample held at 250 °C to induce thermal runaway. The sample held at 270 °C decomposed 7 minutes after reaching isothermal conditions. The mass of samples reduced due to evaporation. The normal boiling point of 2-NT is 225 °C at 14.7 psi.

In the ARSST, the open test cell is heated and contained inside a closed but otherwise cold, pressure vessel with a pad pressure of 220 psi. The pad pressure helps minimize much of the evaporation of the sample. However, vapors of 2-NT escaping from the cell condense on the cold parts of the pressure vessel. The isothermal test at 250 °C, lost 0.66 g of 2-NT sample during the 90-minute test. At the end of the experiment wet cotton wool surrounding the cell was observed. Whether all 0.66 g were lost due to evaporation or whether potential reactions contributed, cannot be concluded from the data collected in this work. As mentioned earlier, this sample changed to a black colored liquid, indicating a reaction took place, but no measurable pressure or temperature increase was observed in

the cell. The same measurement was repeated and after 90 minutes of isothermal operation, the sample was heated to induce decomposition. The results are shown in Figure 41.

An additional measurement was performed with the same mass of 2-NT, with a heating rate of 1.9 °C min^{-1} for an isothermal period of 50 min at 180 °C. For this experiment 1.26 g mass was lost, while the sample color remained yellow, indicating that at this temperature and length of time minimal reaction occurred. From these measurements, it is obvious, that for 2-NT the heating rate affects the evaporation mass, which was substantial in all cases. However, the quantity of evaporated mass during the decomposition measurement could not be evaluated.

The decompositions generated non-condensable gasses and a tar like residue in the cell after each experiment. The sample mass loss due to evaporation and non-condensable gas formation prohibit the results from the present study to be used for thermokinetic calculations of this decomposition. However, the detected decomposition “onset”, in the absence of any additives, was not measurably affected by the conditions of the measurement as can be seen in Figure 41.

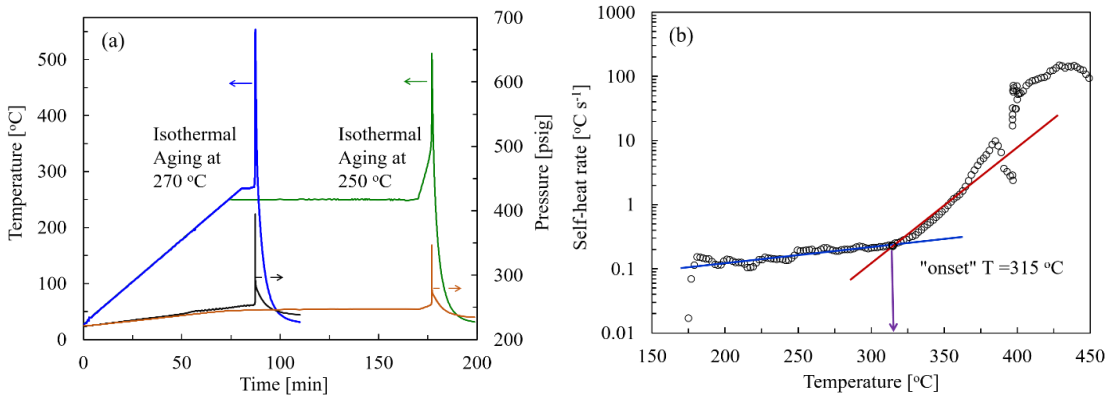

Figure 41. (a) Left: Isothermal aging measurement at 270 °C, Right: Isothermal aging measurement at 250 °C for 90 min., then further heat-up for decomposition. (b) Self-heat rate vs. temperature for the isothermal ageing measurement at 250 °C.

Figure 41 (a) shows the temperature and pressure profiles for two isothermal experiments. The left side shows the temperature and pressure profiles for the isothermal test at 270 °C. Seven minutes after achieving the isothermal condition the sample rapidly decomposed in a thermal run away. On the right side of Figure 41 (a), the temperature and pressure profiles are shown for the isothermal experiment at 250 °C for 90 minutes, after which time no detectable decomposition was observed. An additional heating rate was then applied to induce decomposition.

Figure 41 (b) shows the self-heat profile for the second isothermal experiment. From both Figure 41 (a) and (b), the detected “onset” temperature is not measurably affected by the change in treatment. However, the fact that the sample promptly decomposed at 270 °C indicates the detected “onset” temperature of 310 °C is too high. This value is

closer to that reported by Duh (1997) [12] or even that reported by Sachdev (2005) [30] as discussed in the introduction. In the present study, no temperature or pressure manifestations indicate decomposition for the isothermal measurement at 250 °C, which was the detected "onset" temperature reported by Sachdev (2005) [30]. However, the change in the sample color may indicate the initiation of a runaway, which was not had adequate time to evolve. The decomposition "onset" value of 190 °C as reported in SAX's Dangerous Properties of Industrial Materials [121] was not observed in the isothermal measurements of this work. However, this may be due to the short duration of the isothermal experiments. If detected "onset" is calculated from the temperature or pressure rise profiles of this work (Fig. 15 a and 15b), it would be in agreement with this value.

The ARSST self-heat *vs* temperature profile (Figure 41 b) shows two peaks in the respective curve. This is likely a result of two distinct reactions occurring during the thermal decomposition process. The first reaction happens at a lower temperature and releases less heat, while the second reaction happens at a higher temperature (around 400 °C) and releases substantially more heat. The first reaction might be the C-H alpha attack because it has a lower activation energy compared to the combination of C-NO_2 homolysis and nitro-nitrite rearrangement, which have higher activation energy and may correspond to the second reaction as shown in Figure 21 and Table 6. This dual reaction behavior can be seen in the three repeated tests with pure 2-NT and in the isothermal tests with a "maturing" sample with color change and loss of sample at at 250 °C as shown in Figure 41 (b). In each example the second reaction has the same initiation temperature of approximately 400 °C.

6.6 Effect of Sample Size

Sample size is a very important factor that can influence the observable results in calorimeter studies. For most cases, larger samples sizes will result in more conservative values. In the study, three different samples sizes of 2-NT (1.20 g, 2.37 g and 3.70 g) was used in the ARSST tests. Temperature profile as a function of time, pressure profile as a function of time, self-heat rate as a function of temperature and pressure rate as a function of temperature are shown in Figure 42.

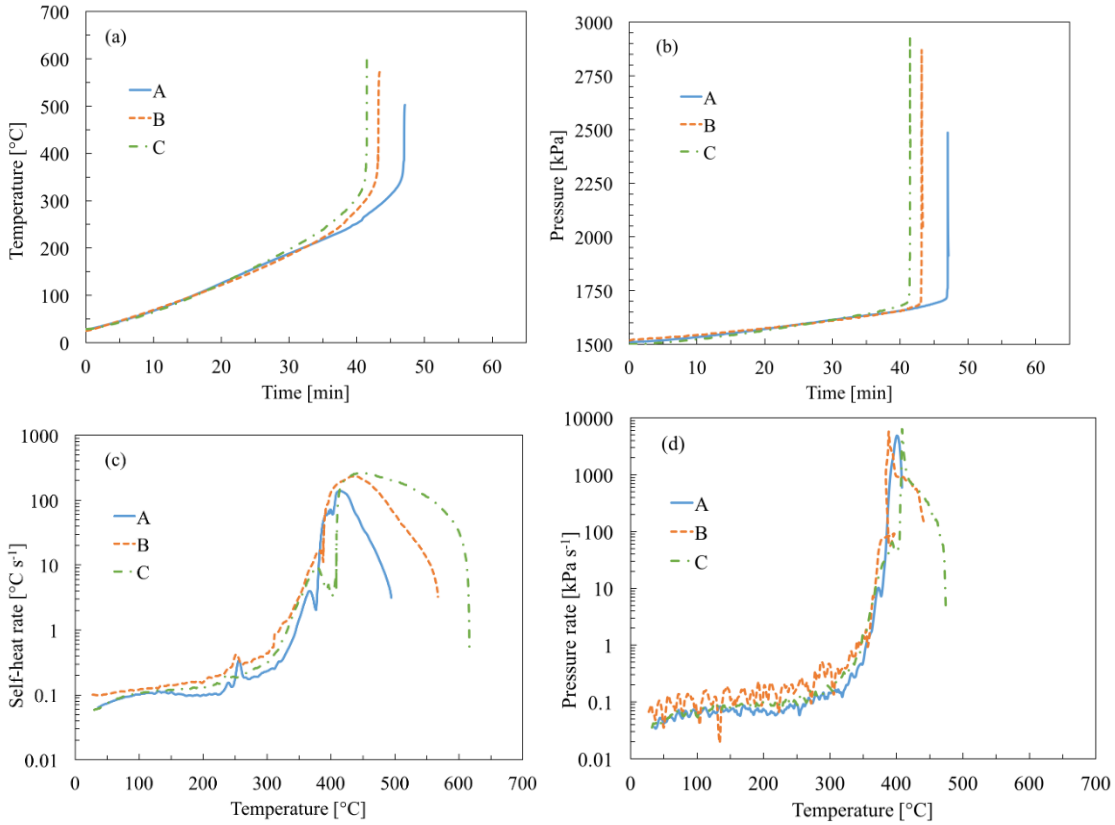

Figure 42. Thermal decomposition of 2-NT for three different sample sizes in ARSST (a) Temperature profile as a function of time (b) Pressure profile as a function of time (c) Self-heat rate as a function of temperature and (d) Pressure rate as a function of temperature.

The thermal properties are summarized in Table 34. The result shows that larger sample sizes can lower the observed onset temperature, which proves the importance of performing large scale tests. Due to the higher thermal inertia (φ) and smaller sample size have smaller values of adiabatic temperature rise ($T_f - T_o$), maximum pressure increase rate $(dT/dt)_{max}$, maximum self-heat rate $(dP/dt)_{max}$ and NCG. This emphasize the

importance of doing the large sample tests and the PHI corrections when using the data from the ARSST.

Table 34. Pure 2-NT ARSST experimental data at various sample sizes

Test No.	A	B	C
Mass (g)	1.20	2.37	3.70
T_o (°C)	326	315	303
T_f (°C)	502	572	617
T_f-T_o (°C)	176	257	314
$(dT\ dt^{-1})_{max}$ (°C s^{-1})	148	235	262
T_{max} (°C)	449	415	449
$(dP\ dt^{-1})_{max}$ (kPa s^{-1})	4854	5733	6348
PHI Factor	1.64	1.37	1.23
NCG (moles)	0.0133	0.0190	0.0026

To protect the APTAC equipment and for the safe operation, only one test was conducted for high temperature range (up to 700 °C). 2.34 g 2-NT was tested in the APTAC equipment and the comparison between two sample sizes in APTAC are summarized in Table 35. Similar trend can be observed that larger sample sizes lead to lower “onset” temperature, higher adiabatic temperature rise, maximum self-heat rate,

maximum pressure rise rate and NCG. For same amount of the sample mass, the tests in ARSST and APTAC give out different results. In APTAC, the "onset" temperature is lower and adiabatic temperature rise is higher, but smaller maximum pressure rise rate and more NCG than ARSST.

Table 35. Compare of different pure 2-NT experiment in APTAC and ARSST

Test No.	2.34 g in APTAC	1.20 g in APTAC	2.34 g in ARSST
T_o (°C)	285	289	310
T_f (°C)	667	415	615
T_f-T_o (°C)	382	126	305
$(dT\ dt^{-1})_{max}$ (°C min^{-1})	115	0.2	229 (high peak) 11 (low peak)
T_{max} (°C)	528	404	441 (high peak) 381 (low peak)
$(dP\ dt^{-1})_{max}$ (kPa s^{-1})	939	101	5880
PHI Factor	2.5	2.9	1.4
NCG (moles)	0.138	0.004	0.016

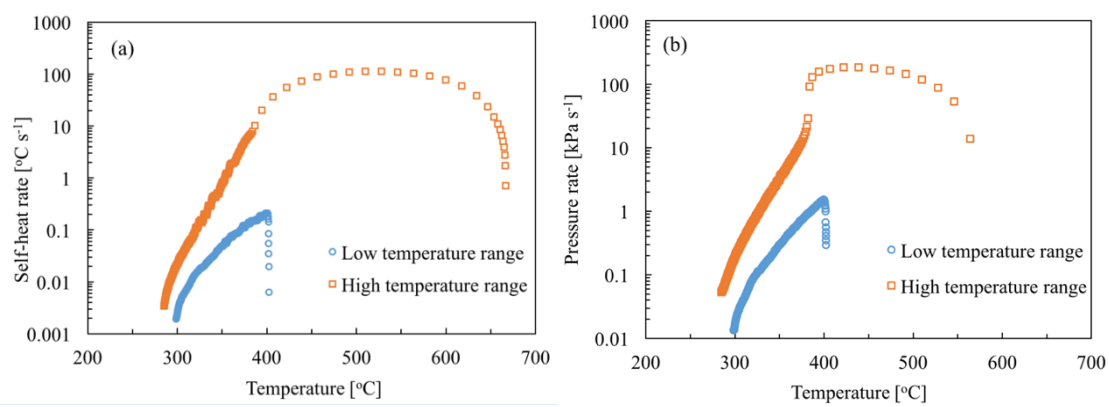

Figure 43. Thermal decomposition of 2-NT for two different sample sizes in APTAC (a) Self-heat rate as a function of temperature and (b) Pressure rate as a function of temperature

7. CONCLUSIONS AND FUTURE WORK

This section summarizes the main findings of the work presented in this dissertation (Section 7.1) and it outlines the opportunities to continue this work (Section 7.2).

7.1 Conclusions

This dissertation involved calorimetry and analytical work for the investigation of mononitrotoluenes (MNT) decomposition (especially 2-NT), which provide inherently safer storage conditions for nitro aromatic compounds. At the normal conditions, MNT is not considered a flammable or combustible material; however, they are strong explosive that can detonate under certain conditions. MNT are associated with several types of hazards including fire and explosion, which have occurred time and again in the past century.

This research advanced the understanding of the root causes associated with MNT explosions, and identified ways to make the MNT storage inherently safer. Among the three isomers, 2-NT is the most reactive approved by ARSST tests and has unique C-H alpha attack mechanisms in the initial phase which worth more investigation. This work focused on the thermokinetics analysis of the 2-NT thermal decomposition and condition-dependent 2-NT decomposition, including the effect of additives, pressure influence, thermal history, temperature, and sample sizes. Differential screening calorimetry (DSC), pseudo-adiabatic calorimetry (ARSST) and adiabatic calorimetry (APTAC) were used to study the characteristics of 2-NT decomposition. Thermodynamic and kinetic parameters

were evaluated; decomposition pathways were analyzed; models were proposed to predict the SADT and TMR of 2-NT; safer conditions for 2-NT storage were identified; and 2-NT hazards and explosion phenomenology were reported with six incompatible substances.

The topics covered in this work involved:

1) The evaluation of the thermal stability of pure MNT using pseudo adiabatic calorimetry (ARSST), to determine its runaway decomposition behaviors, which provided a better understanding of the hazards of MNT. Key parameters, such as the "onset" temperature, maximum self-heating rate, and maximum pressure rise rate have been identified.
2) The investigation of the thermodynamic and kinetic parameters of the 2-NT decomposition using three common calorimetry (DSC, ARSST and APTAC). Besides, the comparisons between the calorimetry were discussed. Further, the safe conditions for 2-NT storage and transportation was determined based on thermokinetics.
3) The identification of promoters for the study of additives through various experiments, including the study of single additive with various amount. Further, this work proposed mathematical models to predict the results of certain additive. Key parameters, such as the "onset" temperature, maximum self-heating rate, and maximum pressure rise rate have been identified.

4) The analysis of the mechanisms of decomposition associated with 2-NT for both pure 2-NT and 2-NT mixture with additives. Thus, the decompositions were explained from a fundamental point of view.
5) The study of the condition-dependent thermal decomposition of 2-NT, including the effect of additives, initial pressure, heating rate, temperature, thermal history, sample size, and isothermal testing.
6) The correction of the experimental results based on thermal inertia factor and analyzed the corrected values. Therefore, the errors introduced by the test cells of the calorimetry were eliminated and more accurate results were obtained.

The main conclusions of this dissertation are summarized here.

Among the three isomers of MNT, 2-NT is the most reactive, then the 4-NT and least reactive is 3-NT. The experimentally measured "onset" temperature of 2-NT decomposition was found to be in the range of 340 °C in the DSC, 310 °C in the ARSST and 290 °C in the APTAC. The detected "onset" temperature depends on the way it is defined, as well as the experimental conditions. In the absence of any additive, there was no evidence that the value of the detected "onset" temperature was affected by the potential mass loss, although there is substantial variability in this value, depending on the evaluation method chosen.

The thermal decomposition of MNT has three stages which are the induction phase, acceleration phase and the decay phase. The induction phase follows the n^{th} order reaction kinetics with n=0. Both the kinetic fitting shows good agreement from DSC and APTAC tests. The calculated activation energy (E_a) is 170 – 174 kJ mol^{-1} and the pre-exponential

factor (A) is $10^{11.60}$-$10^{11.77}$ with linear coefficient (R^2) larger than 99%. The activation energy of 2-NT (170-174 kJ mol^{-1}) at low temperature range (300 °C to 410 °C) shows agreement with the literature value of the reaction 2-nitrotoluene condensed to anthranil and water (167-184 kJ mol^{-1})[49]. Therefore, the main reaction happened during the low temperature is the generation of the water and anthranil. The heat energy obtained from the 2-NT decomposition was 2674 J g^{-1} equivalent to 0.57 g of TNT.

Safe operation conditions for the storage and transportation of 2-NT has been proposed. For the UN 25 kg standard package, U= 2.83 J/(s·m^2·K), S=0.4812 m^2, the temperature of no return (T_{NR}) is 502 to 510 K and the self-accelerating decomposition temperature (SADT) is 490 to 498 K. From the thermal safety diagram of 2-NT (induction time), TMR_{ad} of 24 hr. and TMR_{ad} of 7 days are reached for starting temperatures of 218 °C and 196 °C respectively. The PHI correction is of vital importance for the calorimetry study and especially for the thermokineitcs study, the raw data from the tests should be corrected first before analyzing.

Small quantities of additives such as sodium hydroxide, calcium chloride, sodium sulphate, sodium carbonate and iron (III) oxide have a significant effect on the detected decomposition “onset” temperature. They all can lower the onset temperature of the 2-NT and sodium hydroxide can decrease the “onset” temperature as much as 183 °C. While sodium chloride has limited influences on the 2-NT thermal decomposition. By comparing the data of the thermal analyses performed via ARSST^{TM}, this work assessed the incompatibility rating of hazards on 2-NT with six impurities. In summary, the unstable sequences are proposed as follows:

2-NT + OH^- > 2-NT + iron (III) oxide > 2-NT + CO_3^{2-} > 2-NT + SO_4^{2-} > 2-NT + Cl^-

Previous research has focused on theoretical work and experiments which did not provide any pressure generation data. However, implementation of theoretical methods of hazard screening based thermal data only are not enough for evaluating the hazards and the mitigation methods to avert or minimalize the effects of potential incidents. The rates and magnitudes of the pressure rises is a prerequisite for safe scale up for the process [122]. Previous studies have shown data collected from DSC and TDA tests. Unlike the previous DSC and TDA test, pressure related data, such as maximum pressure rate, pressure vs. time and non-condensable gas is reported in this paper. One mole of 2-NT may generate approximately one mole of NCG in temperatures lower than 600 °C. Iron (III) oxide was found to be the only chemical among the six additives studied that causes a smaller NCG release during 2-NT thermal decomposition. This clearly shows that the thermal decomposition mechanisms for the 2-NT with iron (III) oxide and the other five contaminants are different.

The reasons and the possible mechanisms that lead to the phenomena observed by the addition of each of the six incompatible contaminants have been discussed. The base sodium hydroxide can lower the thermal stability of nitro aromatics due to the positive charge on the nitro atom of nitro group. Sodium carbonate and sodium sulfate, in water generate OH^- thus increasing the solution pH, which lowers the stability of the 2-NT. The chloride ions from the dissolution of sodium chloride and calcium chloride slightly impact the thermal stability of the 2-NT. The higher the concentration of chloride irons, the larger

their influence on the thermal stability of 2-NT. The iron (III) oxide may work as the catalyst to accelerate the reduction reaction of the 2-NT (P1) to 2-toluidine (P22) which competes with the original main reaction of formation of anthranil (P12).

Thermal decomposition of nitroaromatics with α-CH bonds *ortho* to -NO_2 on an aromatic ring are activated by *ortho* –CH substitution, such as 2,4-dinitrotoluene, TNT etc.[7] This mechanism was first evidenced by 2-nitrotoluene turned to anthranil and water upon heating (P1 → P11 → P12). For the nitroaromatic explosives that have the α-CH bond *otho* to the –NO_2, similar impacts from these six contaminants are expected due to the same initial decomposition mechanism.

The effect of confinement was tested by observing 2-NT decomposition under various overhead initial pressures in the ARSST, varying from 50 psi to 220 psi (1.5 MPa). With increasing initial pressure, the "onset" temperature and self-heat rate slightly, and the maximum pressure-rise rate increased dramatically; "onset" and maximum pressure were all higher, and there was more gas generated as P initial increased. As a conclusion, pressure accumulation is hazardous to 2-NT and it is important to keep a low-pressure environment for 2-NT storage and transportation.

2-NT decomposition is also affected by heating rate, and the effect of heating rate was studied using the DSC and ARSST by heating up 2-NT under different heating rates. As a conclusion, when the heating rate is faster or the detected "onset" temperature slightly higher temperatures, the self-heating rate and the pressure-rise rate increase faster, and the reaction occurs more violently. Therefore, if 2-NT is suddenly heated up, the

decomposition is more likely to occur. The thermal decomposition of 2-NT is a low probability but high consequence event.

The thermal history impacts the 2-NT thermal behavior during the decomposition. The longer the induction time, the lower temperature it needs to decomposition. This also prove the autocatalytic reactions for the 2-NT decomposition. The experiments of different sample sizes show that the decomposition of 2-NT would be mitigated with inert material. And of course, with smaller amount of sample size, the decomposition is less violent. Therefore, the size of 2-NT piles should be limited. The APTAC can give more conservative results than ARSST except the maximum pressure rise rate.

φ factor correction is important for both temperature and pressure related data. Use the low thermal inertia or φ factor equipment, do not always provide better large-scale estimations.

Thermal history, heating up rate, confinement effect and sample sizes are complex factors that can influence the thermal behavior of 2-NT.

Overall, this dissertation provides sufficient information to understand the potential hazard related to the MNT decomposition, and it also represents a step forward toward safer conditions for MNT transportation and storage. This work demonstrates the complexity and the multiple studies required for making 2-NT safer. It serves as a foundation to further the understanding of 2-NT. In addition, the data, techniques, approaches utilized in this dissertation illustrate a methodology for the study of the reactive chemicals of interest.

7.2 Future Work

This section provides recommendations for future work, based on the challenges faced during this study. Also some ideas about how to continue the work of 2-NT reactive chemical study.

7.2.1. Calorimetric studies

The experimental and analytical findings of this research can be validated by performing experimental tests at large sample sizes. Due to the severity of the runaway of 2-NT, fast pressure rise and temperature rise rate, obtaining meaningful adiabatic experimental data with large sample sizes were not applicable since it may damage the equipment. Therefore, the PHI factor of 2-NT decomposition in APTAC is large in this research. Though after the PHI correction, the influence from the glass cell can be eliminated. It cannot be guarantee that the heat transfer of the sample and glass are uniform. Alternatively, others such as DSC or microcalorimetry could be a better choice.

Also, to protect the equipment, the power from equipment was turned off after the shutdown criteria (460 °C for ARSST and 410 °C for APTAC). Which means, the data from the calorimeter overpass the shutdown criteria is not adiabatic anymore. Therefore, the current kinetics study was mainly focused on the induction phase (T_o to 410 °C). To get the full picture of the 2-NT thermal decomposition under N_2 atmosphere, other calorimetry is required which are capable of doing the decomposition tests at higher temperature.

Together with the calorimetry used in this research, the analytical tools such as Gas Chromatography (GC), Mass Spectrometry (MS), High performance liquid chromatography (HPLC) and/or X-ray powder diffraction (XRD) will allow to perform in-situ compound analysis to verify the main findings of the 2-NT thermal decomposition during induction phase. Besides, the proposed mechanism of the incompatible components influence can also be validated which will be used to evaluate chemical reactivity for the other nitro aromatic compounds with the same family of contaminants.

7.2.2. Relief valve sizing design

Design Institute for Emergency Relief Systems (DIERS) by AICHE spent $1.6 million to investigate the two-phase vapor-liquid dynamics and the emergency relief systems. The ARSST is based on DIERS two-phase methodology is a useful equipment recognized by OSHA for relief valve sizing design. This easy-to-use device is also capable of generating low phi-factor data for DIERS vent sizing design.

This work has provided big amount of the data for MNT thermal decomposition under different conditions using ARSST varying pad pressures, mass quantities, heating rate and with/without additives etc. This data is valuable for industry to perform the relief valve sizing calculations and predictions. In the industry, reactors, distillation towers, storage tanks or pipelines have different geometry parameters. Engineers can use the pressure and temperature from this research and coupling together with the geometry data of their equipment, to calculate the appropriate sizes for the corresponding relief valves in case of the vapor heating or fire.

7.2.3. Molecular simulation

As shown in the literature review, many researchers have studied the initial decomposition pathways of MNT by applying experimental and simulation methods. The full list of the possible products of the runaway reaction are still unclear. Also, the discrepancies exist between different work required more work to be done in study the decomposition pathway of MNT decomposition reactions. To prove the proposed decomposition mechanisms of the 2-NT thermal decomposition with incompatibles, more study is needed by the molecular simulation together with the experiment.

7.2.4. Effect of surrounding gas atmosphere

This research work focus on the thermal decomposition of nitro aromatic compounds under the nitrogen atmosphere. However, different gas atmosphere might influence nitro aromatics runaway behavior. Different gases can be used as initial overhead pad gas, such as O_2, He, NO_2, NO, CO and CO_2 rich atmosphere. The O_2 may accelerate the reactions due to the trigger of explosion, the H_e may inert the system. For the NO_2, NO, CO and CO_2, researcher should be careful to do the tests since they are hazardous to the health of human being and they may largely change the thermal behavior of nitro aromatics since they are the main products for the reactions as well. The study of this other gas atmosphere can help the firefighting related to nitro aromatics.

REFERENCES

[1] Crowl, D. A., & Louvar, J. F. (2001). Chemical process safety: fundamentals with applications. Pearson Education.

[2] Gonzalez, A. C., Larson, C. W., McMillen, D. F., & Golden, D. M. (1985). Mechanism of decomposition of nitroaromatics. Laser-powered homogeneous pyrolysis of substituted nitrobenzenes. The Journal of Physical Chemistry, 89(22), 4809-4814.

[3] Matveev, V. G., Dubikhin, V. V., & Nazin, G. M. (1978). Radical gas-phase decomposition of nitrobenzene derivatives. Russian Chemical Bulletin, 27(4), 675-678.

[4] Booth, G. (2000). Nitro compounds, aromatic. Ullmann's Encyclopedia of Industrial Chemistry.

[5] Ju, K. S., & Parales, R. E. (2010). Nitroaromatic compounds, from synthesis to biodegradation. Microbiology and molecular biology reviews, 74(2), 250-272

[6] Urbanski T (1964). Chemistry and Technology of Explosives 1. Pergamon Press. pp. 389–91. ISBN 0-08-010238-7. Ledgard, Jared. The preparatory manual of explosives. Lulu. com, 2007.

[7] Gattrell, M. (2014). U.S. Patent No. 8,907,144. Washington, DC: U.S. Patent and Trademark Office.

[8] US EPA (2004). Non-confidential IUR production volume information. US Environmental Protection Agency. Available at: http://www.epa.gov/oppt/iur/tools/data/2002-vol.html and search on CAS number

[9] IARC Working Group on the Evaluation of Carcinogenic Risk to Humans. (1970, January 01). 2-NITROTOLUENE. Retrieved February 09, 2018, from https://www.ncbi.nlm.nih.gov/books/NBK373187/

[10] Six, C.; Richter, F. (2005), "Isocyanates, Organic", Ullmann's Encyclopedia of Industrial Chemistry, Weinheim: Wiley-VCH, doi:10.1002/14356007.a14_611

[11] Chemicals, I. A. (1999, March 10). Air Products' World-Class DNT Facility Now on Stream in Geismar, Louisiana. Retrieved February 09, 2018, from https://www.prnewswire.com/news-releases/air-products-world-class-dnt-facility-now-on-stream-in-geismar-louisiana-75295987.html

[12] Duh, Y. S., Lee, C., Hsu, C. C., Hwang, D. R., & Kao, C. S. (1997). Chemical incompatibility of nitrocompounds. Journal of Hazardous Materials, 53(1-3), 183-194.

[13] Haynes, W. M. (Ed.). (2014). CRC handbook of chemistry and physics. CRC press.

[14] CSB (2003, October). Investigation Report-Fire and Explosion at First Chemical Corporation. Retrieved February 09, 2018, from http://www.csb.gov/first-chemical-corp-reactive-chemical-explosion/

[15] Cutler, D. P., & Brown, A. K. (1996). Investigation into an explosion and fire in a mononitrotoluene manufacturing plant. Journal of hazardous materials, 46(2-3), 169-183.

[16] Harris, G. F. P., Harrison, N., & MacDermott, P. E. (1981). HAZARDS OF THE DISTILLATION OF MONO NITROTOLUMES.

[17] Larrañaga, M. D., Lewis, R. J., & Lewis, R. A. (2016). Hawley's condensed chemical dictionary. John Wiley & Sons.

[18] OSHA. "Chemical Sampling Information | Nitrotoluene." United States Department of Labor. Retrieved February 9, 2018. from https://www.osha.gov/dts/chemicalsampling/data/CH_258200.html

[19] Dunnick, June K., Michael R. Elwell, and John R. Bucher. "Comparative toxicities of o-, m-, and p-nitrotoluene in 13-week feed studies in F344 rats and B6C3F1 mice." Toxicological Sciences 22.3 (1994): 411-421.

[20] EPA. (2014, January). Emerging Contaminants – Dinitrotoluene (DNT). Retrieved February 9, 2018, from https://www.epa.gov/sites/production/files/2014-03/documents/ffrrofactsheet-contaminant-dnt_january2014_final.pdf

[21] Pike, J. (n.d.). Explosives - Nitroaromatics. Retrieved February 09, 2018, from http://www.globalsecurity.org/military/systems/munitions/explosives-nitroaromatics.htm

[22] Guard, U. C. (1978). Department of Transportation, CHRIS-Hazardous Chemical Data. Manual Two, US Government Printing Office, Washington, DC.

[23] Dugal, M. (2005). Nitrobenzene and nitrotoluenes. Kirk-Othmer Encyclopedia of Chemical Technology.

[24] Linstrom, P. J., & Mallard, W. G. (2001). NIST chemistry webbook.

[25] NIOSH. (2014, July 01). O-NITROTOLUENE. Retrieved February 09, 2018, from https://www.cdc.gov/niosh/ipcsneng/neng0931.html

[26] Fuels and Chemicals - Auto Ignition Temperatures. (n.d.). Retrieved February 09, 2018, from https://www.engineeringtoolbox.com/fuels-ignition-temperatures-d_171.html

[27] Gustin, J. L. (1998). Runaway reaction hazards in processing organic nitro compounds. Organic Process Research & Development, 2(1), 27-33.

[28] Grewer, Th. Int. Symp. Loss Prev. Saf. Promot. Process Ind. 1978, No. 1, III-105-113.

[29] Ando, T., Fujimoto, Y., & Morisaki, S. (1991). Analysis of differential scanning calorimetric data for reactive chemicals. Journal of Hazardous Materials, 28(3), 251-280.

[30] Sachdev, A., & Todd, J. (2005). Incident investigation of mono-nitro toluene still explosion. Journal of loss prevention in the process industries, 18(4-6), 531-536.

[31] Yang, L., Pan, Y., Wang, J., Shang, W., Lan, J., & Jiang, J. C. (2017, October). A new method for assessing the thermal hazard of reactive substances. In AIP Conference Proceedings (Vol. 1890, No. 1, p. 040017). AIP Publishing.

[32] Manelis, G. B. (2014). Thermal decomposition and combustion of explosives and propellants. Crc Press.

[33] BAO, S. L., CHEN, W. H., CHEN, L. P., GAO, H. S., & Lü, J. Y. (2013). Identification and thermokinetics of autocatalytic exothermic decomposition of 2, 4-dinitrotoluene. Acta Physico-Chimica Sinica, 29(3), 479-485.

[34] Bateman, T. L., Small, F. H., & Snyder, G. E. (1974). Dinitrotoluene pipeline explosion. A. LCh. E. CEP Loss Prevention, 8, 117-122.

[35] Gustin, J. L. (2002). Influence of trace impurities on chemical reaction hazards. Journal of Loss Prevention in the Process Industries, 15(1), 37-48.

[36] Oxley, J. C., Smith, J. L., Ye, H., McKenney, R. L., & Bolduc, P. R. (1995). Thermal stability studies on a homologous series of nitroarenes. The Journal of Physical Chemistry, 99(23), 9593-9602.

[37] Terrier, F. (1982). Rate and equilibrium studies in Jackson-Meisenheimer complexes. Chemical Reviews, 82(2), 77-152.

[38] Klais, O., & Grewer, T. (1988). Exotherme Zersetzung: Untersuchung der charakteristischen Stoffeigenschaften. VDI Verlag.

[39] Grewer, T., & Rogers, R. L. (1993). Exothermic secondary reactions. Thermochimica acta, 225(2), 289-301.

[40] Zhu, W., Papadaki, M. I., Han, Z., & Mashuga, C. V. (2017). Effect of temperature and selected additives on the decomposition “onset” of 2-nitrotoluene using Advanced Reactive System Screening Tool. Journal of Loss Prevention in the Process Industries, 49, 630-635.

[41] Lee, P. P., & Back, M. H. (1988). Kinetic studies of the thermal decomposition of nitroguanidine using accelerating rate calorimetry. Thermochimica acta, 127, 89-100.

[42] Furman, D., Kosloff, R., Dubnikova, F., Zybin, S. V., Goddard III, W. A., Rom, N., ... & Zeiri, Y. (2014). Decomposition of condensed phase energetic materials: Interplay between uni-and bimolecular mechanisms. Journal of the American Chemical Society, 136(11), 4192-4200.

[43] Oxley, J. C., Smith, J. L., & Wang, W. (1994). Compatibility of ammonium nitrate with monomolecular explosives. 2. Nitroarenes. The Journal of Physical Chemistry, 98(14), 3901-3907.

[44] Muravyev, N. V., Monogarov, K. A., Bragin, A. A., Fomenkov, I. V., & Pivkina, A. N. (2016). HP-DSC study of energetic materials. Part I. Overview of pressure influence on thermal behavior. Thermochimica Acta, 631, 1-7.

[45] Wang, Q., Rogers, W. J., & Mannan, M. S. (2009). Thermal risk assessment and rankings for reaction hazards in process safety. Journal of thermal analysis and calorimetry, 98(1), 225.

[46] Brill, T. B., & James, K. J. (1993). Kinetics and mechanisms of thermal decomposition of nitroaromatic explosives. Chemical reviews, 93(8), 2667-2692.

[47] Nikolaeva, E. V., Chachkov, D. V., Shamov, A. G., & Khrapkovskii, G. M. (2018). Alternative mechanisms of thermal decomposition of o-nitrotoluene in the gas phase. Russian Chemical Bulletin, 67(2), 274-281.

[48] Nazin, G. M., & Manelis, G. B. (1994). Thermal decomposition of aliphatic nitro-compounds. Russian

[49] Fayet, G., Joubert, L., Rotureau, P., & Adamo, C. (2009). A theoretical study of the decomposition mechanisms in substituted o-nitrotoluenes. The Journal of Physical Chemistry A, 113(48), 13621-13627.

[50] Chen, S. C., Xu, S. C., Diau, E., & Lin, M. C. (2006). A computational study on the kinetics and mechanism for the unimolecular decomposition of o-nitrotoluene. The Journal of Physical Chemistry A, 110(33), 10130-10134.

[51] Minier, L. M., Brower, K. R., & Oxley, J. C. (1991). Role of intermolecular reactions in thermolysis of aromatic nitro compounds in supercritical aromatic solvents. The Journal of Organic Chemistry, 56(10), 3306-3314.

[52] Galloway, D. B., Glenewinkel-Meyer, T., Bartz, J. A., Huey, L. G., & Crim, F. F. (1994). The kinetic and internal energy of NO from the photodissociation of nitrobenzene. The Journal of chemical physics, 100(3), 1946-1952.

[53] Tsang, W., Robaugh, D., & Mallard, W. G. (1986). Single-pulse shock-tube studies on C-NO2 bond cleavage during the decomposition of some nitro aromatic compounds. The Journal of Physical Chemistry, 90(22), 5968-5973.

[54] Diez-y-Riega, H., Gunawidjaja, R., & Eilers, H. (2013). Photoluminescence spectroscopy of 2-nitrotoluene and its photo and photothermal decomposition derivatives. Journal of Photochemistry and Photobiology A: Chemistry, 268, 50-57.

[55] He, Y. Z., Cui, J. P., Mallard, W. G., & Tsang, W. (1988). Homogeneous gas-phase formation and destruction of anthranil from o-nitrotoluene decomposition. Journal of the American Chemical Society, 110(12), 3754-3759.

[56] Dacons, J. C., Adolph, H. G., & Kamlet, M. J. (1970). Novel observations concerning the thermal decomposition of 2, 4, 6-trinitrotoluene. The Journal of Physical Chemistry, 74(16), 3035-3040.

[57] Yinon, J. (1982). Mass spectrometry of explosives: Nitro compounds, nitrate esters, and nitramines. Mass Spectrometry Reviews, 1(3), 257-307.

[58] Lifshitz, A., Tamburu, C., Suslensky, A., & Dubnikova, F. (2006). Decomposition of anthranil. single pulse shock-tube experiments, potential energy surfaces and multiwell

transition-state calculations. the role of intersystem crossing. The Journal of Physical Chemistry A, 110(27), 8248-8258.

[59] Cook, M. A., & Abegg, M. T. (1956). Isothermal decomposition of explosives. Industrial & Engineering Chemistry, 48(6), 1090-1095.

[60] Guidry, R. M., & Davis, L. P. (1979). Thermochemical decomposition of explosives. I. TNT kinetic parameters determined from ESR investigations. Thermochimica Acta, 32(1-2), 1-18.

[61] Chen, P. C., & Wu, C. W. (1995). The molecular structures of nitrotoluenes and their thermal decomposition tautomers. Journal of Molecular Structure: THEOCHEM, 357(1-2), 87-95.

[62] Tanaka, G., & Weatherford, C. (2008). Decomposition mechanisms of dinitrotoluene. International Journal of Quantum Chemistry, 108(15), 2924-2934.

[63] Fayet, G., Rotureau, P., Joubert, L., & Adamo, C. (2010). QSPR modeling of thermal stability of nitroaromatic compounds: DFT vs. AM1 calculated descriptors. Journal of molecular modeling, 16(4), 805-812.

[64] Saraf, S. R., Rogers, W. J., & Mannan, M. S. (2003). Application of transition state theory for thermal stability prediction. Industrial & engineering chemistry research, 42(7), 1341-1346.

[65] Fayet, G., Rotureau, P., Joubert, L., & Adamo, C. (2011). Development of a QSPR model for predicting thermal stabilities of nitroaromatic compounds taking into account their decomposition mechanisms. Journal of molecular modeling, 17(10), 2443-2453.

[66] Lu, Y., Ng, D., & Mannan, M. S. (2010). Prediction of the reactivity hazards for organic peroxides using the QSPR approach. Industrial & Engineering Chemistry Research, 50(3), 1515-1522.

[67] Baati, N., Nanchen, A., Stoessel, F., & Meyer, T. (2015). Predictive Models for Thermal Behavior of Chemicals with Quantitative Structure-Property Relationships. Chemical Engineering & Technology, 38(4), 645-650.

[68] Valdes, O. J. R., Moreno, V. C., Waldram, S. P., Véchot, L. N., & Mannan, M. S. (2015). Experimental sensitivity analysis of the runaway severity of dicumyl peroxide decomposition using adiabatic calorimetry. Thermochimica Acta, 617, 28-37.

[69] ASTM E537–12. Standard Test Method for the Thermal Stability of Chemicals by Differential Scanning Calorimetry. Annual Book of ASTM Standards, ASTM, International, West Conshohocken, PA, USA, 2012.

[70] G. Maria, E. Heinzle, Kinetic system identification by using short cut techniques in early safety assessment of chemical processes, J. Loss Prev. Process Ind. 11 (1998) 187–206.

[71] Fauske & Associates, I., FAI/94-25, Reactive system screening tool system manual, methodology and operations. July, 1994.

[72] Kumpinsky, E., A Study on Resol-Type Phenol-Formaldehyde Runaway Reactions. Industrial & Engineering Chemistry Research, 1994. 33(2): p. 285-291.

[73] Grolmes, M.A., Leung, J.C., and Fauske, H.K. Reactive systems vent sizing evaluations. in Proceedings of the International Symposium on Runaway Reactions, CCPS. March 1989. Cambridge, MA.

[74] Burelbach, J. P. (2000, October). Advanced Reactive System Screening Tool (ARSST). In North American Thermal Analysis Society, 28th Annual Conference, Orlando.

[75] Han, Z. (2016). Thermal Stability Studies of Ammonium Nitrate (Doctoral dissertation).

[76] Townsend, D. I., & Tou, J. C. (1980). Thermal hazard evaluation by an accelerating rate calorimeter. Thermochimica Acta, 37(1), 1-30.

[77] Vyazovkin, S., Burnham, A. K., Criado, J. M., Pérez-Maqueda, L. A., Popescu, C., & Sbirrazzuoli, N. (2011). ICTAC Kinetics Committee recommendations for performing kinetic computations on thermal analysis data. Thermochimica acta, 520(1-2), 1-19.

[78] A.K. Burnham, R.K. Weese, A.P. Wemhoff, J.L. Maienschein, A historical and current perspective on predicting thermal cookoff behavior, J. Therm. Anal. Calorim. 89 (2007) 407–415.

[79] S. Vyazovkin, The Handbook of Thermal Analysis & Calorimetry, in: M.E. Brown, P.K. Gallagher (Eds.), Recent Advances, Techniques and Applications, vol. 5, Elsevier, 2008, p. 503.

[80] M.E. Brown, Introduction to Thermal Analysis, 2nd ed., Kluwer, Dodrecht, 2001.

[81] Kossoy, A. and Akhmetshin, Y., Identification of kinetic models for the assessment of reaction hazards. Process Safety Progress, 2007. 26(3): p. 209-220.

[82] Vyazovkin, S., Burnham, A. K., Criado, J. M., Pérez-Maqueda, L. A., Popescu, C., & Sbirrazzuoli, N. (2011). ICTAC Kinetics Committee recommendations for performing kinetic computations on thermal analysis data. Thermochimica acta, 520(1-2), 1-19.

[83] Brown, M. E., Maciejewski, M., Vyazovkin, S., Nomen, R., Sempere, J., Burnham, A. A, ... & Keuleers, R. (2000). Computational aspects of kinetic analysis: part A: the ICTAC kinetics project-data, methods and results. Thermochimica Acta, 355(1-2), 125-143.

[84] Sivapirakasam, S. P., Mohamed, M. N., Surianarayanan, M., & Sridhar, V. P. (2013). Evaluation of thermal hazards and thermo-kinetic parameters of a matchhead composition by DSC and ARC. Thermochimica acta, 557, 13-19.

[85] 2003, Recommendations on the Transport of Dangerous Goods, Manual of Tests and Criteria, 4 revised Ed., United Nations, ST/SG/AC.10/11/Rev.4 (United Nations, New York and Geneva).

[86] 2003, Globally Harmonized System of Classification and Labelling of Chemicals (GHS), United Nations, New York and Geneva.

[87] Semonov, N. N. (1959). Some problems of chemical kinetic and reactivity. Part II.

[88] Sterling, K. B., Cevasco, G. A., Harmond, R. P., & Hammond, L. F. (1997). Biographical dictionary of American and Canadian naturalists and environmentalists. Greenwood Publishing Group.

[89] Kamenetskii, D. F. (1969). Diffusion and heat transfer in chemical kinetics. Plenum Press, New York.

[90] Yaws, C. L. (1999). Chemical properties handbook. McGraw-Hill,

[91] Wilcock, E., & Rogers, R. L. (1997). A review of the phi factor during runaway conditions. Journal of Loss Prevention in the Process Industries, 10(5-6), 289-302.

[92] Fisher, H. G., Forrest, H. S., Grossel, S. S., Huff, J. E., Muller, A. R., Noronha, J. A., ... & Tilley, B. J. (1992). Emergency relief system design using Design Institute for Emergency Relief Systems (DIERS) technology.

[93] Haynes, W. M. (2014). CRC handbook of chemistry and physics. CRC press.

[94] Gao, H. S.; Chen, L. P.; Chen, W. H.; Bao, S. L. Thermochim. Acta 2013, 569, 134. doi: 10.1016/j.tca.2013.07.017

[95] ASTM E698-01. Standard test method (Ozawa and Kissenger) for Arrhenius kinetic constants for thermally unstable materials. doi:10.1520/E0698-01.

[96] Roduit, B., Folly, P., Berger, B., Mathieu, J., Sarbach, A., Andres, H., ... & Vogelsanger, B. (2008). Evaluating SADT by advanced kinetics-based simulation approach. Journal of Thermal Analysis and calorimetry, 93(1), 153-161.]

[97] Lin, W., Wu, S., Shiu, G., Shieh, S., & Shu, C. (2008). Self-accelerating decomposition temperature (SADT) calculation of methyl ethyl ketone peroxide using an adiabatic calorimeter and model. Journal of thermal analysis and calorimetry, 95(2), 645-651.

[98] Buck, P. (1969). Reactions of aromatic nitro compounds with bases. Angewandte Chemie International Edition in English, 8(2), 120-131

[99] Chen, C. Y., & Wu, C. W. (1996). Thermal hazard assessment and macrokinetics analysis of toluene mononitration in a batch reactor. Journal of loss prevention in the process industries, 9(5), 309-316.

[100] Han, Z., Sachdeva, S., Papadaki, M. I., & Mannan, M. S. (2015). Ammonium nitrate thermal decomposition with additives. Journal of Loss Prevention in the Process Industries, 35, 307-315.

[101] Han, Z., Sachdeva, S., Papadaki, M. I., & Mannan, S. (2016). Effects of inhibitor and promoter mixtures on ammonium nitrate fertilizer explosion hazards. Thermochimica Acta, 624, 69-75.

[102] Halle, J. C., & Stern, K. H. (1980). Vaporization and decomposition of sodium sulfate. Thermodynamics and kinetics. The Journal of Physical Chemistry, 84(13), 1699-1704.

[103] Hall, J. Lab Manual for Zumdahl/Zumdahl's Chemistry, 6th ed.; Brooks Cole: Pacific Grove, 2002, Appendix 5.

[104] Thomas Jr, A. M. (1963). Thermal Decomposition of Sodium Carbonate Solutions. Journal of Chemical and Engineering Data, 8(1), 51-54.

[105] Hall, J. Lab Manual for Zumdahl/Zumdahl's Chemistry, 6th ed.; Brooks Cole: Pacific Grove, 2002, Appendix 5.

[106] Housecroft and Sharpe, Inorganic Chemistry, 2nd ed, Prentice-Pearson-Hall 2005, p. 368.

[107] Wei, C., Saraf, S. R., Rogers, W. J., & Mannan, M. S. (2004). Thermal runaway reaction hazards and mechanisms of hydroxylamine with acid/base contaminants. Thermochimica acta, 421(1-2), 1-9.

[108] Buck, P. (1969). Reactions of aromatic nitro compounds with bases. Angewandte Chemie International Edition in English, 8(2), 120-131.

[109] Weast, R. C., Astle, M. J., & Beyer, W. H. (1988). CRC handbook of chemistry and physics (Vol. 69). Boca Raton, FL: CRC press.

[110] Molenda, M., Stengler, J., Linder, M., & Wörner, A. (2013). Reversible hydration behavior of CaCl2 at high H2O partial pressures for thermochemical energy storage. Thermochimica acta, 560, 76-81.

[111] Fanning, J. C. (2000). The chemical reduction of nitrate in aqueous solution. Coordination Chemistry Reviews, 199(1), 159-179.

[112] Janssen, L. J. J., & Barendrecht, E. (1981). The electrochemical reduction of o-nitrotoluene to o-tolidine—I. Coulometry at controlled potential; production aspects. Electrochimica Acta, 26(6), 699-704.

[113] Zilberberg, I., Pelmenschikov, A., Mcgrath, C., Davis, W., Leszczynska, D., & Leszczynski, J. (2002). Reduction of nitroaromatic compounds on the surface of metallic iron: Quantum chemical study. International Journal of Molecular Sciences, 3(7), 801-813.

[114] Agrawal, A., & Tratnyek, P. G. (1995). Reduction of nitro aromatic compounds by zero-valent iron metal. Environmental Science & Technology, 30(1), 153-160.

[115] Keum, Y. S., & Li, Q. X. (2004). Reduction of nitroaromatic pesticides with zero-valent iron. Chemosphere, 54(3), 255-263.

[116] Nefso, E. K., Burns, S. E., & McGrath, C. J. (2005). Degradation kinetics of TNT in the presence of six mineral surfaces and ferrous iron. Journal of hazardous materials, 123(1-3), 79-88.

[117] Pereira, M. C., Oliveira, L. C. A., & Murad, E. (2012). Iron oxide catalysts: Fenton and Fentonlike reactions–a review. Clay Minerals, 47(3), 285-302.

[118] Klausen, J., Troeber, S. P., Haderlein, S. B., & Schwarzenbach, R. P. (1995). Reduction of substituted nitrobenzenes by Fe (II) in aqueous mineral suspensions. Environmental Science & Technology, 29(9), 2396-2404.

[119] Datta, K. J., Rathi, A. K., Gawande, M. B., Ranc, V., Zoppellaro, G., Varma, R. S., & Zboril, R. (2016). Base-Free Transfer Hydrogenation of Nitroarenes Catalyzed by Micro-Mesoporous Iron Oxide. ChemCatChem, 8(14), 2351-2355.

[120] Papadas, I. T., Fountoulaki, S., Lykakis, I. N., & Armatas, G. S. (2016). Controllable synthesis of mesoporous iron oxide nanoparticle assemblies for chemoselective catalytic reduction of nitroarenes. Chemistry–A European Journal, 22(13), 4600-4607.

[121] Lewis, R. J. (1996). Sax's dangerous properties of industrial materials (Vol. 8). New York.

[122] Singh, J., & Simms, C. (2000). The Thermal Screening Unit (TS^ u)-A tool for Reactive Chemical screening. In INSTITUTION OF CHEMICAL ENGINEERS SYMPOSIUM SERIES (Vol. 148, pp. 67-80). Institution of Chemical Engineers; 1999.

[123] Group Values for Estimating Heat Capacities of liquids and solids. Retrieved February 09, 2018, from http://www.umsl.edu/~chickosj/JSCPUBS/cpsupptab.pdf.

[124] Pitsadioti, I., Lapouridis, K., Georgopoulos, S., Antonopoulou, M., & Papadaki, M. (2017). Thermal decomposition of hydroxylamine in aqueous solutions in the presence of NaCl, KCl or Na2SO4 in the temperature range 120° C–140° C. Journal of Loss Prevention in the Process Industries, 49, 177-182.

[125] Barton, K., & Rogers, R. (1997). Chemical reaction hazards. Gulf Professional Publishing.